

University of Oslo

Contralateral Premolars: Validation of Symmetry

A doctoral thesis by Gaute Floer Johnsen



Gaute Floer Johnsen
Institute of Clinical Dentistry, Faculty of Dentistry
University of Oslo
NORWAY
2018

© Gaute Floer Johnsen, 2019

*Series of dissertations submitted to the
Faculty of Dentistry, University of Oslo*

ISBN 978-82-8327-037-2

All rights reserved. No part of this publication may be
reproduced or transmitted, in any form or by any means, without permission.

Cover: Hanne Baadsgaard Utigard.
Print production: Representeralen, University of Oslo.

*God, Thou great symmetry,
Who put a biting lust in me
From whence my sorrows spring,
For all the frittered days
That I have spent in shapeless ways
Give me one perfect thing.*

Anna Wickham, "Envoi," from *The contemplative quarry*, Harcourt, Brace and Co., 1921

Table of Contents

Table of Contents.....	III
Supervisors	1
Acknowledgements.....	2
List of Publications	3
Abbreviations	4
1. Introduction	5
1.1 Symmetry	5
1.1.1 Symmetry versus Asymmetry.....	8
1.1.2 Bilateral Symmetry: Sexual Dimorphism and Attractiveness	9
1.1.3 The Origin and Evolution of Bilateral Symmetry.....	10
1.1.4 Bilateral Symmetry: From Bones to Teeth	10
1.2 Premolars	13
1.2.1 Availability of Premolars	13
1.2.3 Techniques to Investigate Root Canal Morphology.....	13
1.2.4 Symmetry of Dental Anomalies/Aberrations	16
1.3 On the Importance of Knowing Symmetry in Dentistry	17
1.3.1 Dental Anthropology	17
1.3.3 Endodontics	17
1.4 Endodontic Challenges	20
1.4.1 Evaluation of Endodontic Techniques and Materials	20
1.4.1.1 Instrumentation	20
1.4.1.2 Obturation	22
2. Aims of the Research and Hypothesis.....	25
2.1 Aims	25
2.2 Hypothesis	25
3. Methodological Considerations	26
3.1 Background to Micro-CT	26
3.2 Hardware for micro-CT	28
3.3 Software and Image Analysis for micro-CT	28
3.4 Scan Quality Challenges and Artefacts	30

31	
3.5	Landmark based versus Automatic Algorithms 32
3.6	Nickel-Titanium Instruments.....34
3.7	Ethical Considerations.....35
4.	Summary of the Results 36
	Study I.....36
	Study II.....36
	Study III.....36
5.	Discussion..... 37
5.1	Validity and Reliability of Methodologies in Endodontic Research37
5.2	Sample size39
5.3	Geometric Morphometric Analysis42
6.	Conclusions 45
7.	Research Prospects 46
	REFERENCES..... 47
	APPENDIX I 69
	APPENDIX II 70
	APPENDIX III 71
	APPENDIX IV..... 72
	ORIGINAL PAPERS77

Supervisors

Professor Håvard Jostein Haugen, Dr. Ing.

Associate Professor Pia Titterud Sunde, D.D.S., PhD.

Acknowledgements

The present work was conducted as part of the Dual Competence in Dentistry Program at the *Department of Biomaterials* and *Section of Endodontics, Faculty of Dentistry, University of Oslo* during the years 2012-2018.

The completion of this thesis would not have been possible without the enduring personal and scientific support from my two supervisors and mentors, Håvard Jostein Haugen and Pia Titterud Sunde. Your continual motivation and encouragement made me see light at the end of the tunnel when it sometimes seemed as if all hope in completing this endeavor was lost. I am forever grateful.

I am extremely thankful to my knowledgeable co-authors whose expertise and hard-work made the publication of our three papers possible. Sameenah and Sazan, your dedication was truly awe-inspiring. Thank you, Joakim for providing insight and inspiration. I am truly indebted to my co-author, teacher, and true friend and brother from a different mother, Lord Wengenroth. Jonas, thank you explaining difficult concepts in easy-to-understand terms, great technical help with the micro-CT, and never-ending willingness to help me. I will see you the Oktoberfest in the near future, brother!

Words cannot express the sense of gratitude I have to my therapist, counselor, and friend, Hanna Tiainen. Your sense of humor, compassion, and scientific knowledge seem to know no bounds. Thank you.

To all my co-workers and friends at the *Department of Biomaterials* and *Section of Endodontics*, I owe you thanks for sharing your knowledge and expertise.

This thesis would not have been possible without the collaboration the *Section of Orthodontics, Faculty of Dentistry, Institute of Clinical Dentistry, University of Oslo*. Sincere thanks to Professor Lise Espeland, students in the graduate orthodontics program, and willing patients.

To my parents and brothers, thank you for your words of wisdom, support, and love you have always shown me.

I love you, Sonja, C. Gunnar, Alvilde, and Liv Solveig. Thank you, Sonja, for keeping our family afloat and taking care of our home, three kids, and me when this work occupied all of my time and efforts. In the midst of our chaotic existence, you somehow found energy and time to proof-read all of my manuscripts and come with invaluable input. C. Gunnar, you are my favorite son and I want to thank you for helping your mom with household chores, your sisters, and all of our GNs. Alvilde, your smile, spirit and cuddles always remind me of what is important in life. Liv Solveig, you show me how anything is possible for even the smallest of us as long as you are determined and strong-willed. I love you. You now have your husband and daddy back.

Gaute Floer Johnsen

Oslo, September 2018

List of Publications

- PAPER I Johnsen G. F., Sundnes, Wengenroth J., Haugen H. J. *Methodology for Morphometric Analysis and Comparison of Modern Human Contralateral Premolars*. Journal of Computer Assisted Tomography, **2016**, 43 (6), 956-963
- PAPER II Johnsen G. F., Dara S., Asjad, S., Sunde P. T., Haugen H. J. *Anatomic Comparison of Contralateral Premolars*. **2017**, Journal of Endodontics, 40 (4), 617-625
- PAPER III Johnsen G. F., Sunde P. T., Haugen H. J. *Validation of contralateral premolars as the substrate for endodontic comparison studies*. **2018**, International Endodontic Journal, 51 (8), 942-951.

Abbreviations

AAE	American Association of Endodontists
AS	Antisymmetry
CBCT	Cone Beam Computed Tomography
CCD	Charge-Coupled Device
CT	Computed Tomography
DA	Directional Asymmetry
FA	Fluctuation asymmetry
FOV	Field-of-View
Micro-CT	Microscopic Computed Tomography
NCC	Neural Crest Cells
NiTi	Nickel-Titanium
NPL	National Physical Laboratory
PTB	Physikalisch-Technische Bundesanstalt
RA	Retinoic Acid
RB	Reciproc™ Blue system
RCT	Root Canal Treatment
RMS	Resilon™ Monoblock System
RMSE	Root Mean Square Error
SDA	Shape Deviation Analysis
SEM	Scanning Electron Microscopy
SMI	Structure Model Index
VMTK	Vascular Modeling Toolkit
VMTKLab	Vascular Modeling Toolkit Lab

1. Introduction

1.1 Symmetry

The term “symmetry” derives from the Greek words *sum* (meaning ‘with’ or ‘together’) and *metron* (‘measure’), yielding *summetria*. Originally this indicated a relation of commensurability [1]; that something (concept, theory, or a concrete object) is measurable or comparable by a common standard. Symmetry, in both science and everyday life, has fascinated and intrigued humans since ancient times. Symmetry has, both as a concept and as a concrete thing, a particular salience to humans as it is closely related to humans’ inclination for harmony, beauty, and unity. In everyday use the word has two meanings [2]; one philosophical and one mathematical. The artistic usage of the word pertains to the harmony of shapes, colors, and forms in art, but also harmony in the written word such as Petrarchan sonnets and rhyming couplets. This artistic understanding of the word is less strict and applied in a more general/abstract sense than in the purely mathematical usage. At its core, symmetry is therefore a philosophico-mathematical idea by which man has attempted to understand and construct order, beauty, and perfection [2].

In art, symmetry is considered the harmonizing effect proportions and composition may have on different elements so that they are brought together into a unitary whole [1]. This does not require that any of the elements can be mirrored across an imaginary plane or undergo any geometric transformation. Rather, it is more of a conceptual mechanism that unifies the different parts of a sculpture or painting. This rather elusive use of the term symmetry in art means that the notion of symmetry is more of a transcendent experience that goes beyond measurable geometric figures.

Aristoteles writes in one of his principal works, *Metaphysica*, that “(t)he chief forms of beauty are order and symmetry and definiteness, which the mathematical sciences demonstrate in a special degree [3].” The mathematical branch of geometry defines bilateral symmetry, the symmetry of left and right, as an absolutely precise concept [2]. An object is symmetrical if it can be split into two or more identical parts, and these parts are systematically situated in relation to one another [4]. Objects are symmetric by two main types of transformation: reflection or rotation [4]. Reflection, also known as mirror symmetry, and rotation, which is any operation that results in bilateral symmetry, were described succinctly in writing as well as schematically by Hermann Weyl (**Figure 1**) [2]:

“A body, a spatial configuration, is symmetric with respect to a given plane E if it is carried into itself by reflection in E . Take any line l perpendicular to E and any point p on l : there exists one and only one point p' on l which has the same distance from E but lies on the other side. The point p' coincides with p only if p is on E . Reflection in E is that mapping of space upon itself, $S: p \rightarrow p'$, that carries the arbitrary point p into this its mirror image p' with respect to E . A mapping is defined whenever a rule is established by which every point p is associated with an image p' . A rotation around a perpendicular axis, say by 30° , carries each point p of space into a point p' and thus defines a mapping. A figure has rotational symmetry around an axis l if it is carried into itself by all rotations around l .”

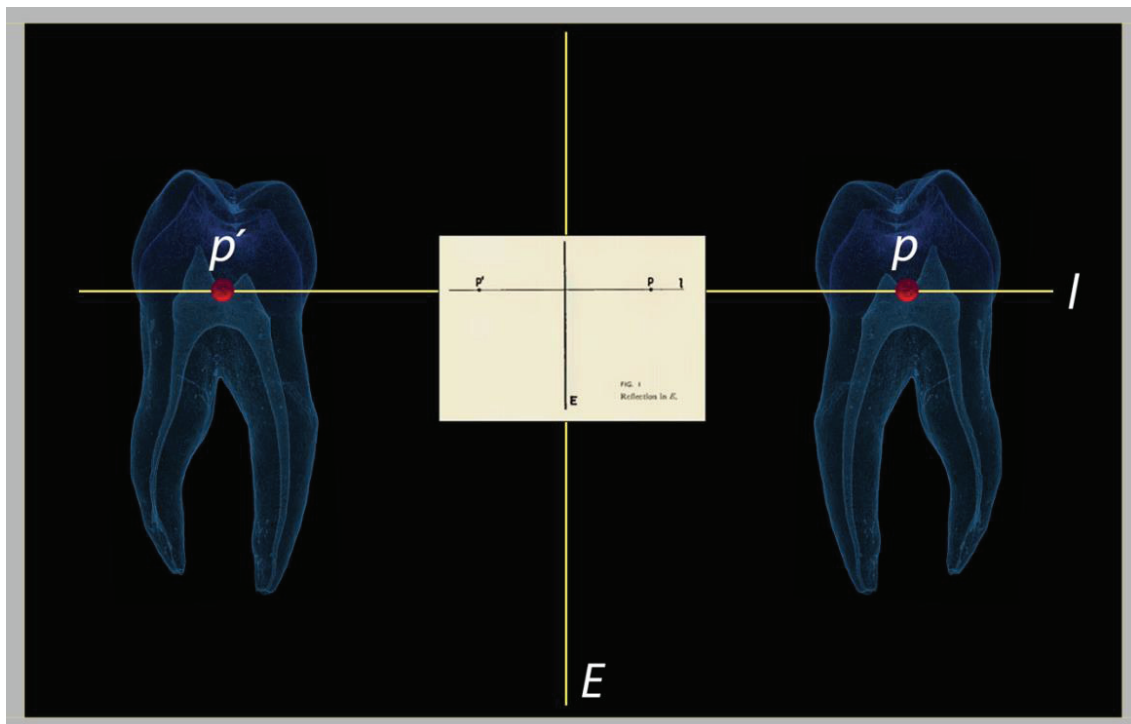


Figure 1. Schematic of reflection/rotation about a line resulting in bilateral symmetry as sketched by Hermann Weyl in his book *Symmetry* [2] and demonstrated with a premolar.

Bilateral symmetry of the face is perhaps the archetypal example of symmetry about a line (**Figure 2**). The imaginary line that bisects the face in the midsagittal plane can be thought of like a mirror, as every point on one side of the mirror plane has its counterpoint on the other side, thus yielding the figure what is called *self-coincident* with *congruent* sides [4]. When a transformation changes an object, like half a face, into a congruent figure it is called an *isometry*, with reflection being *indirect* or *opposite isometry* and rotation being *direct isometry* [4]. When a two dimensional figure like a triangle is mirrored across a line, the corresponding angle turns of the mirror image will be opposite (clockwise and counterclockwise). For three-dimensional structures the corresponding turns are right-handed and left-handed, and the two parts of the figure are called *indirectly* or *oppositely congruent* [4].

Mardia *et al.* [5] make a differentiation between two types of bilateral symmetries observed in the natural world, matching symmetry and object symmetry. Matching symmetry manifests itself as a pair of separate copies at the same distance from an imaginary mirror plane (midsagittal plane), but this symmetry axis does not bisect either of the paired objects [6]. Deer antlers, insect antennae, crayfish claws, primate hands are all examples of matching symmetry where a structure is present in two separate mirror image copies of each other on opposite sides of the anteroposterior axis of bilaterians. The term matching symmetry refers to the way scientists evaluate and analyze the degree of symmetry/asymmetry between mirror image structures [6]: the structures of interest are matched by using one as the reference object and reflecting the test object before superimposition. On the other hand, anatomical structures (objects) with an internal axis

or plane of symmetry such as the human mandible, sternum, pelvis, *etc.* that are bisected with midsagittal plane have object symmetry.

There are other types of symmetry (**Figure 2**) for both two-dimensional objects in one plane (glide reflection [e.g. human footprints]) and three-dimensional solids such as [4]:

- inversion symmetry (e.g. pair of cranks on a bicycle),
- rotatory inversion (e.g. two equal sticks laid across each other at right angles; if the cross is turned through a right angle and inverted, the sticks will have changed places), and
- screw symmetry (e.g. spiral stair case, DNA helix, screw, *etc.*).

These symmetries can be combined and present at the same time for certain objects, and it is clear that the number of symmetry permutations in three dimensions far exceeds those possible in two dimensions.

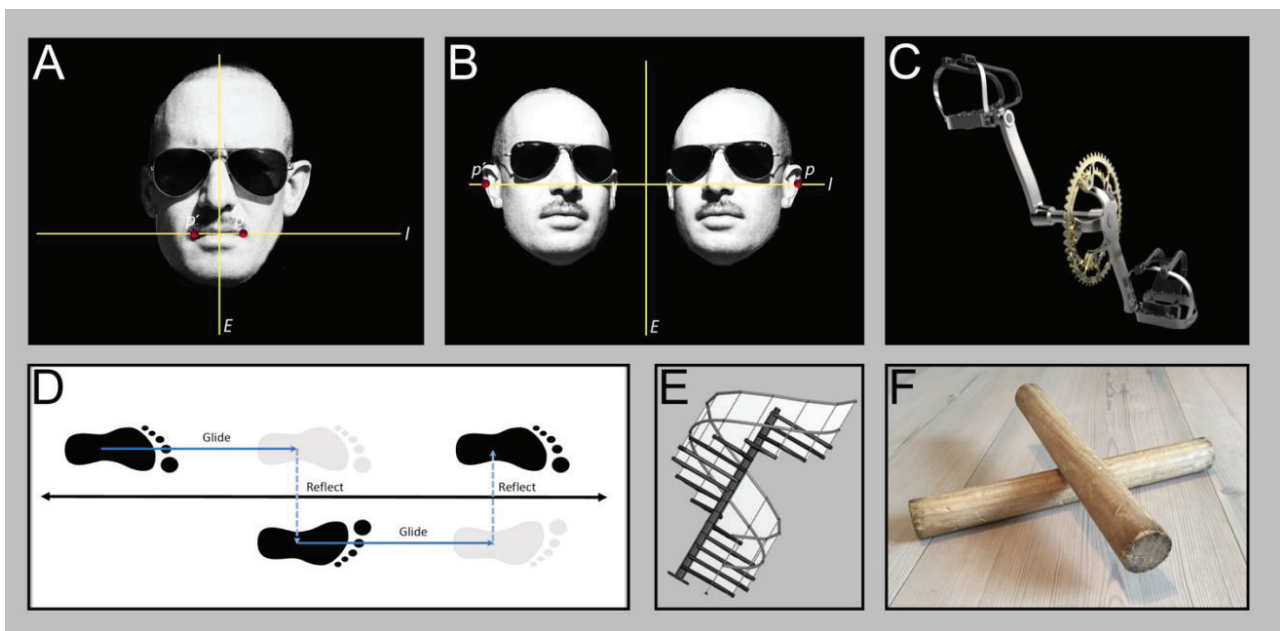


Figure 2. Visualization of different types of symmetries (A-F). The symmetry about the mirror line E in (A) shows how point p has its counterpart p' on the other side (authors' face). The symmetry depicted in (B) shows the reflection about the mirror line E of the authors' twins face resulting in a mirror imaged where for every point there is a corresponding. It follows that corresponding angles are clockwise and anticlockwise. Panel (C) demonstrates inversion symmetry (rotation and reflection about the axis of the bicycle crank). For two-dimensional objects one can also have symmetry in glide reflection (D). Three-dimensional symmetries are numerous as demonstrated with both screw symmetry and rotatory inversion (E and F).

1.1.1 Symmetry versus Asymmetry

To understand the propensity for bilateral symmetry in biology, it is important to appreciate the different forms of asymmetry. The ideal body plan of an organism belonging to the bilaterian clade has perfect symmetry, but this is never really encountered in nature. Imbalances in growth due to selective pressures, environmental challenges, congenital instability or genetic defects can result in patterns of asymmetry that fall into three categories [7, 8]:

1. **Fluctuating Asymmetry (FA):** FA is a random phenotypic deviation from the expected ideal genotypic programmed bilateral symmetry believed to be due to developmental instability from genetic factors (e.g. mutations) and/or environmental challenges (e.g. pathogens, toxins, nutritional) [9]. The use of FA as an indicator of genetic and overall health is controversial and by some described as contentious [6, 10]. Palmer and Strobeck [7] lamented that “FA as a measure of developmental stability is a very small signal easily lost in a tumultuous sea of entropic forces.” There are, however, more recent studies that have found that increased FA is associated with higher BMI in women, more medical conditions [11], and lower IQ and socioeconomic status [9, 12]. See **Figure 3A**.
2. **Directional Asymmetry (DA):** DA is a form of asymmetry whereby a characteristic in a population differ from the left to right side in the same *direction*. Examples of this include male narwhals with their consistently enlarged left canine [13], height differences in ear openings in barn owls [14], and asymmetrically situated internal organs in *Homo sapiens* [15]. See **Figure 3B**.
3. **Antisymmetry (AS):** AS is where the characteristic is consistently of greater or lesser size like in DA but occurs on either side with approximately equal frequency. The fiddler crab (*Uca* spp.) is an example of AS where there are equal distributions of males with the extremely asymmetric enlarged claw being either right- or left-clawed [16]. See **Figure 3C**.

External dental geometric morphometrics have attempted to correlate FA in teeth with both general health and malocclusion. Bailit *et al.* [17] found that they could predict the ranking of dental FA in four different ethnic groups according to degree of external challenges (exposure to illnesses, caloric intake, environment and living conditions, and inbreeding). Khalaf *et al.* [18] found that the degree of FA was low in their study sample of young Caucasian males and females from the United Kingdom where external challenges on average can be expected to be low. When studying the connection between dental FA, Sprowls *et al.* [19] found a positive correlation between increased FA and so-called transverse positional asymmetries as well as dental crowding. The connection between dental FA and overall health is contested, as other studies have not found any biological meaningful correlation with morbidity [20]. Asymmetry is not only manifested in structures either belonging to the object or matching type of symmetry but may also present itself in the midsagittal plan such as a *spina nasalis anterior* deviation or an asymmetric sagittal skull suture resulting in bulging away from the midline [21].

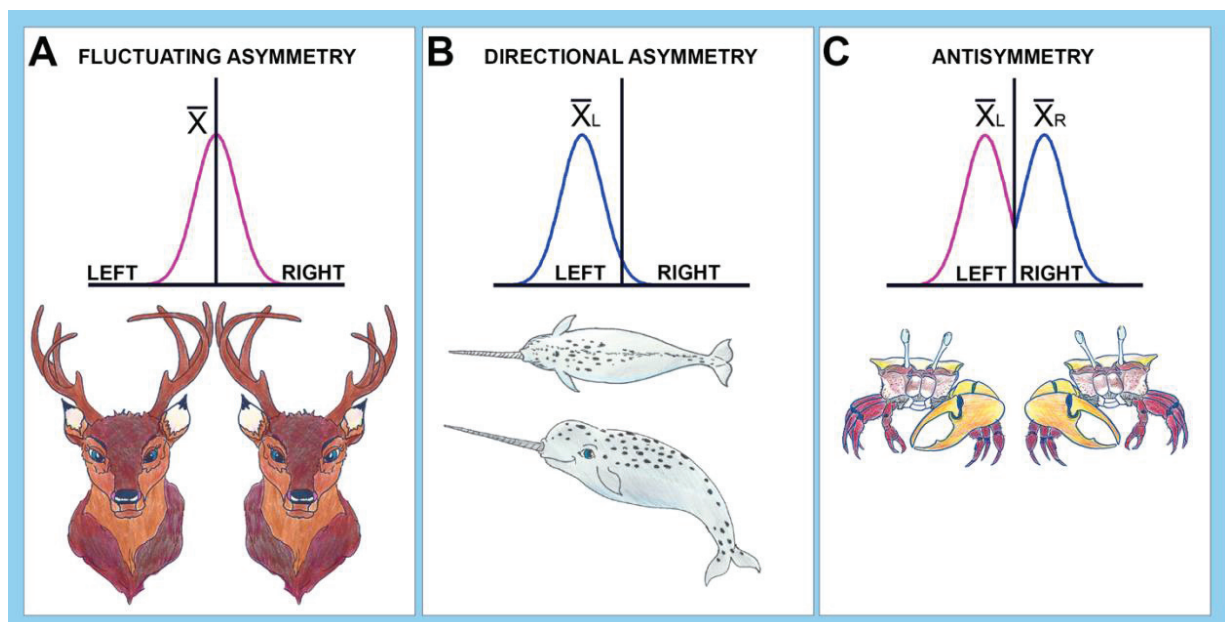


Figure 3. Categories of asymmetry. (A) FA demonstrated by the antlers of elk (*Cervus canadensis*). FA is represented by minor non-directional deviations from perfect symmetry (origin), measured as the differences between corresponding parts on the left and sides of the body (thus, the mean value (\bar{x}) for left–right differences is zero). (B) With DA, morphological lateralization in essentially all individuals of a population is fixed on the same side. The species-specific left placement of the tusk of the Narwhal (*Monodon monoceros*) typifies DA. (c) Populations with random lateralization of contralateral structures, such as seen with the enlarged claws of Banana fiddler crabs (*Uca mjoebergi*), show discrete asymmetries either to the left (pink) or to the right (blue), exhibit AS. Figure after Compagnucci *et al.* [21] by permission from John Wiley and Sons (License number 4423701297049)

1.1.2 Bilateral Symmetry: Sexual Dimorphism and Attractiveness

The human face plays an important role in visual perception (e.g. gender) and for conveying and understanding social cues. Facial expressions and grimaces that are transmitted, either consciously or sub-consciously, are quickly assessed and perceived by the receiver and illicit both physical and psychological reactions. It was previously held as scientific truth that a person's outer appearance could give insight into his/her personality. Historically, many scientists devoted their careers to the study of physiognomy, the assessment of a person's traits and characteristics based on facial features. Physiognomic analysis is now considered a pseudo-science at best. However, with the advent of advanced two- and three-dimensional facial analysis the field has been reincarnated as studies show that people and computers are able to correctly identify gender (sexual dimorphism) based on symmetry with a high degree of accuracy [22, 23].

A high degree of symmetry (low FA) has also been investigated in sexual dimorphism by itself [24] and has been found to correlate positively with perceived facial attractiveness [25, 26].

Symmetry is both visually pleasing and appealing to humans; it has perceptual salience [27]. It permeates the organic and inorganic natural world as well as art, architecture and engineering [2]. The ubiquitous and almost universal presence of bilateral body plans, while radial (rotational) symmetry and other forms can be found as well [6], suggest that symmetry must have become in of and in itself a driving force of sexual selection for the bilaterian clade.

1.1.3 The Origin and Evolution of Bilateral Symmetry

It is believed that the bilaterian body plan burst out of what is known as the Cambrian Explosion approximately 541 million years ago [28]. The main features of vertebrate bilaterians are that they have a front (anterior), back (posterior), top (dorsal), and bottom (ventral). This anteroposterior axis gives their external body bilateral symmetry, e.g. left and right side. The bilaterian blueprint for segmental identity, anteroposterior vectorial patterning, and development of anatomical structures is encoded by conserved common cladistic regulatory genes known as homeotic genes such as *Hox* genes [29]. These regulatory programs for regional specification and morphogenesis are under fine-tuned control by several signaling molecules.

Retinoic acid (RA) (the oxidized form of vitamin A) is an important signaling molecule with several functions in the developing vertebrate embryo [30]. RA plays an important part in establishing the anteroposterior and the left-right embryonic axis along with the formation of the cranial neural crest cells (NCC) [31]. These NCC are vertebrate pluripotent migratory cells that specialize into cells that become responsible for craniofacial development and patterning of bone, cartilage, and teeth [32].

Epithelial-mesenchymal interactions control odontogenesis and the morphodifferentiation of teeth. These interactions are controlled through several complex signaling pathways by a number of different mesenchymal regulatory molecules and their receptors [33]. Furthermore, RA provides a molecular link between the anteroposterior and left-right axis that ensures the bilateral symmetric somitogenesis in vertebrate embryos [30, 34]. The Zebrafish's anterior dentition was lost in evolution. Seritrakul *et al.* [32] demonstrated that Zebrafish exposed to RA during development induced both the formation and bilateral symmetric formation of ectopic anterior dentition.

1.1.4 Bilateral Symmetry: From Bones to Teeth

Apart from the asymmetric arrangement of internal organs, the anatomical structures and limbs of the human body is assumed to exhibit near perfect matching or object symmetry. The clinical relevance is apparent in the case of surgical reconstructions/corrective surgery and a multitude of clinical assessments where the contralateral limb serves as an intra-subject control [35]. Studies on bilateral symmetry of both the physical, densitometric, and structural measurements of the entire femur as well as geometric morphometric features of the proximal femur show substantial symmetry [35, 36]. The implication for both research purposes and surgical procedures is clear when Young *et al.*

[36] also found that demographics (age, weight, height, ethnicity and gender) had no association with asymmetry. The bilateral matching symmetry of the femur is a valuable aid in reproducing the correct femoral size, shape and orientation in hip arthroplasty [37, 38].

Three-dimensional evaluation and comparison of computed tomography (CT) images of the scaphoid bone demonstrate, like the studies on femurs, such a high degree of bilateral matching symmetry that ten Berg *et al.* [39] suggest that the contralateral side is a useful reference in preoperative planning for reconstruction surgery of scaphoid fractures. Other similar two- and three-dimensional comparisons of bilateral anatomical structures support the presumption of bilateral matching and object symmetry in humans for structures such as the talus for surgical planning; metacarpals, humeri and calcanei for mismatching comingled human remains; and for shape and volume deviation analysis of the pelvis [40-43] [44].

The high degree matching symmetry seen in bones and bony structures has also been found in cartilage and fibrocartilaginous tissue in certain outer and inner human anatomical structures such as the outer ear [45] and meniscus [46]. Bilateral symmetry seems pervasive in the human body. It is also present in the normal craniofacial complex [47, 48] with the mandible showing a symmetry of 82.85 (95% confidence interval 80-84.2), in a sample of 952 Brazilian individuals [49]. Thus, one would therefore presume that this would be the case for contralateral teeth.

Studies on the degree of macroscopic similarity between contralateral teeth have been sparse, but there has been interest in the microscopic features such as striae of Retzius in enamel and lines of Owen of the dentin in forensic dentistry. Based on an investigation by two Japanese scientists (T. Fujita and H. Takiguti) the renowned forensic dentist G. Gustafson [50] showed in 1947 that teeth from the same dentition could be matched using the aforementioned lines. His wife, and Sweden's second female with a PhD in dentistry, Anna-Greta Gustafson, confirmed the structural symmetry in contralateral premolars. She demonstrated that gross details such as the dentinoenamel junction and finer details such as irregularities and bending of the enamel prisms were identical in contralateral first premolars [51]. She also states "(...) *occasional exceptions where the condition is not bilateral are no doubt accounted for by some localized disturbance of development (...) such as trauma or infection (...)*." In her thesis [52], she reiterates her findings of identical structural regions in homologous teeth from the same individual. She makes the contention that results from any investigation of the reactions of "enamel are unreliable unless absolutely identical control material has been used" and "experiments on the reactions of enamel to acid or to other destructive substances should be [conducted] on a very great number of teeth, or on homologous teeth."

Jørgensen [53] did not cite the findings or recommendation made by Anna-Greta Gustafson two decades prior, but he did confirm her conclusion on enamel being identical in homologous teeth by testing effect of a given etching acid on different teeth and on 10 pairs of contralateral teeth *ex vivo*. He used the scanning electron microscopy (SEM) monitor to localize identical coordinate values measured from the mesial and incisal border of the labial surface. He concluded that non-contralateral teeth demonstrate

substantial differences in the pattern of the etched enamel and that symmetric areas on pairs of contralateral teeth have almost identical etch patterns. He suggested that “*comparative studies (...) may therefore lead to erroneous conclusions unless the materials are compared from pairs of contralateral teeth [53].*” In a follow-up study, Jørgensen & Shimokobe [54] used contralateral pairs of incisors and canines and confirmed their previous findings when they examined the adaption of flowable restorative materials to etched enamel *ex vivo*.

Brännström and Nordenvall [55] based their methodology on Jørgensen’s findings. They used contralateral teeth in their combined *in vivo* and *ex vivo* etching on dentin and enamel study in an effort to create well-balanced experimental groups. They found variations in the etching effects, but it is unclear how they compared the exact same area of tooth with its corresponding contralateral. Furthermore, since the etching procedures were conducted prior to extraction the enamel surfaces could not be matched as suggested by Anna-Greta Gustafson. Nevertheless, in his presentation of the series of experiments laying the grounds for explaining the hydrodynamic theory, Martin Brännström used contralateral premolars to have one of the homologous teeth serve as the control [56].

Even though matched contralateral teeth have been used as the substrate for certain comparison studies [57-61], they have never become the gold standard [62, 63]. De-Deus [64] suggest using paired and matched teeth for endodontic leakage studies as most studies have only demonstrated differences in anatomy. This principle of using paired and matched teeth can be applied to other studies apart from leakage studies. There are, however, a paucity of detailed and high quality studies on the normal external or internal anatomy of contralateral teeth.

1.1.4.1 Bilateral Symmetry in Premolars

Ludwig [65] identified seven distinct morphological traits that included 19 aspects of the mandibular second premolar. These traits were used by Wood and Green [66] in their study of second premolar morphologic trait similarities in twins to see if they could be used to determine whether twin pairs were mono- or dizygotic. This study has been erroneously cited as evidence for contralateral premolars being almost anatomically identical [58] and that their similarity would remove confounding factors such as root canal anatomy or dentin structure. Unfortunately, Wood and Green only made homolateral (*i.e.* left premolar from twin “A” compared to left premolar from twin “B”) and heterolateral (*i.e.* left premolar from twin “A” compared to right premolar from twin “B”) premolar comparisons, but, as seen in **figure 4** their schematic this is easily misunderstood:

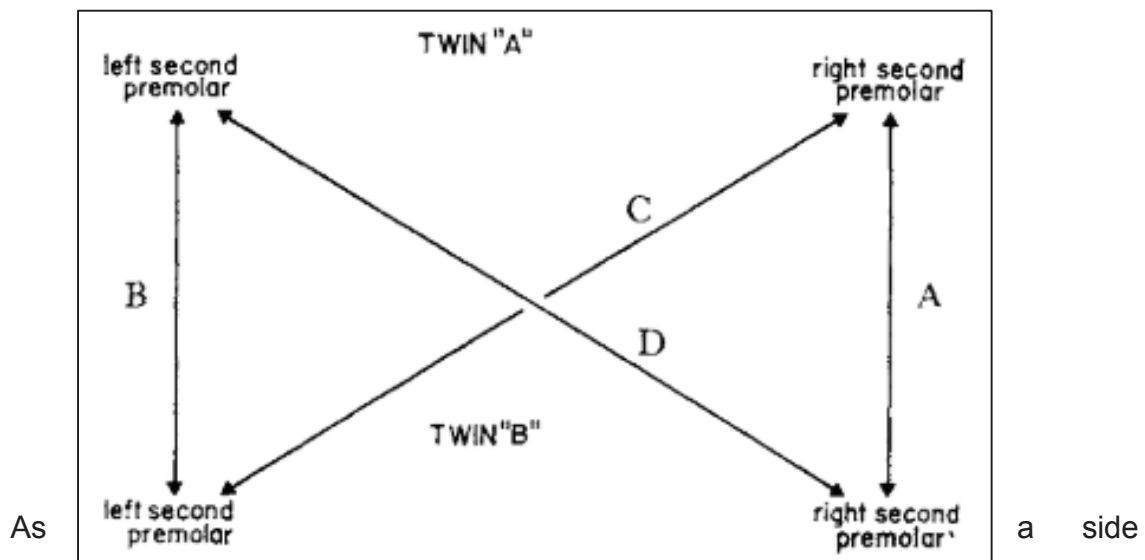


Figure 4. Schematic depicting the intra-pair comparisons done by Wood and Green, 1969. Note how no comparisons within each twin were made.

note, high homolateral concordance (similarity) was positively correlated with monozygosity and was in close agreement with the serologic diagnosis. In other words, a finding of homolateral premolars with high degrees of similarity had a higher chance belonging to identical twins. Their findings of occlusal topology having less variability in identical twins versus fraternal twins has been confirmed in two three-dimensional geometric morphometric studies [67, 68]. Townsend *et al.* speculate that since less asymmetry (both directional and fluctuating) was reported in identical and fraternal twins compared with singletons according to findings made by Boklage, “*there may be something special about the twinning process [69, 70].*”

1.2 Premolars

Paired and matched premolars have been suggested as being a suitable substrate for comparison studies due to their availability and potential to create well-balanced experimental groups [64, 71].

1.2.1 Availability of Premolars

The proportion of children receiving orthodontic treatment in Norway has historically been approximately 30% out of every birth cohort. Overbites and the combination of crowding in the maxilla and mandible are the most common treated malocclusions [72]. In 2017 the Norwegian birth cohort consisted of 56 633 babies [73]. The extraction of premolars to treat crowding and overbites is commonplace, and the access to contralateral premolars as substrates for endodontic comparison studies seems plentiful.

1.2.3 Techniques to Investigate Root Canal Morphology

The root canals' multifarious morphologies, intriguing intricacies, enchanting enigmas, reclusive recesses, twisting tortuosities, and cavernous complexities have always fascinated students of dental anatomy. The founder of the Brooklyn Endodontic Study

Club, inventor of the endodontic explorer DG-16 [74] and root canal anatomist Dr. David Green, stated that “(o)f all the phases of anatomic study in the human system one of the most complex is that of pulp cavity morphology [75].”

Without a thorough and complete appreciation of the normal and abnormal anatomy that is hidden within the tooth, the dental operator cannot be expected to provide state-of-the-art care. It is thanks to researchers like Dr. David Green that endodontic exploration has evolved from the simple sectioning and grinding studies to the complex and visually stunning three-dimensional elucidations of today. The wonderful history of investigating the internal anatomy of teeth deserves a synopsis, and the following is an attempt at presenting its evolution. This brief history of endodontic exploration is by no means exhaustive. It merely presents some of the more important landmark studies.

The first comprehensive and systematic description of root canal anatomy was published by Georg Carabelli in 1844 [76]. The earliest internal investigations were conducted by sectioning teeth in all planes and detailing the anatomy with both measurement data and meticulous illustrations as seen in the works by G.V. Black and E. Mühlreiter [77, 78]. The first to use another technique besides sectioning and grinding was probably Gustav Preiswerk who employed a method he called corrosion technique. He poured molten Wood's metal into the pulp chamber and root canal system before softening of the tooth with *liquor potassae* (a caustic solution) for easy removal of metallic casts [79]. These casts were often incomplete, as the metal could not flow into the finer wefts of the root canal system. In 1907, inspired by Preiswerk, Fischer obtained stunning, though fragile, results by immersing teeth in celluloid-in-acetone solutions before decalcification with hydrochloric acid [80]. He was able to demonstrate the finer details of the root canal systems ramifications and his renditions of the apical delta are quite stunning. Hess made a further improvement by injecting vulcanized rubber prior to decalcification [81], and his excellent vulcanite preparations and impressive illustrations are still valuable to the study of root canal anatomy today. Nevertheless, Hess and his predecessors failed to portray the relation of the canals to the tooth as a whole. The methods described so far also all resulted in the complete destruction of the surrounding tooth substance

Werner Spalteholz introduced his clearing technique (diaphanization) in 1911 for visualization of internal structures of anatomical specimens [82]. Investigators of internal dental anatomy finally had a non-invasive method to render dental tissue translucent. By injecting the *pulp cavity* with either molten metal like P. Adloff did in 1913 or Indian ink as introduced by H. Moral in 1914, it was now finally possible to study the pulp cavity in relation to the outer anatomy [83-85]. These two revolutionary methods did, however, have their shortcomings [86]. The first technique had the potential to produce artifacts and cracks from the molten metal. Also, the molten metal would not penetrate the finer minutia of the root canal system. The India ink does have the ability to penetrate the intricate anastomoses, but the ink would also diffuse into dentinal tubules and obscure the periphery of the canals.

Okumura presented a new classification for root canals from his extensive study of 2148 teeth in 1927 using the technique of dyes and diaphanization [87]. Many have

unfortunately overlooked his studies as they were first published in Japanese. Seeling and Gillis presented in 1973 a simplified method in which the dentin and cementum are made transparent and the pulp tissue is stained dark blue [88]. This technique was refined and utilized (decalcification in hydrochloric acid, placed in potassium-hydroxide solution, Hematoxylin staining of pulp tissue and clearing of teeth using a crystal-clear liquid plastic casting resin after dehydration in alcohol) both by Vertucci *et al.* and by Gulabivala *et al.* in their seminal studies of permanent teeth [87, 89-91]. The canal staining and clearing technique eventually became the gold standard method of studying root canal anatomy [92].

Two-dimensional x-ray has also been used alone and as a supplement to the aforementioned techniques to provide as demonstrated in Augustus Henry Mueller's impressive master thesis from 1932, which was a radiographic study on 1394 incisors, cuspids, and bicuspid [93]. His introduction gives an excellent overview of the investigations of root canal anatomy leading up to his study. However, this method yields an unreliable interpretation of a three-dimensional reality. This would only be attainable when combining computerized methods with radiography.

The first studies attempting to introduce a CAT methodology for three-dimensional imaging of the root canal were carried out in the mid-1980s. Mayo & Montgomery [94] were inspired by non-invasive CAT scan technology, when they injected contrast medium into the root canal system of nine extracted single-rooted permanent human premolars before taking radiographs from several known angles. A computerized digital image-processing program evaluated these radiographs and they were able to calculate the root canals' volume and diameter. Next, they compared their findings with the actual volume and diameter from physical cross-sections. The diameter of the root canal was found to be very accurate (within 1 mm of actual measurements), while the volume was significantly different. The volumetric discrepancy was probably due to voids in the contrast medium. Furthermore, the methodology required trephination and flattening of the occlusal surface prior to injection of contrast medium. Nevertheless, this study showed the promise of CAT and was improved upon the following year using xeroradiography, which yielded superior edge enhancement and enhanced detail when compared with conventional radiographs [95]. Their hope was that future studies would employ the methodology in order to study root canal morphology before and after instrumentation.

The first studies to utilize computerized methodology for this very purpose was Berutti [96]. In 1993 he used microphotographs of five root canal sections from cross-sectioned mesial roots of mandibular molars for superimposition of the root canal before and after instrumentation. Berutti did not include cross-sections of the apical portion like Blašković-Šubat *et al.* did in their study [97]. It provided more detail, but this was also a destructive technique. These two aforementioned studies were in many ways only an elaborate extension of the sectioning and grinding studies of G.V. Black and E. Mühlreiter [77, 78] in the sense that they were destructive and ultimately did not yield sufficient detail of the anatomy. Despite this criticism, at the time they must have provided much incentive and motivation for other dental scientists finding themselves at the dawn of the dental digital age.

The potential of non-destructive, computerized, three-dimensional radiographic technique to the field of endodontics was first explored by Tachibana and Matsumoto [98] in 1990. It was not until the invention of microscopic computed tomography (micro-CT) that the field of endodontic exploration was revolutionized. Much of the work done the first pioneers still give insight to both untrained students and seasoned endodontists alike. Nevertheless, it is interesting to note that none of them were concerned with the presence or absence of bilateral symmetry in normal root canal anatomy.

1.2.4 Symmetry of Dental Anomalies/Aberrations

Despite the lack of studies on the expected anatomy in bilateral teeth, reports on bilateral symmetry of unexpected and aberrant root canal morphology have not been scant in the dental scientific literature [99-109]. However, most of these studies have been on single incidences of bilateral anomalies. The first systematic large scale study of the occurrence of bilateral internal dental aberrations was not undertaken until 1994 [110]. Sabala *et al.* scrutinized a large radiographic material consisting full-mouth series from 501 patients and found 100% bilaterality for rare abnormalities (they classified rare as an anomaly occurring less than 1% in their sample). Overall, they discovered that 60.2% of the aberrations they evaluated (multiple canals, extra roots, fused roots, and atypical shapes or appearances of pulp chambers) occurred with bilaterality. The tooth type with the highest incidence of aberration was the mandibular first premolar (22.8% had a bifurcation of root/canal with 60% bilaterality). Their findings were admittedly limited by being two-dimensional, but their results serve as a reminder that exact matching symmetry is not a default condition in teeth.

The fact that the mandibular first premolar showed the highest incidence of aberrations concurs with previous findings made by Slowey [111]. Slowey, in fact, referred to them as endodontic enigmas. However, this is contrariwise to idea of morphogenetic fields (field theory) in which a “pole” or “key” teeth contribute most to the size and shape of each tooth class (incisors, canines, premolars and molars) (66). The “pole” or “key” teeth show less asymmetry, variation in size and morphology, and are “never” missing due to agenesis. The mandibular pole teeth include the lateral incisor, canine, first premolar, and first molar [70]. The vast variability within the tooth types demonstrated by Slowey (and by the many researchers before and after) clearly show the need for screening and matching of teeth that are to be used in comparative endodontic studies.

Kirthiga *et al.* [112] conducted a descriptive cross-sectional survey among 2111 children to identify twelve morphological features in mixed dentition of 6-10 year old children in Bengaluru city, India. The combined mean (standard deviation) prevalence of symmetry of features was 97.44% (5.56) with a range of 81.4% to 100%. The features were recorded a present or absent, and the study fails to provide any two- or three-dimensional geometric morphometric data. Nevertheless, it supports the idea that bilateral structures are under identical genotypic control.

1.3 On the Importance of Knowing Symmetry in Dentistry

1.3.1 Dental Anthropology

It is common practice for the experienced clinician to use the occlusal pattern and morphology of an intact contralateral tooth as a reference template when restoring its antimere. This is based on both subjective experience and the anecdotal evidence that the occlusal morphology of contralateral teeth is close to identical. This anecdotal evidence and conjecture regarding occlusal matching symmetry made when performing restorative dentistry is not without scientific merit.

Dental anthropology, a subfield of biological anthropology, is the study of the development, eruption, number, size, morphology, modification, wear, and pathology of teeth, among other topics, in order to answer questions like how individuals and populations are related, what pre-historic humans' diet consisted of, and what their general health status was like [113]. According to Diaz *et al.* [114], the analysis of dental morphology by anthropologists strives to understand how so-called Tooth Crown Morphological Traits present in frequency, sexual dimorphism, and bilateral symmetry in order to answer the aforementioned questions as well as give insight in biology, anthropology, dentistry, paleopathology, archeology, and forensic science.

There is according to dental anthropology a high degree of symmetry in dental morphological and geometric traits [115] and the bilaterality of these traits are analyzed when studying the dentition of a given population [20, 114, 116]. Scott *et al.* elucidate that the overall symmetry rates based on the presence or absence of morphological traits fail in the range of 85-95%, but that it is lowered to 50-80% when all forms of asymmetry are considered [115]. This range is due to the varying findings among different populations with regard to fluctuating symmetry, which has been extensively studied in the field of dental anthropology and is believed to increase with inbreeding, deleterious environmental challenges, and in certain genetic disorders [70].

1.3.3 Endodontics

The need for endodontic treatment of contralateral teeth is commonplace. It is of great clinical importance to ascertain if bilateral homonymous teeth are symmetrical in number of roots and root canal configuration/morphology. The use of cone beam computed tomography (CBCT) has made it possible for three-dimensional analysis of dental morphology.

Plotino *et al.* [117] completed the very first *in vivo* CBCT study (Field-of-View (FOV): 15x15cm) evaluating the symmetry of root and root canal morphology of 596 maxillary and mandibular molars in 201 Caucasian (Rome, Italy) men and women in 2013. They noted that there was no previously available data concerning the symmetry of teeth in the endodontic literature even though this information would serve as being highly clinically relevant when treating contralateral teeth. The study evaluated contralateral molars' symmetry according to number of roots and configuration of root canal system according to the Vertucci classification. Exact matching symmetry for the chosen parameters varied from 70%-81%, and they noted that the first mandibular and maxillary molars exhibited

the greatest degree of asymmetry. The clinical relevance is apparent, as missed anatomy in endodontics can be the root cause of clinical failure [118]. Furthermore, it accentuates the need for screening and matching of contralateral teeth destined for *ex vivo* comparative studies as asserted by Xu *et al.* [71] in their CBCT screening proposal for using contralateral premolars for creating balanced experimental groups.

The external and internal morphology of teeth varies according to ethnicity with respect to prevalence of number of roots (*i.e.* radix para-entomolaris in mandibular molars among Inuit populations [119, 120]), shape of *pulp cavity* (*i.e.* C-shape prevalence in Chinese second mandibular molars [121]), and even crown morphology (*i.e.* shoveling in Pima Indians [122]). The fact that anatomical features are not homogenous from one race/ethnicity to the next has led others to investigate the degree of symmetry among different populations. Felsypremila *et al.* [123] examined CBCT scans (FOV: 18x20cm) from 246 patients (3015 teeth) in an Indian subpopulation (Chennai, Tamil Nadu) and evaluated the degree of symmetry in number of roots and morphology when the patient had contralateral teeth according to the Vertucci classification for maxillary and mandibular premolars and molars. They found a percentage of symmetry that varied from 70%-98%, with premolars in ascending order showing the greatest degree of symmetry: maxillary first and second (81.5%), mandibular first (96.1%), and mandibular second (98.3%). Contrariwise, to the findings made by Plotino *et al.* [117], the first maxillary and mandibular molars were more symmetrical than the second molars in both arches.

Table 1 details the symmetry for bilateral homonymous teeth [124-134] on different populations along with the two aforementioned studies. The overall finding from these studies should prompt clinicians to use information from contralateral teeth when considering the expected anatomy/morphology when this data is available.

Table 1. CBCT investigations on different populations with relation to bilateral symmetry for various variables.

STUDY (Authors, year)	ETHNICITY	CBCT BRAND	FOV (cm)	VOXEL SIZE (mm)	VARIABLES	CONTRALATERAL TEETH (n)	SYMMETRY (%)
Felsypremila <i>et al.</i> , 2015 [123]	Indian	Kodak 9500 cone beam 3D (Carestream Health Inc., Rochester, NY)	18x20	-	Number of Roots & Number of Root Canals	Maxillary First Premolar (195)	81.5
						Maxillary Second Premolar (184)	81.5
						Mandibular First Premolar (205)	96.1
						Mandibular Second Premolar (176)	96.3
						Maxillary First Molar (160)	77.5
Plotino <i>et al.</i> , 2013 [117]	Italian	NewTom VGi Vertical Cone Beam (NewTom, Verona, Italy)	15x15	-	Vertucci Root Classification & Number of Root Canals	Maxillary First Molar (45)	71
						Maxillary Second Molar (54)	79.6
						Mandibular First Molar (34)	70.6
						Mandibular Second Molar (54)	81
						Maxillary First and Second Molars (90)	84
Zhang <i>et al.</i> , 2011 [124]	Chinese	3D Accuitomo scanner (Morita, Kyoto, Japan)	4x4 or 6x6	0.125	Vertucci Root Classification & Number of Root Canals	Maxillary First and Second Molars (90)	84
Lin <i>et al.</i> , 2014 [128]	Chinese	NewTom VG scanner (QR srl, Verona, Italy)	-	0.20	Vertucci Root Classification & Number of Root Canals	Mandibular Central Incisors (706)	92.7
						Mandibular Lateral Incisors (706)	89.2
Tian <i>et al.</i> , 2012 [126]	Chinese	3D Accuitomo scanner (Morita, Kyoto, Japan)	-	0.125	Vertucci Root Classification & Number of Root Canals	Mandibular Central Incisors (706)	95.2
						Mandibular Lateral Incisors (706)	93.8
Tian <i>et al.</i> , 2016 [132]	Chinese	NewTom VG, QR srl, (Verona, Italy)	20x25	0.160	Number of Root Canals	Maxillary First Premolar (69)	64
Kayaoglu <i>et al.</i> , 2015 [129]	Turkish	Promax 3D unit (Planmeca, Helsinki, Finland)	8x8	0.160	Number of Roots	MB Root Maxillary First Molar (724)	79
						MB Root Maxillary Second Molar (458)	82.3
						Mandibular Central Incisors (973)	100
Guo <i>et al.</i> , 2014 [127]	5 North American ethnic groups	Sirona Galileos (Sirona Dental Systems, Inc, Long Island City, NY)	15x15	0.30/0.15	Vertucci Root Classification & Number of Roots MB2 Occurrence	Mandibular Lateral Incisors (1008)	100
						Mandibular Canines (1019)	100
						Mandibular Central Incisors (973)	94.8
						Mandibular Lateral Incisors (1008)	89.8
						Mandibular Canines (1019)	93.3
Huang <i>et al.</i> , 2015 [130]	Taiwanese	i-CAT (TM Imaging Sciences International, Hatfield, PA, USA)	-	0.250	Vertucci Root Classification & Number of Roots	MB root in Maxillary First Molars (317)	97.5
Kim <i>et al.</i> , 2012 [125]	Korean	Dinnova system (Willmed, Gwangmyeong, Korea)	10x10	0.167	Number of Root Canals	Maxillary First Molars (317)	98.1
						MB root in Maxillary First Molars (317)	65.6
Kim <i>et al.</i> , 2016 [131]	Korean	Dinnova system (Willmed, Gwangmyeong, Korea)	10x10	0.167	C-shape	Mandibular First Premolar (122)	81.3
						MB Root Maxillary First Molar (395)	88.10
Ratanajirasut <i>et al.</i> , 2018 [133]	Thai	3D Accuitomo CBCT machine (J Morita Manufacturing Corp, Kyoto, Japan)	10x10	0.250	MB2 Occurrence	MB Root Maxillary Second Molar (318)	82.07
						Mandibular Second Molar (453)	70
Shemesh <i>et al.</i> , 2018 [134]	Israeli	Asahi Alich (Alich series; Asahi Roentgen IND, Kyoto, Japan)	8x8	0.155	Vertucci Root Classification	MB Root Maxillary First Molar (215)	80.93
						MB Root Maxillary Second Molar (179)	82.59
						Central Mandibular Incisors (1472)	-70
						Lateral Mandibular Incisors (1508)	

1.4 Endodontic Challenges

Endodontics is the field of dentistry concerned with the morphological, physiological, and pathological aspects of the human dental pulp and periradicular tissues [135]. It is imperative for dentists to have a working knowledge of the possible complexities and irregularities in anatomy of any tooth destined for Root Canal Treatment (RCT). Understanding both irregular and regular morphology/anatomy is fundamental to planning, performing, and the prognosis of successful RCT [136](132). Failing to locate and/or completely biomechanically clean (irrigate) and obturate all canals is a root cause not achieving a successful prognosis of RCT and ultimately endodontic treatment failure [118, 137]. The purpose of RCT is ultimately preventing and treating apical periodontitis through chemo-mechanical instrumentation by preparing the root canal for obturation with a root canal material of choice before sealing with a coronal restoration [138]. Pathogenic ingress through these barriers will lead to (re)infection and failure [139].

Despite the many challenges (persistence of bacteria, inadequate filling of the canal, overextensions of root filling materials, improper coronal seal, untreated canals, and iatrogenic procedural errors) that can prove deleterious to the endodontic prognosis when preventing or treating apical periodontitis, RCT has enjoyed a relatively high rate of success regardless of the outcome measures [140-147]. The very nature of endodontic treatment is a pursuit of perfection judged and predicted with great accuracy from the final radiograph. The esteemed Professor Dag Solmund Ørstavik states succinctly, *“Endodontics will be successful and joyful by producing a final result in the form of a radiographically “perfect” root canal filling, which confirms the quality of the preceding endodontic work [148].”*

Striving for perfection has permeated all aspects of the endodontic discipline and has led to an everlasting endeavor of developing advances in areas such as techniques, instruments, and obturation materials that might improve upon the already high long-term prognosis of RCT.

1.4.1 Evaluation of Endodontic Techniques and Materials

1.4.1.1 Instrumentation

The body of work relating to the variations of the unprepared root canal anatomy is vast and the exploration of this literature in **Chapter 1.2.3** is certainly not exhaustive. It would take over 100 years after Carabelli's first systematic study [76] of root canal anatomy before the first studies on the prepared root canal appeared in the literature. The first mention of histological studies on prepared root canals appeared in a 1928 review. E.H. Hatton listed three primary reasons for failure of root canal treatment: firstly, insufficiently cleaned root canals; secondly, fillings short of the apex; and thirdly, that the diameter of the filling material is considerably less than the diameter of the pulp canal (this was considered most serious) [149]. He stated that, *“The canals are very superficially cleansed and much of the pulp tissue is not removed. It is probably true that all the pulp tissue cannot be removed until the shape, course, and diameter of the canals are modified*

by filing and curetments. Yet the efforts of the operators to remove the pulps, as observed in treated teeth, are frequently pitifully inadequate." His findings are based on histological findings on extracted failed root treated teeth in studies from USA, Switzerland, France, Austria, and elsewhere. It is unclear where any of the renditions of histological sections are taken from, except for one, which is a section typifying "a very poorly treated and filled root canal" by the oral histologist William G. Skillen. Romelli *et al.* [150] reconfirmed the general findings of insufficient debridement of pulpal tissue in instrumented root canals.

In 1968, two studies evaluated the effect mechanical instrumentation had on the morphology of the root canal [151, 152]. Haga [151] instrumented 161 root canals and made two cross sectional cuts at 2 mm and 6 mm from the tip and found in the measuring microscope a high percentage of inadequate preparations (75-81.3%) in all of the categories of canals except the maxillary central incisors. Inadequate preparation was defined as failure to remove voids and irregularities and was in general always greater at the 6 mm level than at the 2 mm level. Gutierrez and Garcia [152] inspected rubber molds of the internal anatomy in a microscope at magnifications of up to 40x after instrumentation of 120 extracted maxillary incisors and canines. After cleaving the teeth in twain, they found that that the 78.33% of the incisors' and 85% of the canines' root canals had "*been badly negotiated*" and that the "*lack of regularity was due to the presence of prolongations, very much like fins of a fish (...).*"

Davis *et al.* [153] confirmed the finding of untouched irregularities (lateral canals, fins, webbings, and irregularly shaped foramina) in their beautifully detailed silicone models of the post-debridement canal anatomy of 217 teeth after dissolution of tooth substance with 5% nitric acid. Much like the earliest studies on root canal anatomy, the first evaluations of instrumentation were destructive in nature. Furthermore, even when they started applying modern computer-assisted tomography [94] they only considered the morphology and root canal walls post-instrumentation, which made it impossible to precisely quantify the instruments ability to shape the canals.

Bramante et al. [154] acknowledged the lack of methods allowing for accurate comparison of pre- and post-instrumented canals. They devised a reassembly setup where teeth were sectioned at three different levels before instrumentation, removed, and the profile of the root canal was traced from a projection of the transparency of each section. The sections were positioned back into the jig, the teeth were instrumented, before removal and tracing of the instrumented canals. Though crude and two-dimensional when compared to modern techniques, the methodology allowed for statistical analysis and calculation of changes in area from pre- to post-instrumentation.

Berutti [96] was inspired by the aforementioned setup and elaborated upon it by conducting computerized analysis of the first five apical millimeters below the bifurcation of mesial roots from first permanent mandibular molars. Microphotograph outlines of five cross-sections (pre- and post-instrumentation) per root were digitized and it was possible to superimpose the models graphically for three-dimensional visual inspection. Furthermore, it was possible to acquire metric measurements and data for both volumes and surfaces. Even if the experiment did not include information regarding the apical

portions and was destructive in nature, it certainly gave a glimpse into what the future had in store for endodontic research in terms of computer-aided tomography.

McComb and Smith [155] were the first to describe the smear layer in instrumented root canals with SEM, and since their pioneer study, the use of SEM has provided much insight into the effects of instrumentation and chelation. However, there has been a lack of reproducibility and standardization in these studies. The attempt to correlate presence or absence of smear layer with sealability has been described as “pointless” [64]. Among other shortcomings in these types of studies, the effect of root canal anatomy and differences in dentin physiology (sclerotic and irregular secondary dentin) have not been accounted for [156].

The use of micro-CT in endodontic research revolutionized the field allowing for the non-destructive comparison of pre- versus post-instrumentation data such as debris accumulation, anatomy (morphology, transportation, centering ability, SMI), changes in volume, and surface, from different types of instruments and kinematics [157-163].

Finally, a recent paper [164] integrated histology, SEM, and micro-CT into a correlative analysis in order to evaluate the untouched surfaces of the same root canals after instrumentation and irrigation. Innovative well-conceived studies, like this one, that integrate the best of different techniques like this give valuable insights into the effects that our armamentarium have on the hard tissue, soft tissue, and the biofilm.

1.4.1.2 Obturation

One-hundred years ago, one of the most infamous proponents of extractions in lieu of endodontics and the Focal Infection Theory (*oral sepsis*) [165], Dr. Weston A. Price, presented probably the first report on the physical properties of root filling materials (mainly gutta-percha) and root fillings ability to hinder bacterial infection of sterilized teeth [166]. The main conclusions on the physical properties, and the root fillings' ability to seal off the extracted teeth from infection [166], was that “(w)e are using materials which do not have the properties that our needs require” and “(e)xhaustive researches should be made to develop adequate root filling materials.” Furthermore, he concluded that the apparent initial success of root canal therapy must be due to what he called “an apparently tolerant nature” and the inevitable failure of the root fillings is attributed to the contraction of the materials leading to leakage and ingress of bacteria.

The following 100 years have seen a plethora of materials for obturation, but even more so, an inexhaustible production of testing methods for evaluating endodontic filling materials. The other work of Price on rabbits and case reports of improvements of medical conditions have been discredited due to the eventual dismissal of Focal Infection Theory and his research not meeting the stringent standards of modern dental research [167].

The “Washington Study” [168, 169] found that poorly performed obturation was responsible for 58.66% of endodontic failures, which was misconstrued to mean that the obturation itself was responsible for success or failure. There are, indeed, studies that have shown resolution and healing of apical periodontitis without obturation [170, 171], but these do not by any means disprove the importance of an impregnable root canal seal.

Cleaning or shaping together with the obturation complete the classical triad in endodontic treatment [172], and modern endodontics now place the emphasis on the biomechanical cleaning and shaping steps. The American Association of Endodontists (AAE) states the following in one of its pamphlets [173]: “*what you take out of a root canal may be more important than what you put in*”, which echoes the similar statement made by Eberly in 1898.

The AAE statement encompasses the paradigm shift in endodontics from performing root canals in order to simply fill dead spaces (Hollow Tube Theory) in the 1930s [174, 175] to the treatment or prevention of periapical infection. The Hollow Tube Theory has since been debunked and apical periodontitis is considered a microbiological challenge [176-179]. The statement, however, does not mitigate the value of a technically well performed root canal judged radiographically. It is important to keep in mind the prognostic value of a good quality root filling with satisfactory lengths [180, 181] as these two parameters have been associated with the absence of periapical lesions in epidemiological studies [182, 183]. Ray & Trope [184] showed that the quality of the coronal restoration was more important for the periapical health than the technical quality of the endodontic treatment (obturation). This was challenged by the findings made in the duplicate study by Tronstad *et al.* [185] who also found that a good coronal restoration in combination with good endodontic quality is important, but poor obturation resulted in a poor outcome regardless of the quality of the coronal restoration.

The interest in assessing the quality of the root canal in terms of deficits (voids) and leakage has therefore been of great interest to the endodontic research community since the possibly the first one conducted by Weston A. Price [166]. Brayton *et al.* [186] echoed the concerns of Price stating that “*(...) gutta-percha placed in a root canal by the lateral condensation technique [with standard root canal sealer] is inadequate as a filling*” when evaluating root fillings after teeth were decalcified and dissolved away. Their group from Tufts University School of Dental Medicine conducted a series of studies on conventional and experimental root canal materials [186-191], which was prompted by the lack of success-and-failure studies providing insight into the role of the various root canal filling materials effect on the outcome of root canal treatment and their ability to seal off the root canal. Their studies on lateral condensation technique with gutta-percha [186, 188] found a lack of correlation with the radiographs, the fillings showed voids, irregularities, and did not reveal root canal variations as demonstrated in their in morphological study of instrumented root canals [153].

A follow-up study [187] compared the results from lateral condensation technique with models of Kloroperka and Chloropercha after decalcification and dissolution with nitric acid [153]. They found more homogeneity and better replication of root canal anatomy in both these two chloroform-based techniques than in models from lateral condensation technique. The Kloroperka technique used a master gutta-percha cone which fitted 2 mm short of the apex. Chloroform was added to Kloroperka powder (19.6%, rosin 11.8%, gutta-percha 19.6%, zinc oxide 49.0%) to make a thick creamy mix. The cone was dipped into the Kloroperka mixture and is inserted into the canal. Successive cones were added in

the same manner with firm pressure using spreaders or pluggers until the canal was completely obturated. In the Chloropercha technique, a master cone was also fitted 2 mm short of the apex. Next, gutta-percha was dissolved in chloroform to make a creamy mix. The fitted cone was dipped into the mix and placed in the canal. Subsequent cones were added with very firm pressure from root canal pluggers until the canal was obturated. Chloropercha was deemed better than Kloroperka but concerns about contraction/shrinkage and porosity were raised. Their conclusion regarding lack of conformity to root canal regularities and shrinkage resulted in the histological study of three experimental root canal materials; root filling consisting of silicone elastomer and adhesive (Silastic 382 elastomer and Silastic Medical Adhesive type A) or a pure poly-hydroxy-ethyl-methacrylate root filling (Hydron, Hydron Technologies, FL, USA) (185). The *in vitro* & *in vivo* preliminary findings for Hydron were very promising [192-194], but a subsequent long-term study showed poorer results with Hydron versus gutta-percha and AH-26 [195]. Furthermore, other independent studies on histological responses and leakage found that Hydron did not fulfill the manufactures promises concerning physical/clinical properties as it elicited severe inflammatory responses, demonstrated more leakage than conventional root filling materials, and was resorbable [196-198].

The search for advanced root filling materials that complete the quest for three-dimensional obturation and the creation of a monoblock [199] seemed possible with the polymer based Resilon core material and methacrylate based sealer RealSeal/SE [200-203]. However, like the story of the hopeful but hapless Hydron, the once promising revolutionary Resilon was recently found to be 5.7 times more likely to fail than teeth filled with gutta-percha and AH Plus sealer in a long- term clinical outcome study with a retrospective case-control design [204].

Former methods to evaluate obturation were destructive and invasive in nature. Micro-CT technique has become the common non-destructive method used to evaluate root fillings materials in terms of voids and ability to obturate root canals three-dimensionally [205-208].

2. Aims of the Research and Hypothesis

2.1 Aims

The overall objective of this thesis was to develop a valid and reliable *in silico* methodology for *ex vivo* endodontic comparative studies using contralateral premolars. An additional purpose was to provide a greater insight into the anatomy and morphology of the *pulp cavity* of contralateral premolars. The working hypothesis was that contralateral premolars are anatomically identical, and the primary aim was to provide insight into their degree of similarity and matching symmetry by:

- Qualitatively and quantitatively describing and comparing the similarity of the anatomy/morphology of contralateral premolars' *pulp cavity* in terms of shape deviation analysis (SDA) and simple morphometric geometric parameters (**Study I**).
- Assess and compare the morphology of contralateral premolars' *pulp cavity* in terms of anatomic characteristics such as length, canal width, dentinal thicknesses, accessory canals, root canal configurations, isthmi, C-shapes, root canal orifices, and apical foramina (**Study II**).

The secondary aim was to use micro-CT technology and metrology software to validate the use of contralateral premolars in endodontic comparison studies by comparing their *root canal systems* before and after canal instrumentation with one instrumentation system. Furthermore, to determine whether contralateral premolar will yield non-significantly different outcomes regarding shaping ability (volume), degree of twisting and three-dimensional shape changes (**Study III**).

2.2 Hypothesis

The overall hypothesis was that using screened and matched contralateral premolars would yield non-significant results in a comparative endodontic study using the same biomechanical instrumentation system, and thereby providing a model and standard for endodontic comparative studies.

3. Methodological Considerations

3.1 Background to Micro-CT

Conventional radiographs (*i.e.* periapical radiograph) are two-dimensional, direct (no reconstruction; immediate conversion to grey-scales), and exhibit spatial summation. The ability to acquire multi-planar reconstructions (three-dimensional images) of the internal structure of an object (*i.e.* jaw or tooth) probably represents the single most important dental diagnostic developmental step in the evolution of oral radiology since the first dental radiograph by Otto Walkhoff in 1896.

The slice-by-slice internal view and translation in any plane along any axis of an object would not be possible without the complicated mathematical algorithms for reconstruction of that object through a technique first known as computerized axial tomography (CAT) or now simply CT. The original tomographic techniques were based on axial one-dimensional direct imaging (*i.e.* panoramic) or two-dimensional reconstructions from for example fan beam CT. Today, CBCT has allowed for true three-dimensional reconstruction from a grey-scale cloud (three-dimensional dataset). Tomography is a Greek compound from the words “τόμος *tomos* (slice, cutting, sharp)” and “γράφω *graphō*” (representation by means of lines, writing) [209].

The underlying principle for any radiographic technique is based on the interaction between ionizing radiation and matter. The x-rays from the source transverses the object of study and within the object, the intensity of the x-ray is weakened (attenuated). The attenuation is due to reduction in beam intensity both by absorption (photoelectric) and deflection (scattering). The attenuated ionizing radiation is detected by a sensor (11 Megapixel (4000x2300) 12-bit digital charge coupled device (CCD)-camera coupled to scintillator (converts x-rays into visible light) in the Skyscan 1172) or phosphor plate. Both the CT and CBCT reconstructions utilize the Beer Lambert Law ($I = I_0 \cdot e^{-\mu x}$), where I is the detected X-ray intensity at a detector pixel after passing through an object of thickness x , I_0 is the incident X-ray intensity at the same pixel, and μ is the attenuation coefficient of the specimen's material. This is what is called attenuation-based scanning, and the scanning software uses this relation to generate a quantifiable shadowgraph [210]. This CT number is proportional to the degree to which the material within the voxel has attenuated the x-ray beam. It represents the absorption (photoelectric), or linear attenuation coefficient, of that particular volume in the object of study. The degree of photoelectric interaction varies directly with the third power of the atomic number of the absorber, and it is this difference in absorption that makes it possible to produce any radiographic image [211].

The mathematical basis for the CT technique is based on a 1917 mathematical relation known as the *Radon transform* (the inverse Radon transform is applied for CT), which in short proves that an n-dimensional object can be reconstructed from its (n-1)-dimensional projections [212]. The mathematical principle of the *Radon transform* allows us to reconstruct any point along an ideal line. In radiology, this ideal line is the X-ray and with the inverse *Radon transform*, we can reconstruct any grey-scale along this X-ray.

The result is an image from one-dimensional projections seen as two-dimensional axial slices composed of distinct grey-scale pixels.

The mathematical basis presented by Cormack in 1964 and 1965 [213, 214] laid the foundation for cross-sectional imaging reconstruction in the CT scanner. They also implemented the mathematics that show that a function can be reconstructed from values of its line integrals [215]. The CT scanner was invented by Hounsfield [216], and the first clinical machine was installed at the Atkinson Morley Hospital in Wimbledon in 1971 [217]. In the case of CBCT (the X-ray bundle has a cone shaped geometry), the volumetric reconstruction process is accomplished through the so-called back-projection algorithm method of the attenuation coefficients using the *Feldkamp algorithm* [218]. The mathematical principle behind the reconstruction is different from the *Radon transform*, as the *Feldkamp algorithm* allows for the reconstruction of, for example, teeth, into a grey-scale cloud. The results of this imaging process is a three-dimensional volumetric dataset consisting of voxels (volumetric pixels). This radiographic technique allows for the multi-planar non-destructive internal inspection and computation of a volume. The CBCT has many clinical applications including: medical, industrial, and research.

Micro-CT in biological applications and materials testing had been around since the 1960s, when Elliott and Dowker published their paper on the investigation of a carious lesion in enamel. Their paper contained both contour maps and images with half-tones along with the possibility of quantitative data [219]. The apparatus from their first paper was modified with an axis to rotate the specimen and used again in a follow-up paper in 1982 [220]. Even if the paper only presented a two-dimensional slice of a tropical freshwater snail, the resolution of 15 μm was revolutionary. This was the first suggestion of micro-CT ("X-ray micro-tomography) based on the principles of CAT and served as a major stepping-stone into the modern world of micro-CT technology. Present day micro-CT technology has the ability to collect multiple adjoining slices of volumetric data simultaneously. The technology evolved rapidly and resolutions of better than 10 μm were soon attainable along with the generation of 3D tomographic images [215, 221]. Today, resolutions in the nano-resolution (submicron) region are attainable.

The endodontic research community quickly realized the potential of CT-technology already in the 1980s as a means of non-destructively and non-invasively studying the internal anatomy of teeth. However, the first CT scanners with slice widths of 2 mm did not offer fine enough resolutions for detailed study (94). The invention of the CBCT machine NewTom-9000 in 1998 allowed for resolutions down to 0.3 mm voxel size [222], and today small FOVs in modern CBCTs can offer <0.1mm voxel size [223]. The effective spatial resolution in CBCT devices is always lower than the published resolutions. This is due to the inevitable influences of patient movement (motion blur) and scatter effects. In clinical/practical applications, this means that one cannot expect higher accuracy than 0.5 mm [224]. It is important to make the distinction between the terms destructive and invasive. Although, micro-CT is a non-destructive technique it is invasive when it comes to the study of human dental anatomy. This is because the studies using micro-CT are on extracted teeth (*ex vivo*).

The seminal study by Nielsen *et. al* in 1995 truly launched micro-CT technology into the realm of endodontic research. This paper demonstrated micro-CT's capability to

evaluate external/internal morphology, changes from instrumentation in terms of surface/volume, degree of canal transportation, and transportation at a resolution of 127 μm [225]. The application for this technology in dental education was soon realized along with the possibility for detailed qualitative and quantitative studies of morphology and instrumentation/obturation/retreatment [160, 205, 206, 226-236].

3.2 Hardware for micro-CT

The contralateral premolars in **Study I-III** were all scanned with the Skyscan 1172 (Bruker microCT, Kontich, Belgium) *in vitro* desktop micro-CT. It employs a microfocus X-ray source and a tungsten source target with a variable range over 20-100kV (10W). Adjustment of applied voltage and use of different X-ray filters (0.5mm Al, 1.0mm Al, 0.5m Al/40 μm Cu, 0.25mm Cu) allow for modification of the polychromatic X-ray energy spectrum generated by the source target (233). Furthermore, it has a spot size of <5 μm and a 11 Megapixel (4000x2300) 12-bit digital CCD camera with a 50mm FOV. It has the ability to detect 1 μm at its highest resolution to 25 μm (continuous variable pixel size) due to its *adaptive geometry*. Image reconstruction is accomplished using a modified Feldkamp algorithm for cone beam [237].

The adaptive geometry offered in the Skyscan 1172 means that it has a variable specimen magnification for scanning. This is possible because the x-ray camera can be moved closer or further away from the source, which allows for increased X-ray detection efficiency and scanning speed over a wide range of resolutions [237]. Newer scanners, like the Skyscan 2211, which is multimodal, allow for both the sample stage and x-ray camera being adjusted nearer or farther away from the source. This means that it can scan samples on the nano scale as long as the sample is small and close enough to the source.

3.3 Software and Image Analysis for micro-CT

Visualization and analysis of the micro-CT image data in **Study I - III** was completed using the standard SkyScan (Bruker microCT, Kontich, Belgium) Image analysis software. The software package consists of CTAn (CT analyzer; builds 3d models from micro-CT scans and measures 2D and 3D morphometric parameters), CTVol (CT volume; provides a virtual 3D viewing environment by surface rendering), and CTVOx (CT voxel; provides a virtual 3D viewing environment by volume rendering).

The precise and valid analysis, visualization, and comparison of the various parameters of the root canal geometries in **Study I - III** relies on the user-dependent thresholding (visual and histogramical estimation) of the binarized dataset to extricate the root canal volume from the surrounding phases (tooth structure) [238]. The image data are transformed to 8 bits for analysis by the reconstruction software (the dynamic range is 256 shades of gray) before thresholding. Thresholding can be a major source of error in micro-CT analysis when dealing with interfaces (*i.e.* tissues, materials) with overlapping ranges [239]. Binarization of the root canal and hard tissue was readily performed as there is a clear delineation between air and tooth structure.

The comprehensive metrology software, Geomagic (Geomagic, Morrisville, NC,

USA) was used for geometric and morphometric shape deviation analyses in **Study I and III**. The software has been validated by several international governmental agencies. The Physikalisch-Technische Bundesanstalt (PTB) is Germany's technical authority for metrology and physical safety engineering. The PTB is a scientific and technical authority under the auspices of the Federal Ministry for Economic Affairs and Energy. The institute fulfils the requirements for calibration and testing laboratories as defined by the EN ISO/IEC 1705 international standard, and as such is Germany's highest authority when it comes to correct and reliable measurements [240]. In 2005, Geomagic Qualify™ computer-aided inspection software received the highest accuracy certification from PTB by passing their standards for surface- and curve-fitting algorithms. Fitting results were accurate to less than 0.1 micrometers in length and 0.1 arcseconds (1/36,000 of a degree) in angle compared to the official reference value. In 2017, the PTB evaluated Geomagic Control X™ (formerly Qualify™), and again found "*all deviations of the algorithms under test (...) below the maximum permissible errors (MPE) for all quality characteristics [241].*" The metrological software has also received certification for accuracy from the American National Institute of Standards and Technology (NIST) and the United Kingdom's National Measurement Institute: the National Physical Laboratory (NPL). NPL found that Geomagic Control X™ "*comfortably satisfied, with all performance values for location, orientation, size and angle parameters being, respectively, less than 10^{-9} μm , 10^{-14} radians, 10^{-5} μm and 10^{-14} radians [240].*"

The Vascular Modeling Toolkit Lab (VMTKLab) application (Orobix, Bergamo, Italy) was used for extraction of the centerlines and the geometric characterization of their torsion (degree of twisting) in **Study III**. The deviation from a straight line is measured as its curvature, while torsion is the local nonconformity of the line lying on the osculating plane. In other words, torsion describes how sharply a line is twisting in space [242]. VMTKLab has a user-friendly interface with a number of algorithms part from the Vascular Modeling Toolkit (VMTK) and other open-source libraries for segmentation, geometric characterization, network analysis, hemodynamic modeling and visualization of vascular structures from medical images [243]. VMTK is what is known as an image-based modeling framework, which, unlike commercially available counterparts, is open-source and free. Herein lies VMTK's major advantage as it allows for reproducibility and a high degree of validity [243-246].

Extraction of the centerline was the only subjective operator-dependent step as the placement of seed points was done manually. When using VMTKLab for the study of vessels, the operator identifies individual vascular segments for segmentation from large vascular networks by placing seed points. This step in the process was implemented intentionally in order to make location of the subset of vessels of interest reproducible, and also because more automated segmentation methods require extensive model editing for mesh generation [243]. In the case of root canal geometries, the segment was already identified, and the generation of centerlines was not affected by the placement of seed points on the most coronal and apical extremities of the model. VMTKLab processes centerline generation automatically after placement of seed points by using the script *vmtkcenterlines* (**Figure 5**). The centerline is a line extending from the origin to the terminal point of the canal, and is defined by "*inscribed spheres (the largest sphere which can fit within the surface), taking the sphere at the point for the centerline [244].*"

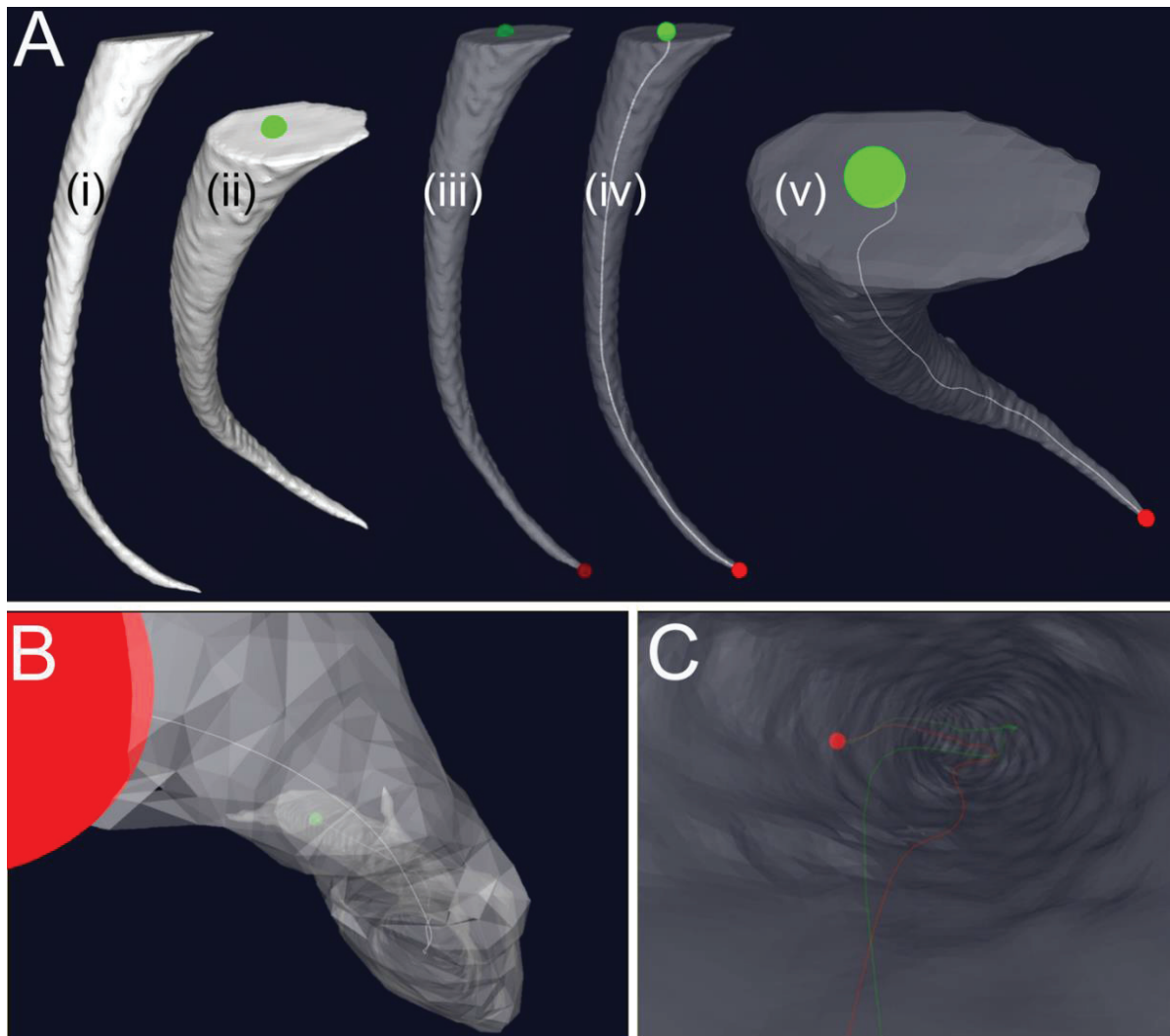


Figure 5. Panel A shows the stepwise (i-v) centerline creation in Orobix VMTKLab on a three-dimensional polydata object (root canal space) (i). The process starts with placement of the coronal green source seed (ii) followed by placement of the apical red target seed (iii) before computation and visualization of centerline (iv and v) and panel B. The centerlines pre- (green) and post-instrumentation (red) visualized simultaneously from the coronal source seed can be appreciated in panel C.

3.4 Scan Quality Challenges and Artefacts

Micro-CT has replaced the primitive methods of studying root canal anatomy and has become the gold standard for laboratory studies. It is invasive because it can only assess teeth *ex vivo*. Being a powerful non-destructive imaging tool, it can lead to clinical applications such as the development of new techniques. It also allows for comparative analysis of existing approaches in endodontic treatment, and enhancement of dental education in preclinical and clinical stages [247]. CBCT certainly has its applications as both a diagnostic aid in clinical endodontics. However, along with the clearing technique,

it is inferior to micro-CT in identifying correct canal anatomy [248]. The resolution possible for CBCT is improving, and newer scanners have voxel sizes lower than 80 μ m. However, there are challenges to acquiring accurate images at such high spatial resolutions due to, for example, patient movement.

A major impediment to improving the spatial resolution of CBCT is also that the image noise (seen as graininess) is inversely proportional to the product of the pixel step size and the square of the number of photons detected [249]. This means that when the pixel size, is reduced by a factor of two, the number of photons must be increased 4-fold in order to keep the signal-to-noise ratio constant [249]. The quality of micro-CT image acquisition is, just like CBCT, hampered by noise in addition to several other types of artefacts.

There are four main types of CT-artefacts: patient (specimen) based, physics based, hardware based, and helical & multichannel artefacts. Some of these artefacts include ring, scatter, noise, extinction, beam hardening, aliasing, and motion artefacts (**Figure 6**) [250-252]. Both ring and beam-hardening reduction algorithms exist, but it has been largely unknown if these reductions tools will have an effect on endodontic research outcomes. Queiroz *et al.* subjectively and objectively evaluated the influence of these two artefact reduction tools [253]. They found no statistically significant difference for canal volume or canal surface for a total of thirteen assessed ring and beam-hardening reduction protocols when applied according to the observer's visual preference [252].

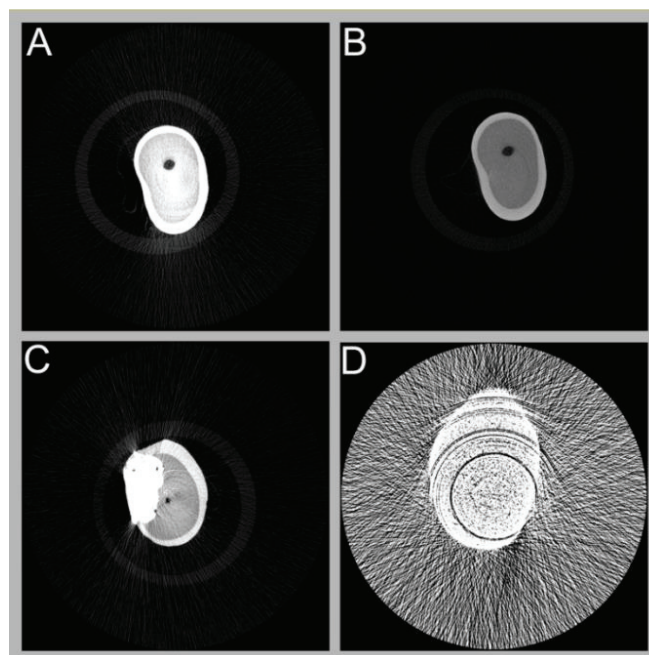


Figure 6. A miscalibrated or defective detector creates ring artefact centered on the center of rotation (A). The level axial slice in panel B is identical to A. The quality is greatly improved in B with ring and beam-hardening reduction algorithms. Beam hardening, noise and scattering from a composite filling (C). Beam hardening, noise, and scattering (D) caused by a metallic crown has resulted in streaks and bands, impairing the quality of the images. Ring artefact can be seen in panels A, C, and D.

3.5 Landmark based versus Automatic Algorithms

A major strength of the methodology used in **Study I and III** is its ability to yield quantitative information on morphometric parameters independent of landmark placement. This makes for a highly automated and efficacious procedure for matching teeth for experimental testing. The accuracy is mainly limited by the software's ability to both align and co-register geometries. The method consists of a two-step iterative closest point algorithm [254, 255]. The first step finds the rigid transformation that brings the geometries into an approximated alignment in X, Y, Z-planes followed by the fine-tuned second step, which co-registers the models for SDA. The automatic alignment requires approximately 90% of common data for success. Furthermore, the registration step, which finds common areas of curvature and orients overlapping portions of scans together, requires 10% overlap for the geometries to be co-registered before SDA. Setting tolerances as low as possible and increasing both sample size and iterations increases the accuracy of both these processes.

Another method to superimpose geometries, in addition to landmark-based methods and the surface-based registration presented herein, is voxel-based registration. This registration process can also be highly automated [256]. Here the software performs registration on greyscale voxels, and by using the intensity gray scale for each voxel it can compare the difference of the geometries [256]. Nevertheless, using voxel-based or surface-based shape deviation analysis of geometries with identical color-coded points (black and white) as in **Study I and III** seems arbitrary.

The standard methods to study and compare anatomical structures in three dimensions have largely been landmark-based. These methodologies have their apparent shortcomings as they often require extensive training for identifying the anatomical structures (inaccessible to non-experts), are prone to inter-examiner variability as reproducibility of landmarks is challenging, and are time consuming [257, 258]. The opposite methodologies are landmark-independent and evaluate surfaces comprehensively in terms of morphometry. There are a multitude of algorithms used to perform these automated surface analyses that are applied in similarity estimation and matching of 3D objects [259, 260]. Recent studies have demonstrated that landmark-independent methods had higher degrees of validity and reproducibility in addition to offering a more comprehensive analysis (**Figure 7**) compared to the landmark-dependent methods [258, 261, 262].

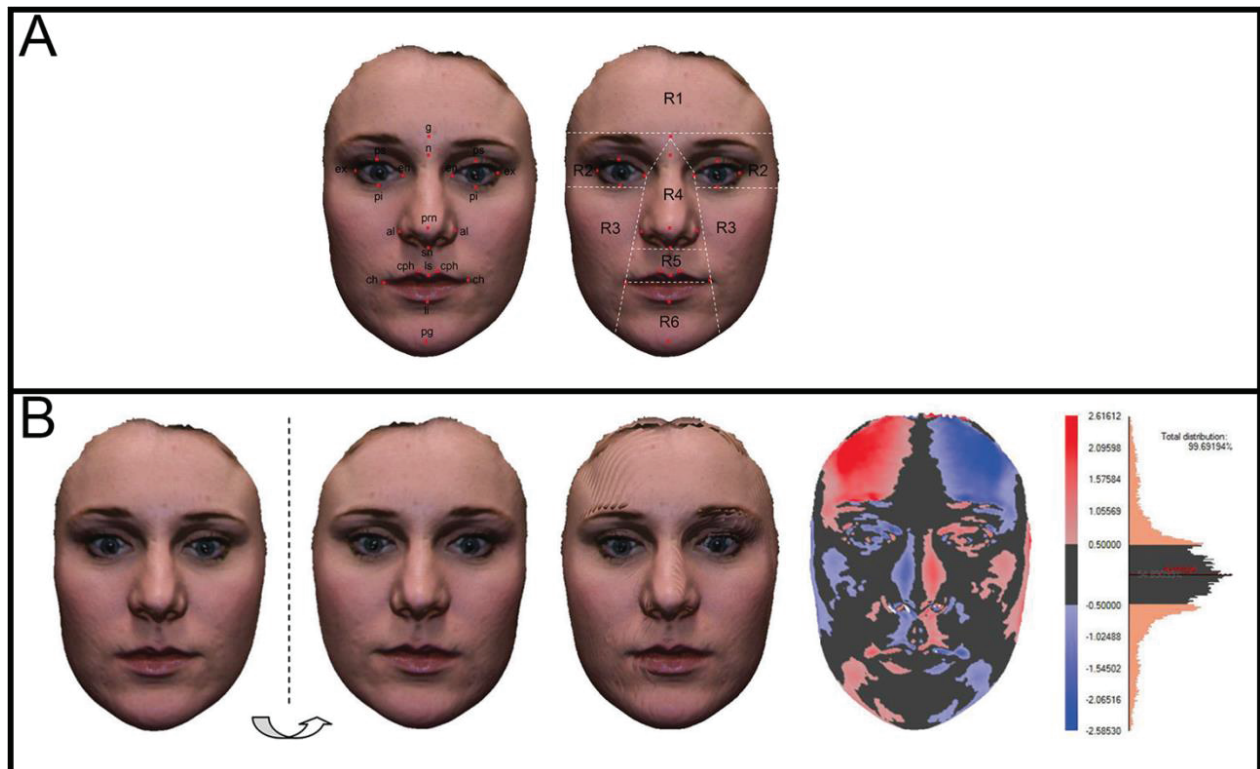


Figure 7. Depiction of landmark (A) and surface-based (B) three-dimensional analyses of facial asymmetry (Alqattan, M. and Djordjevic, J. Comparison between landmark and surface-based three-dimensional analyses of facial asymmetry in adults. *Eur J Orthod.* 2017. 37(1):1-12. Reprinted by permission of Oxford University Press (Lisence number 4418180579013.)

The extensive evaluation of the similarity between contralateral premolars in **Study I and III** included comprehensive SDA, which proved an efficacious and valid method for matching teeth destined for endodontic comparative studies. The scanning precision (*unpublished data*) was determined by rescanning a premolar at a different point in time, but with otherwise identical micro-CT and reconstruction settings [263]. The three-dimensional models were aligned and compared using 3D deviation in Geomagic (**Figure 8**), and the precision of the scanning was determined to be subvoxel (Root Mean Square Error (RMSE) = 0.048 μ m; average 3D deviation (SD) = 0.0148 / -0.0424 μ m (0.0291).

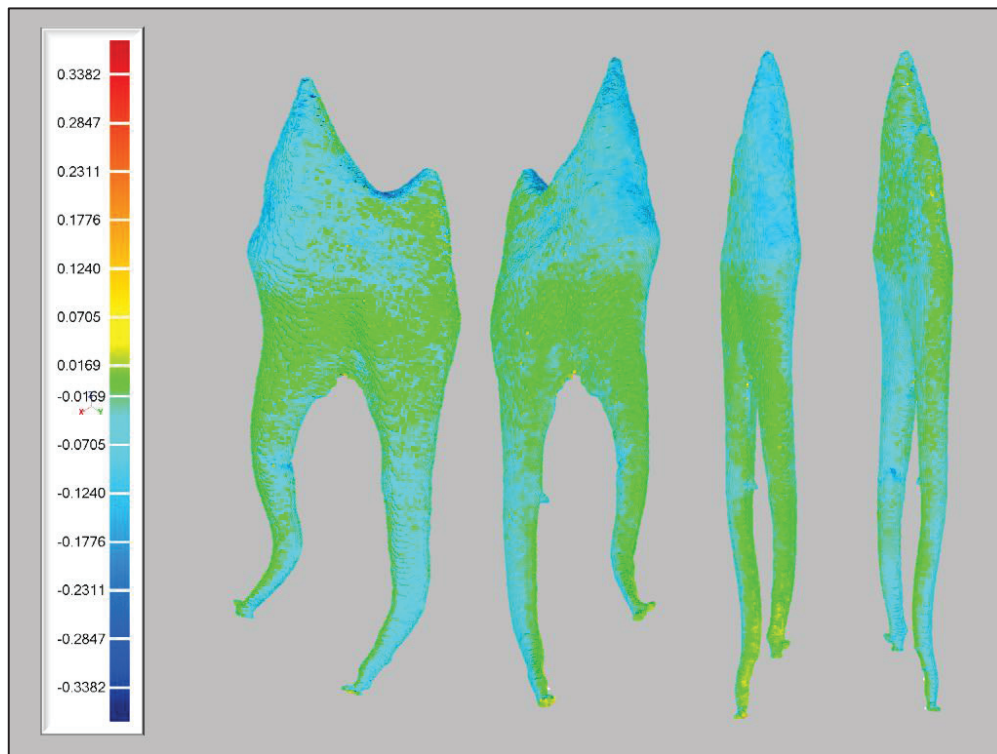


Figure 8. Precision testing scans with SDA in Geomagic Control demonstrating near perfect matching of surface models viewed in four different perspectives. The deviation color maps show deviations within the range of approximately $\pm 0.04\mu\text{m}$.

3.6 Nickel-Titanium Instruments

Shaping of the root canal system has historically been achieved by different modes of manual [264] and rotary instrumentation since William H. Rollins first introduced the rotational endodontic handpiece in 1889 [265]. The greatest advancement in endodontic instruments shaping ability came with the introduction of nickel-titanium (NiTi) files in 1988 due to their superior metallurgical characteristics of shape memory and super elasticity [266]. In recent years, single-file reciprocating NiTi file systems, which were based on the *balanced force* concept introduced [264, 267], have become commonplace.

The mechanical characteristics of the original NiTi files have been improved through different types of cross-sections, various flute designs, taper variations, and improvements in the manufacturing processes (electro-polishing, electro-discharge machining, and thermal treatment protocols) [268]. Recently, NiTi-file systems that undergo a proprietary metallurgical temperature treatment resulting in files with a blue surface color (titanium oxide layer) and, at the same time, creating a predetermined shape memory have been introduced [269]. An example of this next generation of such files is the RECIPROC blue system (RB), which consists of the three different files each with their own size and taper. All three files have the characteristic S-shape cross section and constant taper over the first 3 mm of their working part before a decreasing taper until the shaft of the instrument [270].

In preliminary studies, the RB files have demonstrated increased flexibility and cyclic fatigue resistance [271-273]. Although studies have shown less resistance to bending and cyclic fatigue for the RB files, as of yet there are no studies that have evaluated these files' shaping ability and ability to respect the original root canal anatomy in matched contralateral premolars. The RB files make up the endodontic shaping system that undergraduate dental students are trained to master at the University of Oslo. This was part of the reason for choosing this system for **Study III**. However, the choice of system could very well have been arbitrary as the purpose of the study was to see if a given shaping system used in contralateral premolar roots would result in statistically non-significant differences.

The instrumentation of the contralateral premolars in **Study III** was performed in the ambient conditions of the laboratory, while other studies have instrumented extracted teeth immersed in 37°C water bath with an irrigant solution also having the same temperature. Azim *et al.* used this as their protocol knowing that heat-treated instruments, such as RB used in **Study III**, can undergo phase transformation [162, 274], which affects the fatigue life of the instrument. The choice of using ambient conditions versus the methodology of Azim *et al.* would not affect the outcome of **Study III** as the conditions were identical for all the samples, but future endodontic comparative studies may implement this in order to closer approximate *in vivo* conditions.

3.7 Ethical Considerations

The experimental use and storage of biological samples, such as extracted teeth, is limited by journal specific regulations in addition to institutional, national, and international guidelines/legislation. This PhD project was performed according to the all pertinent Norwegian, international (Declaration of Helsinki), and institutional (University of Oslo) legislation and regulations regarding health and medical research.

The Regional Committee for Medical and Health Research Ethics of South East Norway evaluated the project and found it not to necessitate disclosure as it was "*Technical and methodological development work that uses anonymized biological material.*" The contralateral premolars were all extracted for orthodontic reasons. The patients (or legal guardians) were given written and oral information about the project prior to acquiring written consent to have their extracted teeth included in the study. The consent of the patient and the guardian was obtained in accordance with the Norwegian Health Research Act (Lov 2008-06-20 nr 44), Chapter 4, § 13 and section 20. The extracted teeth were anonymized, except for sex and age, and consent could not be withdrawn, in accordance with §16.

4. Summary of the Results

This dissertation is based upon the results from three studies in contralateral premolars before and after biomechanical root canal preparation. The studies were conducted out at the *Department of Biomaterials* and the *Department of Endodontics, Institute of Clinical Dentistry, Faculty of Dentistry, University of Oslo*.

Study I

In **Study I**, an *in silico* methodology on *ex vivo* teeth was established for the morphometric geometric analysis and comparison of contralateral premolars. Using micro-CT, forty-one intact premolar pairs (n = 82) extracted from 28 patients were evaluated using geometric morphometric shape deviation analysis of the pulp spaces after mirroring, automatic alignment, and co-registration with semi-automated software. Geometric parameters compared included volume, surface, and surface over volume. This was the first study of its kind to quantitatively compare contralateral premolars three-dimensionally with high resolution tomography. An improved understanding of the similarity of contralateral premolars was reached and set a new standard for internal validation of teeth to be used in endodontic comparative studies.

Study II

In **Study II**, a micro-computed tomography investigation qualitatively and quantitatively assessed and compared the morphology of contralateral premolars in terms of length, canal width, dentinal thicknesses, accessory canals, root canal configurations, isthmi, C-shapes, root canal orifices, and apical foramina. The contralateral premolars showed a high degree of symmetry in linear measurements. There was also matching symmetry in terms of root canal configurations and root canal orifice shapes. There were noticeable variations between contralaterals in the apical portion as well as some instances of major anatomic asymmetry such as radicular *dens invaginatus*.

Study III

In **Study III**, the effect of a reciprocating file system for biomechanical preparation in forty-four contralateral roots from twenty-eight contralateral premolars was evaluated in terms of volume, SDA, and degree of twisting. Contralateral premolar root canals were associated with similar changes in terms of volume, three-dimensional shape and degree of twisting from pre- to post-instrumentation. There was no differences between the pairs pre- and post-instrumentation, and the study validated contralateral premolars as samples for root canal comparison studies. The study gave further validation for using contralateral premolar roots in endodontic comparative studies.

5. Discussion

5.1 Validity and Reliability of Methodologies in Endodontic Research

The purpose of RCT is the prevention and treatment of apical periodontitis (134). This is accomplished through the process of chemo-mechanical instrumentation in order to both reduce the bacterial challenge in case of an established infection and prepare the root canal system for obturation with a material of choice before sealing off the entire pulp cavity with a coronal restoration [138]. No current root filling material or technique fulfills all the requirements for an ideal obturation [275], and research is ongoing to improve sealability and make materials impervious to bacterial ingress. The eventual leakage and ingress of pathogens will eventually lead to (re)infection and failure of the endodontic treatment [139]. The sealing off of the root canal system and entombment of remaining bacteria has therefore always been considered an important step of RCT. Due to this fact, it has been commonplace to compare and rank different root canal materials' sealing ability by using a myriad of microleakage tests [139]. There seems to be no limit to the ingenuity of design and variability in these microleakage methodologies, but the prevailing lack of standardization in testing calls into question their clinical credibility [64, 276].

One of the earliest studies looking at *in vitro* microleakage was done in 1939 through evaluation of both dye and bacteria ingress through temporary fillings in glass capillary tubes [277]. Since then, several other methodologies have been utilized to measure the efficacy of endodontic barriers. These include, but are certainly not limited to, radioactive isotopes, electrochemical circuits, capillary flow porometry, fluid filtration systems, calibrated latex microsphere percolation, glucose, and leakage of endotoxins and bacteria [191, 278-286]. In terms of clinical relevance, human teeth are preferred due to the fact that morphological, chemical composition and physical property differences should be considered when interpreting results of leakage test using other substrates [287]. However, many leakage tests utilizing human teeth and having otherwise well-conceived experimental designs, lack information about donors [288], storage [289], and matching information beyond tooth type [290]. It is interesting to note that even studies intending to evaluate the validity of leakage tests have not performed sample size calculations, adequate morphometric geometric matching of teeth nor adequately detailed medical history, age, or indications for extractions [288, 291]. Because of this, these types of bench-top experiments have long been subject to controversy due to questionable clinical relevance. They often lack a sound design, have no control of confounding factors, contain statistical errors, and there is a prevailing absence of standardization [64, 292-298].

In the mid-1970s only 2.9 % of all studies in JOE pertained to leakage, but by 1990 the popularity of publishing studies on leakage reached such pinnacle that there was a 1:4.3 ratio between leakage studies and other endodontic articles in the two "main" endodontic journals, namely Journal of Endodontics (JOE) and International Endodontic Journal (IEJ) [292]. As a matter of fact, among the 100 top-cited articles from the last 50 years of Endodontic research from 2013, studies evaluating microleakage (coronal or apical) ranked number one ($n = 12$) in the field [299]. The IEJ celebrated its 50th year in

2017 and its Editorial Board ranked Wu and Wesselink's critical appraisal [292] of endodontic leakage studies from 1993 among the top 6 most influential articles [300]. The main message from this article is that *"(i)t seems that more research should be done on leakage study methodology, rather than continuing to evaluate the sealing ability of different materials and techniques by methods that apparently provide little relevant information."* In other words, the endodontic literature has been saturated by comparative studies lacking a sound scientific foundation supporting reliable conclusion. De-Deus' editorials in 2007, 2008, and 2012 [64, 276, 301] were echoes from the past reiterating Wu and Wesselink's largely unanswered call for studies validating methodology. The prevailing lack of standardization in leakage testing has *"most of the time (...) demonstrate[d] the effect of canal anatomy rather than the variable of interest, that is, the root filling or technique [64]."*

Sealability remains, however, an ever-important topic for endodontic research, as the dental community would benefit from a standardized, reliable and validated laboratory leakage testing method that could successfully screen and reliably rank materials/techniques with a meaningful correlation to clinical performance. Until such a model exist, results from endodontic comparative studies are of limited clinical application and have no prognostic value. The use of clinical trials to evaluate new endodontic materials for their performance is expensive, time-consuming, and even potentially ethically questionable. It would be ideal to be able to predict clinical outcomes based on validated laboratory tests. Certain laboratory test exist that demonstrate correlation with clinical outcome for dental composites (flexural strength, fracture toughness, wear, and hardness) but *"the overall clinical success of dental composites is multi-factorial and therefore is unlikely to be predicted accurately by even a battery of in vitro test methods [302]."*

The AAE clearly states that the use of a new endodontic material or treatment method should not be employed unless its use in patient care is based on adequate laboratory, biological, and clinical studies [303]. The most important criterion for a root filling material is clinical success observed over time. A considerable amount of time may pass from the introduction of a material until systematic clinical studies are available. This makes it difficult for dentists to assess whether or not to use a new material. The first information available is usually laboratory data and animal testing, which usually examines completely specific properties of the material (*i.e.* leakage). This type of information is frequently used for advertising purposes. Systematic studies on the material from its use in patients' teeth measured against clinical success criteria is not necessary in order to sell a material. Therefore, it may take a long time before such data is available. It is therefore prudent to assess the documentation of a material based on the type of studies available and critically appraise what level of evidence pyramid these belong to [172]. The "state-of-the-art" is not the same as what is considered the "standard-of-care," which is when the material/technique has generally been adopted by the profession for a specific purpose and proven clinically efficacious [304].

In 2003 the Resilon Research LLC (Madison, CT, USA) introduced a thermoplastic synthetic polymer-based (polyester) root canal filling system called the Resilon™ Obturation System along with a dual curable dental resin composite sealer (Epiphany

Root Canal Sealant (Pentron Clinical Technologies)) [202]. The “Resilon Revolution” promised superior sealability with the creation of what became known as a monoblock seal (Resilon Monoblock System [RMS] [201]). It was absolutely considered “state-of-the-art”, but the following will demonstrate how there is no guarantee for a material being part of what is deemed “standard-of-care” even if the material can perform adequately in laboratory, biological, and clinical studies.

There was a sentiment presented in the first articles evaluating Resilon™ that gutta-percha based root fillings were the weak link in endodontic therapy and they “*leak at an alarming rate*” [202]. This assertion was largely based on leakage studies [282, 305-307] with clear methodological flaws and potential systematic errors [296] as well as epidemiological cross-sectional studies of apical periodontitis prevalence [184, 308] in urban populations with no control over how or when the RCT was performed (*i.e.* adequate aseptic technique). In any case, several preliminary studies on everything from physical properties [203], leakage [202, 289, 309, 310], cytotoxicity [311, 312], animal studies [201, 313, 314], and clinical outcome studies [315, 316] with short observational time (maximum 25 months) demonstrated statistically indistinguishable or superior properties compared with conventional or other new root filling materials. Based on the available data from laboratory, biological, and clinical studies at the time, no one could have predicted the downfall of Resilon™.

There were some studies and theoretical criticisms of Resilon™ finding that it was no better than conventional root filling materials and actually sometimes worse. The findings from these studies were related to its degradation [317-321], potentially high C-factor and interfacial bond stresses [322], lower push-out and shear bond strengths [323, 324], and reduced short- and long-term sealability [290, 325-328]. However, sound scientific skepticism and divergent findings when new materials are introduced is nothing new. Nevertheless, these studies offer plausible explanations to why Barborka *et al.* [204] found a 5.7 higher chance of failure in their retrospective case-control study in which they compared the long-term (average approximately 6 years) clinical outcomes in teeth obturated with RMS versus gutta-percha and AH-Plus.

The failure of Resilon™ to fulfill its potential as the replacement for conventional gutta-percha root fillings demonstrates how too much emphasis placed on poorly validated and unreliable leakage tests can lead to dental outcome disasters. A lack of validation of methodologies in the leakage studies carried out on the lowest level of the evidence pyramid on gutta-percha root fillings gave impetus to invest time, money, and, worst of all, patients’ health and wellbeing into a material that over time proved to be a disastrous alternative.

5.2 Sample size

It is of utmost importance to have an appropriate sample size when conducting experimental trials in order to ensure reliable answers to the research question. Too small sample sizes may prevent a real difference between mean scores being statistically significant. The sample size has to be large enough to yield statistically valid data and

not too large as to exceed limitations set by allocated means available to the researcher. It is necessary to determine optimal sample sizes prior to an experiment. Several factors influence sample size [329]:

- Expected drop-out rate
- Access to samples
- Study desing
- Budget
- Acceptable level of significance (p -value)
- Power of the study (the probability that a statistical test will yield a significant result; a low power casts doubt on the conclusion).
- Expected effect size (d). Effect size is the quantification of the difference between groups; effect size points to the degree to which a phenomenon or difference is present in the population. A small difference (= effect) between mean scores is not likely to be significant if the samples are very small.
- Underlying event rate in the population
- Standard deviation in the population.

When comparing two different therapies in (endodontic) comparative studies it is common to set a *null hypothesis* (H_0) to be rejected. The H_0 being: there is no difference between the therapies (techniques/materials) on the outcome [330]. It is important to keep in mind that failure to reject the H_0 only means just that. In other words, if we are unable to reject the H_0 it only means that there is not enough evidence to show any difference and not that it is true. When performing hypothesis testing it is possible to commit two types of errors: Type I Error (α) and Type II Error (β).

The first (Type I Error) is set by the level of significance (p -value), which is the risk we are willing to accept to commit such an error. A p -value of 0.05 means that we are accepting a 5% chance that we are going to reject the H_0 even if it is in fact true. Type II Error is failing to reject a false null hypothesis. Type II Errors are prone to occur if the sample size has not been made sufficiently large and the H_0 is accepted even when it is false, but there were not enough samples included to detect that difference.

The power is usually set at 80%, *i.e.* one is willing to accept a 20% chance of not rejecting the null hypothesis when it is actually false ($1-\beta$, where β is the probability of Type II Error (20%)) [331]. The two errors are the false-positive (Type I) and the false-negative (Type II) results [332]. The possibility of committing these types of errors can be reduced by performing sample size and effect size calculations.

The increase of sample size will lead to more precision as individual differences and chance will matter less, but “*an increase in sample size reaches a point where the effect over precision is meaningless* [332].” Ethical and economic considerations are also important incentives for not having sample sizes that are larger than necessary. Matched and well-balanced groups can provide researchers with smaller sample sizes with sufficient power that will give reliable answers. This approach can deal with challenges, for example the natural variance of bone [333], that would require a larger sample size for biomechanical testing in an unpaired design.

The general anatomic matching symmetry of contralateral bones for both mechanical, densitometric morphometric, and geometric parameters has the potential to reduce the sample number by anywhere from half to one tenth [35, 36, 40, 333-335]. Sample size reduction by 25% can be achieved using bilateral research designs ($\sigma = 0.05$, $\beta = 0.20$) in cartilage tissue engineering [336], and similar reduction in endodontic research would significantly reduce the cost and time it takes to conduct *ex vivo* and *in vivo* research.

Calculating the paired-design sample size reduction factor (λ_p) based on the sample sized for unpaired and paired study designs for contralateral premolars is given by the following equation [333, 337]:

$$\lambda_p = \frac{N_m}{N_u} \approx (1 - R) \quad \text{Eq. 1}$$

Where N_m is the total number of premolar roots in a paired design, N_u is the number of premolar roots in an unpaired design, and R is the correlation coefficient (linear regression analysis in SigmaPlot) between the left and right. According to Barker *et al.*, *the validity of the right sided term in Equation 1 as a measure of λ_p “depends on the degree of homoscedasticity [same variance] between left and right parameters with similar variances between groups leading to an accurate approximation of λ_p [333].”*

The desired σ (two-sided) and β was set to 0.05 and 0.20, respectively, for calculation of the number of matched (N_m) specimens needed to detect a bilateral percentage difference of 15% (δ_{BPD}) in premolar size using the following sample estimate equations (**Equation 2**) (346, 347, 350):

$$N_m = 2Z_Q^2 \frac{\sigma_D^2}{\delta^2} \quad \text{Eq. 2}$$

Where σ_D is the standard deviation of the differences between the contralateral parameters, δ is the minimum detectable difference between left and right, $Z_Q = Z_\sigma + Z_\beta$ ($Z_Q = 2.8$ (σ (two-sided) = 0.05 and $\beta = 0.20$) [329]). The minimum desired detectable difference between left and right ($\delta_{BPD} = 15\%$) is converted to an absolute number ($\delta = \text{mean}(L,R) \delta_{BPD} / 100$) [333].

The size of the mean difference between contralateral measurements is, according to Sumner *et al.* [334], dependent upon systematic biological asymmetry in addition to systematic measurement error. Furthermore, the magnitude of the standard deviation is a measure of fluctuating asymmetry and random measurement error. With regards to our findings, there was a high level of contralateral homoscedasticity and no evidence of systematic biological asymmetry or systematic measurement error in the mean contralateral differences evaluated for sample size and regression analysis. These results along with standard deviations for six out of the nine measurements (**Table 2** in **APPENDIX II**) being larger than the means, indicate a very high degree of bilateral symmetry of the root canal volumes and diameters [333, 334]. **Table 3** in **APPENDIX III** shows the paired design sample reduction factors (λ_p), correlation coefficients, and mean

sample estimates to detect differences in contralateral pairs of 15% for selected parameters. **Figure 10** in **APPENDIX IV** show scatter plots comparing contralateral premolar roots with fitted linear regression lines with no difference between the left and right [338]. The overall finding is a very high degree of similarity for premolar contralaterals giving a substantial reduction in sample number for comparison studies.

5.3 Geometric Morphometric Analysis

The goal of any comparative study is to create well-balanced experimental groups. This is, of course, also what researchers aim to accomplish in endodontic *ex vivo* research. Unfortunately, even recent studies often lack sufficient information about the exact origin of the extracted teeth, the origin of teeth in regard to age or sex, and storage prior to inclusion. There is also no matching of shape/morphology beyond Vertucci's classification [90] and homogeneity of simple geometric parameters [157, 159, 162, 339-341].

A recent study by Guimaraes *et. al* [342] made a creditable effort in creating well-balanced experimental groups. They used thirteen pairs of single-rooted oval shaped contralateral premolars with known storage medium and age to compare two different endodontic instrumentation systems. Furthermore, a sample size calculation was performed prior to experimentation, but the contralateral premolars were not matched on overall geometric morphometric similarity. However, they asserted that the lack of statistically significant difference in the initial canal volume and surface confirm the validity of using contralateral teeth. This assertion is supported by the findings from the SDA analysis and anatomical evaluation of similarity in **Study I - III** but cannot be made based on simple geometric values of volume and surface area alone.

Two recent articles by Gustavo De-Deus' group compared the shaping ability outcomes of different root canal instrumentation systems on matched teeth. The teeth were selected from a pool of teeth with unknown storage prior to inclusion in the studies [269, 343]. In both instances, they conducted *a priori* sample size calculations based on previous studies [344, 345]. The two previous studies that were used for sample size calculations in the recent articles [269, 343] matched teeth based on two-dimensional curvature, root canal configurations, volumes, and lengths of root canals. In addition to root canal configuration and simple geometric parameters, the teeth were matched based on a method called the structure model index (SMI), which gives a numerical value characterizing the structure of trabecular bone in bone research as being either plate-like (SMI = 0), rod-like (SMI = 3) or spherical (SMI = 4) [346]. The SMI was first used in the geometrical analysis of unprepared three-rooted maxillary molars in order to rate the roundness of the mesio-buccal, disto-buccal and palatal canals. The index was also used to assess endodontic instruments' ability to create rounder canals [347]. The root canals in the studies by De-Deus' group had already matched the geometries according to configuration and other factors, and it is unknown if the lack of statistically significant difference between the SMI has any real bearing on the matching of teeth to be used in endodontic comparative studies.

Study I - III did not consider the SMI for the matching or comparison of root canal anatomy. The SMI is applicable for characterization of primitive and convex geometries

by comparing the surface area of a structure before and after an infinitesimal dilation to its volume [348]. The SMI has been the “*de facto* standard for measuring the rod- and plate-like geometry in 3-dimensional trabecular bone images [348].” However, findings by Salmon *et al.* strongly suggest that the SMI is confounded by the concavities present in real bone geometries and that the SMI algorithm therefore should not be used anymore for evaluation of trabecular bone [348].

The confounding concave surfaces that may be found in trabecular bone can be manifested as saddle curves, troughs, or bowls [348]. It is apparent from the abundant literature on the internal anatomy of teeth that root canals are not smooth and well-defined tubes. The great variation within the course of any given root canal system may contain all of the three aforementioned concavities that are known to confound the SMI. The question is then if the shortcomings of SMI in relation to trabecular bone described in the paper by Salmon *et al.* [348] are applicable to root canal geometries and if similar SMI values can be used for matching purposes. In other words, do SMI values without statistical significance indicate morphological likeness? Phil L. Salmon states “*SMI might be OK for root canals since most of the curvature is convex. It is concave surfaces where SMI becomes biased by porosity and percent volume and thus compromised* [349].”

It remains uncertain whether or not the SMI can be considered a 3D geometric morphometric approach for comparing similarity of root canals comprehensively. Furthermore, it is a common understanding to assume that the root canal is convex tube as described by a myriad of morphological studies. The potential of SMI as a supplement to SDA by Geomagic for morphological matching of root canal geometries should be explored further in future research. If SMI would prove to be a valid method for matching teeth, it would be a valuable time-saver as it is an integrated algorithm in CTan.

Previous odontometric studies [18, 350, 351] have found evidence of considerable fluctuating asymmetry for the external anatomy of teeth. This was calculated by measuring one dimensional distances or superimposition of traced photos. The use of simple one-dimensional parameters has been suggested to cause measurement errors due to variable reference points as well as not giving sufficient information about the teeth’s morpho-geometric whole [352]. Although valuable, these studies do not “*facilitate detailed assessments of how genetic, epigenetic, and environmental factors contribute the final tooth form* [70].” The emergence and accelerated evolution of comprehensive metrology software has ushered forward the era of *dental phenomics* [70, 353], which allows for the geometric morphometric comparison of external and internal dental structures and how they relate to genetic, epigenetic, and environmental factors.

Probst demonstrated a very high degree of matching symmetry for anterior teeth’s crown morphology (centrals, laterals, and canines) using advanced metrology software in his PhD thesis [354] and also in two sub-subsequent articles based on his thesis [352, 355]. Our evaluation (*unpublished data*) of geometric morphometric comparison of the contralateral premolars external anatomy support their findings ($n = 41$ contralateral pairs: mean RMSE (SD) = 180.26 (103.84) μm ; mean Transformed D_{avg} = 246.40 (103.76) μm) (**Figure 9** in **APPENDIX I**). The assumption made by Zehnder *et al.* [58] that contralateral

teeth (premolars) are anatomically identical (twin teeth) does indeed seem plausible despite the lack of evidence to back up their assertion.

6. Conclusions

The main aim of this thesis was to develop a valid and reliable *in silico* methodology for *ex vivo* endodontic comparative studies using matched contralateral premolars. The three studies that comprise this thesis demonstrate how to make a comprehensive evaluation of the degree of similarity between contralateral premolars using micro-CT and metrology software prior to conducting an endodontic comparative study.

The results from this thesis lead to the conclusion that contralateral premolars can be used to reliably test differences between endodontic techniques/materials. This thesis has shown that contralateral premolars do not have a significant amount of variation in anatomy, and this will therefore not be a confounding factor in comparison studies.

The validation of this test system sets a new standard for endodontic comparison studies.

The main conclusions from **Study I – III** are as follows:

- Contralateral premolar *pulp cavities*, in general, exhibit matching symmetry in terms of volume, surface, and surface over volume, and SDA (**Study I**)
- Contralateral premolars have matching symmetry in lengths, root canal widths, and dentinal thickness (**Study II and III**)
- Contralateral premolars demonstrate fluctuating asymmetry in the apical portion, in terms of accessory canals, C-shapes, and isthmi (**Study II**).
- Removal of the apical 3 mm is recommended when it may influence the outcome (*i.e.* leakage studies) (**Study II**).
- Canal instrumentation of contralateral premolars produce non-significantly different geometric and morphometric changes in volume, degree of twisting (torsion), and three-dimensional shape (**Study III**).
- Although this study has found that contralateral premolars have a high degree of symmetry, variations in the apical third and anatomic aberrations such as dens invaginatus underscore the need for micro-CT scanning and comparison of contralateral premolars intended for use in endodontic comparison studies (**Study II**).

The results presented in this thesis contribute to a greater understanding and knowledge of the root canal anatomy of contralateral premolars, which will have impact and relevance for clinicians and researchers alike. This includes dental forensics, pre-clinical education, dental anthropology, and endodontic comparative research.

The overall hypothesis that using screened and matched contralateral premolars will yield non-significant results in a comparative endodontic study using the same biomechanical instrumentation system cannot be rejected. We have thereby provided a new model and set a new standard for endodontic comparative studies.

7. Research Prospects

The findings in the present thesis pave the way for interesting future studies in the fields of dental anthropology, dental forensics, craniofacial developmental biology (twin studies), as well as endodontic *ex* and *in vivo* comparative studies.

Existing research is scant in the area of anthropological differences in degree of root canal symmetry beyond number of canals and root canal configuration. Future research in dental anthropology should include SDA of contralateral teeth.

No statistically significant difference existed between the degree of similarity between male and female root canal geometries in **Study I**. Statistically significant differences between the sexes would warrant recruitment of the sex with the highest degree of left-right symmetry. Furthermore, this may also be useful in identification of gender in dental forensics. Prospective research should include a larger sample size from each sex to explore whether this holds true for both the external and internal anatomy of contralateral premolars.

In the realm of craniofacial developmental biology, the methodology for presented in the present thesis could provide additional insight into the role of genetic, epigenetic and environmental factors during dental development. Also, further studies may reveal a high degree of similarity of root canal geometries in identical twins and as such be a potential method to determine twin zygosity.

Future endodontic comparative studies on instrumentation techniques, irrigation protocols, obturation *etc.* should be conducted in screened and matched contralateral teeth. Further enhancements on current methodology and suggested future research includes development of fully automated SDA or topology matching processes [259, 260] for quick retrieval of geometries *in silico* from large repositories of teeth. It is even conceivable to match the teeth from different individuals (**Figure 8**) to be used for testing if they are within a certain range of morphological similarity. The range, or lowest acceptable similarity coefficient, would certainly rely on further validation has yet to be determined. This type of database repository of pulp spaces would open up for extremely time and cost-efficient *ex vivo* studies.

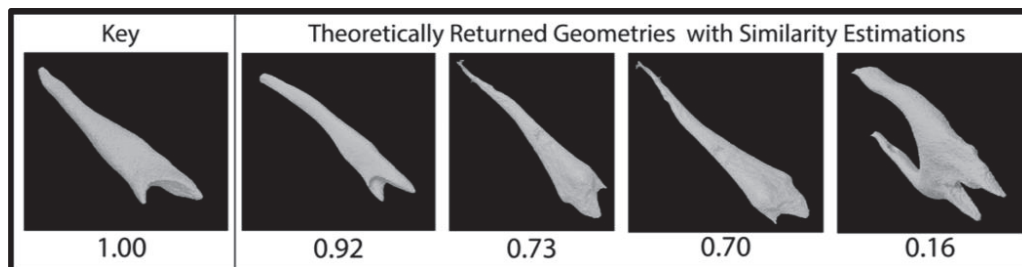


Figure 8. Depiction of theoretical topology matching for fully automatic similarity estimation and retrieval of root canal geometries from database. The selected configuration and morphology for a hypothetical comparison experiment is shown as the key and the models returned with the highest similarities are shown to the right. Figure modified from modification done by Jonas Wengenroth based on Hilaga *et al.* [258].

REFERENCES

1. Brading, K., E. Castellani, and N. Teh. The Stanford Encyclopedia of Philosophy "Symmetry and Symmetry Breaking" 2017. 31.12.2018 [cited 01.03.2018]; Available from: <https://plato.stanford.edu/archives/win2017/entries/symmetry-breaking/>.
2. Weyl, H., *Symmetry*. **1952**, Princeton: Princeton University Press. 168.
3. Aristotle, *The Complete Works of Aristotle*. **1992**, IntelLex Corp. Princeton University Press (The Jowett Copyright Trustees): Princeton, New Jersey, USA.
4. Lockwood, E.H. and R.H. Macmillan, *Geometric symmetry*. **1978**, Cambridge: Cambridge University Press. 228.
5. Mardia, K.V., F.L. Bookstein, and I.J. Moreton. Statistical assessment of bilateral symmetry of shapes. *Biometrika*, **2000**; 87:285-300.
6. Klingenberg, C.P., M. Barluenga, and A. Meyer. Shape analysis of symmetric structures: Quantifying variation among individuals and asymmetry. *Evolution*, **2002**; 56:1909-1920.
7. Palmer, A.R. and C. Strobeck. Fluctuating Asymmetry - Measurement, Analysis, Patterns. *Annu Rev Ecol Syst*, **1986**; 17:391-421.
8. Valen, L.V. A Study of Fluctuating Asymmetry. *Evolution*, **1962**; 16:125-142.
9. Pound, N., D.W. Lawson, A.M. Toma, S. Richmond, A.I. Zhurov, and I.S. Penton-Voak. Facial fluctuating asymmetry is not associated with childhood ill-health in a large British cohort study. *Proc Biol Sci*, **2014**; 281.
10. Van Dongen, S. Associations among facial masculinity, physical strength, fluctuating asymmetry and attractiveness in young men and women. *Ann Hum Biol*, **2014**; 41:205-213.
11. Milne, B.J., J. Belsky, R. Poulton, W.M. Thomson, A. Caspi, and J. Kieser. Fluctuating asymmetry and physical health among young adults. *Evol Hum Behav*, **2003**; 24:53-63.
12. Ozener, B. Fluctuating and directional asymmetry in young human males: effect of heavy working condition and socioeconomic status. *Am J Phys Anthropol*, **2010**; 143:112-120.
13. Caillois, R. The Myth of the Unicorn. *Diogenes*, **1982**; 1-23.
14. Coles, R.B. and A. Guppy. Directional hearing in the barn owl (*Tyto alba*). *J Comp Physiol A*, **1988**; 163:117-133.
15. Palmer, A.R. Symmetry breaking and the evolution of development. *Science*, **2004**; 306:828-833.
16. Rosenberg, M.S. The systematics and taxonomy of fiddler crabs: A phylogeny of the genus *UCA*. *J Crustacean Biol*, **2001**; 21:839-869.
17. Bailit, H.L., P.L. Workman, J.D. Niswander, and C.J. MacLean. Dental asymmetry as an indicator of genetic and environmental conditions in human populations. *Hum Biol*, **1970**; 42:626-638.
18. Khalaf, K., C. Elcock, R.N. Smith, and A.H. Brook. Fluctuating dental asymmetry of multiple crown variables measured by an image analysis system. *Arch Oral Biol*, **2005**; 50:249-253.

19. Sprowls, M.W., R.E. Ward, P.L. Jamison, and J.K. Hartsfield. Dental Arch Asymmetry, Fluctuating Dental Asymmetry, and Dental Crowding: A Comparison of Tooth Position and Tooth Size Between Antimeres. *Semin Orthod*, **2008**; 14:157-165.
20. DiBennardo, R. and H.L. Bailit. Stress and dental asymmetry in a population of Japanese children. *Am J Phys Anthropol*, **1978**; 48:89-94.
21. Compagnucci, C., J. Fish, and M.J. Depew. Left-right asymmetry of the gnathostome skull: its evolutionary, developmental, and functional aspects. *Genesis*, **2014**; 52:515-527.
22. Little, A.C., B.C. Jones, C. Waitt, B.P. Tiddeman, D.R. Feinberg, D.I. Perrett, C.L. Apicella, and F.W. Marlowe. Symmetry is related to sexual dimorphism in faces: data across culture and species. *Plos One*, **2008**; 3:1-8.
23. Xia, B.G., B. Ben Amor, H. Drira, M. Daoudi, and L. Ballihi. Combining face averageness and symmetry for 3D-based gender classification. *Pattern Recong*, **2015**; 48:746-758.
24. Djordjevic, J., A.M. Toma, A.I. Zhurov, and S. Richmond. Three-dimensional quantification of facial symmetry in adolescents using laser surface scanning. *Eur J Orthod*, **2014**; 36:125-132.
25. Grammer, K. and R. Thornhill. Human (*Homo sapiens*) facial attractiveness and sexual selection: the role of symmetry and averageness. *J Comp Psychol*, **1994**; 108:233-242.
26. Rhodes, G., F. Proffitt, J.M. Grady, and A. Sumich. Facial symmetry and the perception of beauty. *Psychon B Rev*, **1998**; 5:659-669.
27. Locher, P. and C. Nodine. The Perceptual Value of Symmetry. *Comput Math Appl*, **1989**; 17:475-484.
28. Zhang, Z.F. and G.A. Brock. New evolutionary and ecological advances in deciphering the Cambrian explosion of animal life. *J Paleontol*, **2018**; 92:1-2.
29. Peterson, K.J. and E.H. Davidson. Regulatory evolution and the origin of the bilaterians. *P Natl Acad Sci USA*, **2000**; 97:4430-4433.
30. Vermot, J. and O. Pourquie. Retinoic acid coordinates somitogenesis and left-right patterning in vertebrate embryos. *Nature*, **2005**; 435:215-220.
31. Wasiak, S. and D. Lohnes. Retinoic acid affects left-right patterning. *Dev Biol*, **1999**; 215:332-342.
32. Seritrakul, P., E. Samarut, T.T. Lama, Y. Gibert, V. Laudet, and W.R. Jackman. Retinoic acid expands the evolutionarily reduced dentition of zebrafish. *FASEB J*, **2012**; 26:5014-5024.
33. Ramanathan, A., T.C. Srijaya, P. Sukumaran, R.B. Zain, and N.H. Abu Kasim. Homeobox genes and tooth development: Understanding the biological pathways and applications in regenerative dental science. *Arch Oral Biol*, **2018**; 85:23-39.
34. Kawakami, Y., A. Raya, R.M. Raya, C. Rodriguez-Esteban, and J.C. Izpisua Belmonte. Retinoic acid signalling links left-right asymmetric patterning and bilaterally symmetric somitogenesis in the zebrafish embryo. *Nature*, **2005**; 435:165-171.
35. Pierre, M.A., D. Zurakowski, A. Nazarian, D.A. Hauser-Kara, and B.D. Snyder. Assessment of the bilateral asymmetry of human femurs based on physical, densitometric, and structural rigidity characteristics. *J Biomech*, **2010**; 43:2228-2236.

36. Young, E.Y., J. Gebhart, D. Cooperman, and N.U. Ahn. Are the left and right proximal femurs symmetric? *Clin Orthop Relat Res*, **2013**; 471:1593-1601.
37. Suh, K.T., J.H. Kang, H.L. Roh, K.P. Moon, and H.J. Kim. True femoral anteversion during primary total hip arthroplasty: use of postoperative computed tomography-based sections. *J Arthroplasty*, **2006**; 21:599-605.
38. Lindner, C., G.A. Wallis, and T.F. Cootes. Increasing shape modelling accuracy by adjusting for subject positioning: an application to the analysis of radiographic proximal femur symmetry using data from the Osteoarthritis Initiative. *Bone*, **2014**; 61:64-70.
39. ten Berg, P.W., J.G. Dobbe, S.D. Strackee, and G.J. Streekstra. Three-Dimensional Assessment of Bilateral Symmetry of the Scaphoid: An Anatomic Study. *Biomed Res Int*, **2015**; 2015:547250.
40. Islam, K., A. Dobbe, A. Komeili, K. Duke, M. El-Rich, S. Dhillon, S. Adeeb, and N.M. Jomha. Symmetry analysis of talus bone: A Geometric morphometric approach. *Bone Joint Res*, **2014**; 3:139-145.
41. Garrido-Varas, C., R. Rathnasinghe, T. Thompson, and Y. Savriama. A new method to pair-match metacarpals using bilateral asymmetry and shape analysis. *J Forensic Sci*, **2015**; 60:118-123.
42. Karell, M.A., H.K. Langstaff, D.J. Halazonetis, C. Minghetti, M. Frelat, and E.F. Kranioti. A novel method for pair-matching using three-dimensional digital models of bone: mesh-to-mesh value comparison. *Int J Legal Med*, **2016**; 130:1315-1322.
43. Lynch, J.J. An Automated Two-Dimensional Form Registration Method for Osteological Pair-Matching. *J Forensic Sci*, **2018**; 63:1236-1242.
44. Kumar, A.Y., M. El-Rich, J.L. Jaremko, and K. Duke, Symmetry of the Pelvis using Volume and Deviation Analysis, in 22nd Congress of the European Society of Biomechanics. **2016**: Lyon, France.
45. Claes, P., J. Reijniers, M.D. Shriver, J. Snyders, P. Suetens, J. Nielandt, G. De Tre, and D. Vandermeulen. An investigation of matching symmetry in the human pinnae with possible implications for 3D ear recognition and sound localization. *J Anat*, **2015**; 226:60-72.
46. Yoon, J.R., H.I. Jeong, M.J. Seo, K.M. Jang, S.R. Oh, S. Song, and J.H. Yang. The use of contralateral knee magnetic resonance imaging to predict meniscal size during meniscal allograft transplantation. *Arthroscopy*, **2014**; 30:1287-1293.
47. Katsumata, A., M. Fujishita, M. Maeda, Y. Arijii, E. Arijii, and R.P. Langlais. 3D-CT evaluation of facial asymmetry. *Oral Surg Oral Med Oral Pathol Oral Radiol Endod*, **2005**; 99:212-220.
48. Kwon, T.G., H.S. Park, H.M. Ryoo, and S.H. Lee. A comparison of craniofacial morphology in patients with and without facial asymmetry--a three-dimensional analysis with computed tomography. *Int J Oral Maxillofac Surg*, **2006**; 35:43-48.
49. Thiesen, G., B.F. Gribel, K.B. Kim, K.C.R. Pereira, and M.P.M. Freitas. Prevalence and Associated Factors of Mandibular Asymmetry in an Adult Population. *J Craniofac Surg*, **2017**; 28:e199-e203.
50. Gustafson, G. Microscopic examination of teeth as a means of identification in forensic medicine. *J Am Dent Assoc*, **1947**; 35:720-724.
51. Gustafson, A.G. The similarity between contralateral pairs of teeth. *Odontol Tidskr*, **1955**; 63:245-248.

52. Gustafson, A.G., A Morphologic Investigation of Certain Variations in the Structure and Mineralization of Human Dental Enamel. **1959**, Berlingska Boktryckeriet: Lund, Sweden.
53. Jorgensen, K.D. Contralateral symmetry of acid etched enamel surfaces. *Scand J Dent Res*, **1975**; 83:26-30.
54. Jorgensen, K.D. and H. Shimokobe. Adaptation of resinous restorative materials to acid etched enamel surfaces. *Scand J Dent Res*, **1975**; 83:31-36.
55. Brannstrom, M. and K.J. Nordenvall. The effect of acid etching on enamel, dentin, and the inner surface of the resin restoration: a scanning electron microscopic investigation. *J Dent Res*, **1977**; 56:917-923.
56. Brannstrom, M. Sensitivity of dentine. *Oral Surg Oral Med Oral Pathol*, **1966**; 21:517-526.
57. Mehlhaff, D.S., J.G. Marshall, and J.C. Baumgartner. Comparison of ultrasonic and high-speed-bur root-end preparations using bilaterally matched teeth. *J Endod*, **1997**; 23:448-452.
58. Zehnder, M., H.U. Luder, M. Schatzle, E. Kerosuo, and T. Waltimo. A comparative study on the disinfection potentials of bioactive glass S53P4 and calcium hydroxide in contra-lateral human premolars ex vivo. *Int Endod J*, **2006**; 39:952-958.
59. Sedgley, C.M. and H.H. Messer. Are endodontically treated teeth more brittle? *J Endod*, **1992**; 18:332-335.
60. Viapiana, R., A.T. Moinzadeh, L. Camilleri, P.R. Wesselink, M. Tanomaru Filho, and J. Camilleri. Porosity and sealing ability of root fillings with gutta-percha and BioRoot RCS or AH Plus sealers. Evaluation by three ex vivo methods. *Int Endod J*, **2016**; 49:774-782.
61. Goracci, C., J. Juloski, R. Schiavetti, P. Mainieri, A. Giovannetti, A. Vichi, and M. Ferrari. The influence of cement filler load on the radiopacity of various fibre posts ex vivo. *Int Endod J*, **2015**; 48:60-67.
62. Hjortsjo, C., G. Jonski, A. Young, and E. Saxegaard. Etching effect of acidic fluorides on human tooth enamel in vitro. *Arch Oral Biol*, **2014**; 59:1328-1333.
63. Endal, U., Y. Shen, J. Ma, Y. Yang, and M. Haapasalo. Evaluation of Quality and Preparation Time of Retrograde Cavities in Root Canals Filled with GuttaCore and Cold Lateral Condensation Technique. *J Endod*, **2018**; 44:639-642.
64. De-Deus, G. Research that matters - root canal filling and leakage studies. *Int Endod J*, **2012**; 45:1063-1064.
65. Ludwig, F.J. The mandibular second premolars: morphologic variation and inheritance. *J Dent Res*, **1957**; 36:263-273.
66. Wood, B.F. and L.J. Green. Second premolar morphologic trait similarities in twins. *J Dent Res*, **1969**; 48:74-78.
67. Su, C.Y., P.M. Corby, M.A. Elliot, D.A. Studen-Pavlovich, D.N. Ranalli, B. Rosa, J. Wessel, N.J. Schork, T.C. Hart, and W.A. Bretz. Inheritance of occlusal topography: a twin study. *Eur Arch Paediatr Dent*, **2008**; 9:19-24.
68. Kabban, M., J. Fearn, V. Jovanovski, and L. Zou. Tooth size and morphology in twins. *Int J Paediatr Dent*, **2001**; 11:333-339.
69. Boklage, C.E., Method and Meaning in the Analysis of Developmental Asymmetries, in Culture, Ecology and Dental Anthropology J. Lukacs, Editor. **1992**, Kamla-Raj Enterprises: Delhi, India 147-156.

70. Townsend, G.C., A. Brook, R. Yong, and T. Hughes, Tooth Classes, Field Concepts, and Symmetry, in A companion to dental anthropology, J.D. Irish and G.R. Scott, Editors. **2016**, John Wiley & Sons: Chichester, UK ; Malden, MA. 540 pages.
71. Xu, J., M.Y. Shao, H.Y. Pan, L. Lei, T. Liu, L. Cheng, T. Hu, and P.M. Dummer. A proposal for using contralateral teeth to provide well-balanced experimental groups for endodontic studies. *Int Endod J*, **2016**; 49:1001-1008.
72. Baastad, A., L. Haugen, J. Herje, E. Hviding, P. Lüdemann, A. Løken, S. Rødseth, W.I. Tønder, and L.V. Ulvenes. Analyse av stønadsutbetalingene til tannbehandling ved tilstander som omfattes av «forskrift om stønad til dekning av utgifter til undersøkelse og behandling hos tannlege og tannpleier for sykdom» punkt 8- Bittanomalier. **2014**; 63.
73. SSB. Statistics Norway - Births. 2018. 06.03.2018 [cited 2018 20.03.2018]; Available from: <https://www.ssb.no/en/befolkning/statistikker/fodte>.
74. Gutmann, J.L. Historical Perspectives III. The DG 16 explorer. *J Hist Dent*, **2014**; 62:110.
75. Green, D. Morphology of the pulp cavity of the permanent teeth. *Oral Surg Oral Med Oral Pathol*, **1955**; 8:743-759.
76. Carabelli, G., Kupfertafeln zu v. Carabelli's Anatomie des Mundes. **1844**, Wien: Bei Braumüller und Seidel. 68.
77. Black, G.V., Descriptive anatomy of the Human Teeth. **1890**, Philadelphia: The Wilmington Dental Manufacturing Co.
78. Mühlreiter, E. and T. de Jonge-Cohen, Anatomie des menschlichen Gebisses. **1928**, Leipzig: Arthur Felix.
79. Preiswerk, G., Atlas and Text-Book of Dentistry Including Diseases of the Mouth - Authorized Translation from German. **1909**, Philadelphia, Pennsylvania, USA: W.B. Saunders Company.
80. Fischer, G. Zur Anatomie der Wurzelkanäle.[Anatomy of root canals]. *Zahnartzl Rundsch*, **1954**; 63:693-697.
81. Hess, W., E. Zürcher, and W.H. Dolamore, The anatomy of the root-canals of the teeth of the permanent dentition. **1925**, New York: Wm. Wood & co. 2 p. L., iii-vii, 199 p. incl. plates.
82. Spalteholz, W., Über das Durchsichtigmachen von menschlichen und tierischen Präparaten und seine theoretischen Bedingungen, nebst Anhang: Über Knochenfärbung - On transparentized human and animal specimens, including notes on bone staining. **1914**, Leipzig: S. Hirzel. 93 p.
83. Fanibunda, K.B. A method of measuring the volume of human dental pulp cavities. *Int Endod J*, **1986**; 19:194-197.
84. Adloff, P. The history of development of the human dental system, together with comments on the question of prelacteal dentition, the so-called concrecence theory and the general development of the bite of mammals. *Arch Mikrosk Anat*, **1913**; 82:1-38.
85. Moral, H. Ueber pulpaausgüsse. *Deutsche Monatsschrift für Zahnheilkunde*, **1914**; 32:617-624.
86. Barker, B.C., K.C. Parsons, P.R. Mills, and G.L. Williams. Anatomy of root canals. I. Permanent incisors, canines and premolars. *Australian dental journal*, **1973**; 18:320-327.

87. Okumura, T. Anatomy of the root canals. *J Am Dent Assoc*, **1927**; 632-635.
88. Seelig, A. and R. Gillis. Preparation of cleared specimens for pulp cavity studies. *J Dent Res*, **1973**; 52:1154.
89. Vertucci, F., A. Seelig, and R. Gillis. Root canal morphology of the human maxillary second premolar. *Oral Surg Oral Med Oral Pathol*, **1974**; 38:456-464.
90. Vertucci, F.J. Root canal anatomy of the human permanent teeth. *Oral Surg Oral Med Oral Pathol*, **1984**; 58:589-599.
91. Gulabivala, K., T.H. Aung, A. Alavi, and Y.L. Ng. Root and canal morphology of Burmese mandibular molars. *Int Endod J*, **2001**; 34:359-370.
92. Neelakantan, P., C. Subbarao, and C.V. Subbarao. Comparative evaluation of modified canal staining and clearing technique, cone-beam computed tomography, peripheral quantitative computed tomography, spiral computed tomography, and plain and contrast medium-enhanced digital radiography in studying root canal morphology. *J Endod*, **2010**; 36:1547-1551.
93. Mueller, A.H., *The Anatomy of the Root Canals of the Incisors, Cuspids, and Bicuspid of the Permanent Dentition*, in Loyola University. **1932**, Loyola University: Chicago. 77.
94. Mayo, C.V., S. Montgomery, and C. de Rio. A computerized method for evaluating root canal morphology. *J Endod*, **1986**; 12:2-7.
95. Gullickson, D.C. and S. Montgomery. The study of root canal morphology using a digital image processing technique. *J Endod*, **1987**; 13:158-163.
96. Berutti, E. Computerized analysis of the instrumentation of the root canal system. *J Endod*, **1993**; 19:236-238.
97. Blaskovic-Subat, V., B. Smojver, B. Maricic, and J. Sutalo. A computerized method for the evaluation of root canal morphology. *Int Endod J*, **1995**; 28:290-296.
98. Tachibana, H. and K. Matsumoto. Applicability of X-ray computerized tomography in endodontics. *Endod Dent Traumatol*, **1990**; 6:16-20.
99. Chauhan, R., S. Singh, and A. Chandra. A rare occurrence of bilateral C-shaped roots in mandibular first and second premolars diagnosed with the aid of spiral computed tomography. *J Clin Exp Dent*, **2014**; 6:e440-443.
100. Holliday, R. and E. Beecroft. Bilateral mandibular premolar dens invaginations: a case report. *Case Rep Dent*, **2012**; 2012:474013.
101. Chauhan, R. and S. Singh. Endodontic management of three-rooted maxillary second premolar in a patient with bilateral occurrence of three roots in maxillary second premolars. *J Clin Exp Dent*, **2012**; 4:e317-320.
102. Gopal, S., G. John, K. Pavan Kumar, S. Latha, S. Latha, and S. Kallepalli. Endodontic Treatment of Bilateral Maxillary First Premolars with Three Roots Using CBCT: A Case Report. *Case Rep Dent*, **2014**; 2014:505676.
103. Dankner, E., S. Friedman, and A. Stabholz. Bilateral C shape configuration in maxillary first molars. *J Endod*, **1990**; 16:601-603.
104. Canger, E.M., S. Kayipmaz, and P. Celenk. Bilateral dens invaginatus in the mandibular premolar region. *Indian journal of dental research : official publication of Indian Society for Dental Research*, **2009**; 20:238-240.
105. Alani, A.H. Endodontic treatment of bilaterally occurring 4-rooted maxillary second molars: case report. *J Can Dent Assoc*, **2003**; 69:733-735.

106. Jafarzadeh, H. Endodontic treatment of bilaterally occurring three-rooted maxillary premolars: a case report. *N Z Dent J*, **2007**; 103:37-38.
107. Zeng, C., Y. Shen, X. Guan, X. Wang, M. Fan, and Y. Li. Rare Root Canal Configuration of Bilateral Maxillary Second Molar Using Cone-beam Computed Tomographic Scanning. *J Endod*, **2016**; 42:673-677.
108. Burton, D.J., R.O. Saffos, and R.B. Scheffer. Multiple bilateral dens in dente as a factor in the etiology of multiple periapical lesions. *Oral Surg Oral Med Oral Pathol*, **1980**; 49:496-499.
109. Badole, G.P., M.M. Warhadpande, P.R. Shenoi, C. Lachure, and S.G. Badole. A rare root canal configuration of bilateral maxillary first molar with 7 root canals diagnosed using cone-beam computed tomographic scanning: a case report. *J Endod*, **2014**; 40:296-301.
110. Sabala, C.L., F.W. Benenati, and B.R. Neas. Bilateral root or root canal aberrations in a dental school patient population. *J Endod*, **1994**; 20:38-42.
111. Slowey, R.R. Root canal anatomy. Road map to successful endodontics. *Dent Clin North Am*, **1979**; 23:555-573.
112. Kirthiga, M., M. Manju, R. Praveen, and W. Umesh. Prevalence of aberrant dental morphological details in 6-10 year old school children in an Indian population. *Contemp Clin Dent*, **2015**; 6:S175-180.
113. Dental Anthropology Association. 2018. [cited 2018 10.04.2018]; Available from: <http://www.dentalanthropology.org/>.
114. Diaz, E., L. Garcia, M. Hernandez, L. Palacio, D. Ruiz, N. Velandia, J. Villavicencio, and F. Moreno. Frequency and variability of dental morphology in deciduous and permanent dentition of a Nasa indigenous group in the municipality of Morales, Cauca, Colombia. *Colomb Med (Cali)*, **2014**; 45:15-24.
115. Scott, G.R., C.G. Turner, G. Townsend, and M.a. Martínón-Torres, *The anthropology of modern human teeth : dental morphology and its variation in recent and fossil Homo sapiens*. Second edition. ed. Cambridge studies in biological and evolutionary anthropology. **2017**, Cambridge, United Kingdom ; New York, NY: Cambridge University Press.
116. Mosharraf, R., B. Ebadian, Z. Ali, A. Najme, S. Niloofar, and K. Leila. Occlusal morphology of mandibular second molars in Iranian adolescents. *Indian journal of dental research : official publication of Indian Society for Dental Research*, **2010**; 21:16-19.
117. Plotino, G., L. Tocci, N.M. Grande, L. Testarelli, D. Messineo, M. Ciotti, G. Glassman, F. D'Ambrosio, and G. Gambarini. Symmetry of root and root canal morphology of maxillary and mandibular molars in a white population: a cone-beam computed tomography study in vivo. *J Endod*, **2013**; 39:1545-1548.
118. Cantatore, G., E. Berutti, and A. Castellucci. Missed anatomy: frequency and clinical impact. *Endod Topics*, **2006**; 15:3-31.
119. Curzon, M.E. and J.A. Curzon. Three-rooted mandibular molars in the Keewatin Eskimo. *J Can Dent Assoc (Tor)*, **1971**; 37:71-72.
120. Curzon, M.E.J. Miscegenation and Prevalence of 3-Rooted Mandibular First Molars in Baffin-Eskimo. *Community Dent Oral Epidemiol*, **1974**; 2:130-131.
121. von Zuben, M., J.N.R. Martins, L. Berti, I. Cassim, D. Flynn, J.A. Gonzalez, Y. Gu, J. Kottoor, A. Monroe, R. Rosas Aguilar, M.S. Marques, and A. Ginjeira. Worldwide Prevalence of Mandibular Second Molar C-Shaped Morphologies

- Evaluated by Cone-Beam Computed Tomography. *J Endod*, **2017**; 43:1442-1447.
122. Scott, G.R., R.H. Potter, J.F. Noss, A.A. Dahlberg, and T. Dahlberg. The dental morphology of Pima Indians. *Am J Phys Anthropol*, **1983**; 61:13-31.
 123. Felsypremila, G., T.S. Vinothkumar, and D. Kandaswamy. Anatomic symmetry of root and root canal morphology of posterior teeth in Indian subpopulation using cone beam computed tomography: A retrospective study. *Eur J Dent*, **2015**; 9:500-507.
 124. Zhang, R., H. Yang, X. Yu, H. Wang, T. Hu, and P.M. Dummer. Use of CBCT to identify the morphology of maxillary permanent molar teeth in a Chinese subpopulation. *Int Endod J*, **2011**; 44:162-169.
 125. Kim, Y., S.J. Lee, and J. Woo. Morphology of maxillary first and second molars analyzed by cone-beam computed tomography in a Korean population: variations in the number of roots and canals and the incidence of fusion. *J Endod*, **2012**; 38:1063-1068.
 126. Tian, Y.Y., B. Guo, R. Zhang, X. Yu, H. Wang, T. Hu, and P.M. Dummer. Root and canal morphology of maxillary first premolars in a Chinese subpopulation evaluated using cone-beam computed tomography. *Int Endod J*, **2012**; 45:996-1003.
 127. Guo, J., A. Vahidnia, P. Sedghizadeh, and R. Enciso. Evaluation of root and canal morphology of maxillary permanent first molars in a North American population by cone-beam computed tomography. *J Endod*, **2014**; 40:635-639.
 128. Lin, Z., Q. Hu, T. Wang, J. Ge, S. Liu, M. Zhu, and S. Wen. Use of CBCT to investigate the root canal morphology of mandibular incisors. *Surg Radiol Anat*, **2014**; 36:877-882.
 129. Kayaoglu, G., I. Peker, M. Gumusok, C. Sarikir, A. Kayadugun, and O. Ucok. Root and canal symmetry in the mandibular anterior teeth of patients attending a dental clinic: CBCT study. *Braz Oral Res*, **2015**; 29.
 130. Huang, Y.D., J. Wu, R.J. Sheu, M.H. Chen, D.L. Chien, Y.T. Huang, C.C. Huang, and Y.J. Chen. Evaluation of the root and root canal systems of mandibular first premolars in northern Taiwanese patients using cone-beam computed tomography. *J Formos Med Assoc*, **2015**; 114:1129-1134.
 131. Kim, S.Y., B.S. Kim, and Y. Kim. Mandibular second molar root canal morphology and variants in a Korean subpopulation. *Int Endod J*, **2016**; 49:136-144.
 132. Tian, X.M., X.W. Yang, L. Qian, B. Wei, and Y. Gong. Analysis of the Root and Canal Morphologies in Maxillary First and Second Molars in a Chinese Population Using Cone-beam Computed Tomography. *J Endod*, **2016**; 42:696-701.
 133. Ratanajirasut, R., A. Panichuttra, and S. Panmekiate. A Cone-beam Computed Tomographic Study of Root and Canal Morphology of Maxillary First and Second Permanent Molars in a Thai Population. *J Endod*, **2018**; 44:56-61.
 134. Shemesh, H., Kavalarchik E., Levin A., Ben Itzhak J., Levinson O., Lvovsky A., Solomonov M. Root Canal Morphology Evaluation of Central and Lateral Mandibular Incisors Using Cone-beam Computed Tomography in an Israeli Population. *Int Endod J*, **2018**; 44:51-55.
 135. Eleazer, P.D., G.N. Glickman, S.B. McClanahan, T.D. Webb, and B.C. Justman. Glossary of Endodontic Terms [AAE Web site]. [Electronic Glossary] 2012. [cited 2015 October 4]; 8th:[Glossary]. Available from: <http://www.aae.org/glossary/>.

136. Vertucci, F.J. Root canal morphology and its relationship to endodontic procedures. *Endod Topics*, **2005**; 10:3-29.
137. Tabassum, S. and F.R. Khan. Failure of endodontic treatment: The usual suspects. *Eur J Dent*, **2016**; 10:144-147.
138. Ørstavik, D. and T.R. Pitt Ford, *Essential endodontology : prevention and treatment of apical periodontitis*. 2nd ed. **2008**, Oxford, UK: Blackwell Munksgaard. 478.
139. Verissimo, D.M. and M.S. do Vale. Methodologies for assessment of apical and coronal leakage of endodontic filling materials: a critical review. *J Oral Sci*, **2006**; 48:93-98.
140. Friedman, S., S. Abitbol, and H.P. Lawrence. Treatment outcome in endodontics: the Toronto Study. Phase 1: initial treatment. *J Endod*, **2003**; 29:787-793.
141. Strindberg, L.Z., The dependence of the results of pulp therapy on certain factors: an analytic study based on radiographic and clinical follow-up examinations. *Acta odontologica scandinavica Suppl.* **1956**, Stockholm,.
142. Engstrom, B. and M. Lundberg. The correlation between positive culture and the prognosis of root canal therapy after pulpectomy. *Odontol Revy*, **1965**; 16:193-203.
143. Kerekes, K. and L. Tronstad. Long-term results of endodontic treatment performed with a standardized technique. *J Endod*, **1979**; 5:83-90.
144. Eriksen, H.M., D. Orstavik, and K. Kerekes. Healing of apical periodontitis after endodontic treatment using three different root canal sealers. *Endod Dent Traumatol*, **1988**; 4:114-117.
145. Azim, A.A., J.A. Griggs, and G.T. Huang. The Tennessee study: factors affecting treatment outcome and healing time following nonsurgical root canal treatment. *Int Endod J*, **2016**; 49:6-16.
146. Ng, Y.L., V. Mann, and K. Gulabivala. Tooth survival following non-surgical root canal treatment: a systematic review of the literature. *Int Endod J*, **2010**; 43:171-189.
147. Peters, L.B. and P.R. Wesselink. Periapical healing of endodontically treated teeth in one and two visits obturated in the presence or absence of detectable microorganisms. *Int Endod J*, **2002**; 35:660-667.
148. Ørstavik, D., *Endodontiske Materialer* **2012**.
149. Hatton, E.H., J.A. Marshall, U.G. Rickert, J.R. Blayney, and E.M. Hall. *Methods and Fundamentals in the Allied Sciences Essential to Successful Root-Canal Surgery*. *Dental Cosmos*, **1928**; 70:249-263.
150. Romelli, J.A., J.J. Laiolo, A. Navia, E. Reboredo, and R. Reig. [The relation in endodontia between the instruments and the internal topography of the teeth]. *Rev Odontol (B Aires)*, **1953**; 41:551-556.
151. Haga, C.S. Microscopic measurements of root canal preparations following instrumentation. *J Br Endod Soc*, **1968**; 2:41-46.
152. Gutierrez, J.H. and J. Garcia. Microscopic and macroscopic investigation on results of mechanical preparation of root canals. *Oral Surg Oral Med Oral Pathol*, **1968**; 25:108-116.
153. Davis, S.R., S.M. Brayton, and M. Goldman. The morphology of the prepared root canal: a study utilizing injectable silicone. *Oral Surg Oral Med Oral Pathol*, **1972**; 34:642-648.

154. Bramante, C.M., A. Berbert, and R.P. Borges. A methodology for evaluation of root canal instrumentation. *J Endod*, **1987**; 13:243-245.
155. McComb, D. and D.C. Smith. A preliminary scanning electron microscopic study of root canals after endodontic procedures. *J Endod*, **1975**; 1:238-242.
156. De-Deus, G., C. Reis, and S. Paciornik. Critical appraisal of published smear layer-removal studies: methodological issues. *Oral Surg Oral Med Oral Pathol Oral Radiol Endod*, **2011**; 112:531-543.
157. Espir, C.G., C.A. Nascimento-Mendes, J.M. Guerreiro-Tanomaru, L.G. Freire, G. Gavini, and M. Tanomaru-Filho. Counterclockwise or clockwise reciprocating motion for oval root canal preparation: a micro-CT analysis. *Int Endod J*, **2018**; 51:541-548.
158. Robinson, J.P., P.J. Lumley, P.R. Cooper, L.M. Grover, and A.D. Walmsley. Reciprocating root canal technique induces greater debris accumulation than a continuous rotary technique as assessed by 3-dimensional micro-computed tomography. *J Endod*, **2013**; 39:1067-1070.
159. Brasil, S.C., M.F. Marceliano-Alves, M.L. Marques, J.P. Grillo, M. Lacerda, F.R.F. Alves, J.F. Siqueira, Jr., and J.C. Provenzano. Canal Transportation, Unprepared Areas, and Dentin Removal after Preparation with BT-RaCe and ProTaper Next Systems. *J Endod*, **2017**; 43:1683-1687.
160. Peters, O.A., K. Schonenberger, and A. Laib. Effects of four Ni-Ti preparation techniques on root canal geometry assessed by micro computed tomography. *Int Endod J*, **2001**; 34:221-230.
161. Espir, C.G., C.A. Nascimento-Mendes, J.M. Guerreiro-Tanomaru, B.C. Cavenago, M.A. Hungaro Duarte, and M. Tanomaru-Filho. Shaping ability of rotary or reciprocating systems for oval root canal preparation: a micro-computed tomography study. *Clin Oral Investig*, **2018**.
162. Azim, A.A., L. Piasecki, U.X. da Silva Neto, A.T.G. Cruz, and K.A. Azim. XP Shaper, A Novel Adaptive Core Rotary Instrument: Micro-computed Tomographic Analysis of Its Shaping Abilities. *J Endod*, **2017**; 43:1532-1538.
163. Versiani, M.A., K.K.T. Carvalho, J.F. Mazzi-Chaves, and M.D. Sousa-Neto. Micro-computed Tomographic Evaluation of the Shaping Ability of XP-endo Shaper, iRaCe, and EdgeFile Systems in Long Oval-shaped Canals. *J Endod*, **2018**; 44:489-495.
164. Siqueira, J.F., Jr., A.R. Perez, M.F. Marceliano-Alves, J.C. Provenzano, S.G. Silva, F.R. Pires, G.C.S. Vieira, I.N. Rocas, and F.R.F. Alves. What happens to unprepared root canal walls: a correlative analysis using micro-computed tomography and histology/scanning electron microscopy. *Int Endod J*, **2018**; 51:501-508.
165. Hunter, W. An Address ON THE RÔLE OF SEPSIS AND OF ANTISEPSIS IN MEDICINE. *The Lancet*, **1911**; 177:79-86.
166. Price, W.A. Report of Laboratory Investigations on the Physical Properties of Root Filling Materials and the Efficiency of Root Fillings for Blocking Infection from Sterile Tooth Structures. *The Journal of the National Dental Association*, **1918**; 5:1260-1280.
167. Pallasch, T.J. and M.J. Wahl. Focal infection: new age or ancient history? *Endod Topics*, **2003**; 4:32-45.

168. Ingle, J.I. A standardized endodontic technique utilizing newly designed instruments and filling materials. *Oral Surg Oral Med Oral Pathol*, **1961**; 14:83-91.
169. Ingle, J.I., *Endodontics*. **1965**, Philadelphia,: Lea & Febiger. 656.
170. Klevant, F.J. and C.O. Eggink. The effect of canal preparation on periapical disease. *Int Endod J*, **1983**; 16:68-75.
171. Sabeti, M.A., M. Nekofar, P. Motahary, M. Ghandi, and J.H. Simon. Healing of apical periodontitis after endodontic treatment with and without obturation in dogs. *J Endod*, **2006**; 32:628-633.
172. Johnsen, G.F., H. Valen, and D. Østavik, *Endodontiske materialer : skyllemidler, sealere og obturerende materialer*. Dentale materialer. S. 1080-1088.
173. AAE, *Endodontics: Colleagues for Excellence - Root Canal Irrigants and Disinfectants*, AAE, Editor. **2011**, American Association of Endodontists.
174. Dixon, C.M. and U.G. Rickert. Tissue Tolerance to Foreign Materials**From the School of Dentistry, University of Michigan.*Read before the Section on Histology, Physiology, Pathology, Bacteriology and Chemistry (Research) at the Seventy-Fourth Annual Session of the American Dental Association, Buffalo, N. Y., Sept. 14, 1932. *The Journal of the American Dental Association (1922)*, **1933**; 20:1458-1472.
175. Rickert, U.G. and C.M. Dixon. The controlling of root surgery. in *Transactions of the Eighth International Dental Congress*. **1931**: Fédération Dentaire Internationale, Paris.
176. Kakehashi, S., H.R. Stanley, and R.J. Fitzgerald. The Effects of Surgical Exposures of Dental Pulp in Germ-Free and Conventional Laboratory Rats. *Oral Surg Oral Med Oral Pathol*, **1965**; 20:340-349.
177. Moller, A.J., L. Fabricius, G. Dahlen, A.E. Ohman, and G. Heyden. Influence on periapical tissues of indigenous oral bacteria and necrotic pulp tissue in monkeys. *Scand J Dent Res*, **1981**; 89:475-484.
178. Torneck, C.D. Reaction of rat connective tissue to polyethylene tube implants. I. *Oral Surg Oral Med Oral Pathol*, **1966**; 21:379-387.
179. Torneck, C.D. Reaction of rat connective tissue to polyethylene tube implants. II. *Oral Surg Oral Med Oral Pathol*, **1967**; 24:674-683.
180. Sjogren, U., B. Hagglund, G. Sundqvist, and K. Wing. Factors affecting the long-term results of endodontic treatment. *J Endod*, **1990**; 16:498-504.
181. Ng, Y.L., V. Mann, S. Rahbaran, J. Lewsey, and K. Gulabivala. Outcome of primary root canal treatment: systematic review of the literature -- Part 2. Influence of clinical factors. *Int Endod J*, **2008**; 41:6-31.
182. Kirkevang, L.L., D. Orstavik, P. Horsted-Bindslev, and A. Wenzel. Periapical status and quality of root fillings and coronal restorations in a Danish population. *Int Endod J*, **2000**; 33:509-515.
183. Kirkevang, L.L., M. Vaeth, and A. Wenzel. Tooth-specific risk indicators for apical periodontitis. *Oral Surg Oral Med Oral Pathol Oral Radiol Endod*, **2004**; 97:739-744.
184. Ray, H.A. and M. Trope. Periapical status of endodontically treated teeth in relation to the technical quality of the root filling and the coronal restoration. *Int Endod J*, **1995**; 28:12-18.

185. Tronstad, L., K. Asbjornsen, L. Doving, I. Pedersen, and H.M. Eriksen. Influence of coronal restorations on the periapical health of endodontically treated teeth. *Endod Dent Traumatol*, **2000**; 16:218-221.
186. Brayton, S.M., S.R. Davis, and M. Goldman. Gutta-percha root canal fillings. An in vitro analysis. I. *Oral Surg Oral Med Oral Pathol*, **1973**; 35:226-231.
187. Goldman, M. Evaluation of two filling methods for root canals. *J Endod*, **1975**; 1:69-72.
188. Larder, T.C., A.J. Prescott, and S.M. Brayton. Gutta-percha: a comparative study of three methods of obturation. *J Endod*, **1976**; 2:289-294.
189. Benkel, B., D. Rising, L. Goldman, H. Rosen, M. Goldman, and J. Kronman. Use of a hydrophilic plastic as a root canal filling material. *J Endod*, **1976**; 2:196-202.
190. Rising, D.W., M. Goldman, and S.M. Brayton. Histologic appraisal of 3 experimental root canal filling materials. *J Endod*, **1975**; 1:172-177.
191. Goldman, L.B., M. Goldman, J.H. Kronman, and J.M. Letourneau. Adaptation and porosity of poly-HEMA in a model system using two microorganisms. *J Endod*, **1980**; 6:683-686.
192. Goldman, L.B., M. Goldman, J.H. Kronman, and C. Kliment. Results of Clinical-Trial of Hydronr Root-Canal Filling Material. *J Dent Res*, **1978**; 57:162-162.
193. McNamara, J.R., G.S. Heithersay, and O.W. Wiebkin. Cell responses to Hydron by a new in-vitro method. *Int Endod J*, **1992**; 25:205-212.
194. Reid, R.J., D.F. Wilson, K.K. Chau, G.S. Heithersay, and P.S. Heijkoop. Tissue responses to Hydron, assessed by intramuscular implantation. *Int Endod J*, **1992**; 25:199-204.
195. Reid, R.J., P.V. Abbott, J.R. McNamara, and G.S. Heithersay. A five-year study of Hydron root canal fillings. *Int Endod J*, **1992**; 25:213-220.
196. Murrin, J.R., A. Reader, D.W. Foreman, M. Beck, and W.J. Meyers. Hydron versus gutta-percha and sealer: a study of endodontic leakage using the scanning electron microscope and energy-dispersive analysis. *J Endod*, **1985**; 11:101-109.
197. Tanzilli, J.P., A.J. Nevins, and B.G. Borden. A histologic study comparing Hydron and gutta-percha as root canal filling materials in monkeys. *J Endod*, **1981**; 7:396-401.
198. Langeland, K., B. Olsson, and E.A. Pascon. Biological evaluation of Hydron. *J Endod*, **1981**; 7:196-204.
199. Tay, F.R. and D.H. Pashley. Monoblocks in root canals: a hypothetical or a tangible goal. *J Endod*, **2007**; 33:391-398.
200. Raina, R., R.J. Loushine, R.N. Weller, F.R. Tay, and D.H. Pashley. Evaluation of the quality of the apical seal in Resilon/Epiphany and Gutta-Percha/AH Plus-filled root canals by using a fluid filtration approach. *J Endod*, **2007**; 33:944-947.
201. Shipper, G., F.B. Teixeira, R.R. Arnold, and M. Trope. Periapical inflammation after coronal microbial inoculation of dog roots filled with gutta-percha or resilon. *J Endod*, **2005**; 31:91-96.
202. Shipper, G., D. Orstavik, F.B. Teixeira, and M. Trope. An evaluation of microbial leakage in roots filled with a thermoplastic synthetic polymer-based root canal filling material (Resilon). *J Endod*, **2004**; 30:342-347.

203. Teixeira, F.B., E.C. Teixeira, J.Y. Thompson, and M. Trope. Fracture resistance of roots endodontically treated with a new resin filling material. *J Am Dent Assoc*, **2004**; 135:646-652.
204. Barborka, B.J., K.F. Woodmansey, G.N. Glickman, E. Schneiderman, and J. He. Long-term Clinical Outcome of Teeth Obturated with Resilon. *J Endod*, **2017**; 43:556-560.
205. Hammad, M., A. Qualtrough, and N. Silikas. Evaluation of root canal obturation: a three-dimensional in vitro study. *J Endod*, **2009**; 35:541-544.
206. Jung, M., D. Lommel, and J. Klimek. The imaging of root canal obturation using micro-CT. *Int Endod J*, **2005**; 38:617-626.
207. Metzger, Z., R. Zary, R. Cohen, E. Teperovich, and F. Paque. The quality of root canal preparation and root canal obturation in canals treated with rotary versus self-adjusting files: a three-dimensional micro-computed tomographic study. *J Endod*, **2010**; 36:1569-1573.
208. Moeller, L., A. Wenzel, A.M. Wegge-Larsen, M. Ding, and L.L. Kirkevang. Quality of root fillings performed with two root filling techniques. An in vitro study using micro-CT. *Acta Odontol Scand*, **2013**; 71:689-696.
209. Liddell, H.G. and R. Scott. A Greek-English Lexicon 1940. [cited; Available from: <http://www.perseus.tufts.edu/hopper/text?doc=Perseus%3Atext%3A1999.04.0057%3Aentry%3Dgraph%2F>].
210. Ritman, E.L. Current status of developments and applications of micro-CT. *Annu Rev Biomed Eng*, **2011**; 13:531-552.
211. White, S.C. and M.J. Pharoah, Oral Radiology: Principles and Interpretation. **2004**, Missouri: Mosby. 742.
212. Radon, J. On the Determination of Functions from Their Integral Values along Certain Manifolds. *IEEE Trans Med Imaging*, **1986**; 5:170-176.
213. Cormack, A.M. Representation of a Function by Its Line Integrals with Some Radiological Applications. *J Appl Phys*, **1963**; 34:2722-2727.
214. Cormack, A.M. Representation of Function by Its Line Integrals with Some Radiological Applications. II. *J Appl Phys*, **1964**; 35:2908-2913.
215. Flannery, B.P., H.W. Deckman, W.G. Roberge, and K.L. D'Amico. Three-Dimensional X-ray Microtomography. *Science*, **1987**; 237:1439-1444.
216. Hounsfield, G.N. Computerized transverse axial scanning (tomography). 1. Description of system. *Br J Radiol*, **1973**; 46:1016-1022.
217. Wolpert, S.M. Neuroradiology classics. *AJNR Am J Neuroradiol*, **2000**; 21:605-606.
218. Feldkamp, L.A., L.C. Davis, and J.W. Kress. Practical Cone-Beam Algorithm. *J Opt Soc Am A Opt Image Sci Vis*, **1984**; 1:612-619.
219. Elliott, J.C., S.E. Dowker, and R.D. Knight. Scanning X-ray microradiography of a section of a carious lesion in dental enamel. *J Microsc*, **1981**; 123:89-92.
220. Elliott, J.C. and S.D. Dover. X-ray microtomography. *J Microsc*, **1982**; 126:211-213.
221. Morton, E.J., S. Webb, J.E. Bateman, L.J. Clarke, and C.G. Shelton. Three-dimensional x-ray microtomography for medical and biological applications. *Phys Med Biol*, **1990**; 35:805-820.

222. Mozzo, P., C. Procacci, A. Tacconi, P.T. Martini, and I.A. Andreis. A new volumetric CT machine for dental imaging based on the cone-beam technique: preliminary results. *Eur Radiol*, **1998**; 8:1558-1564.
223. Kiljunen, T., T. Kaasalainen, A. Suomalainen, and M. Kortensniemi. Dental cone beam CT: A review. *Phys Med*, **2015**; 31:844-860.
224. Brullmann, D. and R.K. Schulze. Spatial resolution in CBCT machines for dental/maxillofacial applications-what do we know today? *Dentomaxillofac Radiol*, **2015**; 44:20140204.
225. Nielsen, R.B., A.M. Alyassin, D.D. Peters, D.L. Carnes, and J. Lancaster. Microcomputed tomography: an advanced system for detailed endodontic research. *J Endod*, **1995**; 21:561-568.
226. Dowker, S.E., G.R. Davis, and J.C. Elliott. X-ray microtomography: nondestructive three-dimensional imaging for in vitro endodontic studies. *Oral Surg Oral Med Oral Pathol Oral Radiol Endod*, **1997**; 83:510-516.
227. Dowker, S.E., G.R. Davis, J.C. Elliott, and F.S. Wong. X-ray microtomography: 3-dimensional imaging of teeth for computer-assisted learning. *Eur J Dent Educ*, **1997**; 1:61-65.
228. Bjorndal, L., O. Carlsen, G. Thuesen, T. Darvann, and S. Kreiborg. External and internal macromorphology in 3D-reconstructed maxillary molars using computerized X-ray microtomography. *Int Endod J*, **1999**; 32:3-9.
229. Rhodes, J.S., T.R. Ford, J.A. Lynch, P.J. Liepins, and R.V. Curtis. Micro-computed tomography: a new tool for experimental endodontology. *Int Endod J*, **1999**; 32:165-170.
230. Peters, O.A., A. Laib, P. Ruegsegger, and F. Barbakow. Three-dimensional analysis of root canal geometry by high-resolution computed tomography. *J Dent Res*, **2000**; 79:1405-1409.
231. Bergmans, L., J. Van Cleynenbreugel, M. Wevers, and P. Lambrechts. A methodology for quantitative evaluation of root canal instrumentation using microcomputed tomography. *Int Endo J*, **2001**; 34:390-398.
232. Jin, G.C., S.J. Lee, and B.D. Roh. Anatomical study of C-shaped canals in mandibular second molars by analysis of computed tomography. *J Endod*, **2006**; 32:10-13.
233. Lee, J.K., B.H. Ha, J.H. Choi, S.M. Heo, and H. Perinpanayagam. Quantitative three-dimensional analysis of root canal curvature in maxillary first molars using micro-computed tomography. *J Endod*, **2006**; 32:941-945.
234. Hammad, M., A. Qualtrough, and N. Silikas. Three-dimensional evaluation of effectiveness of hand and rotary instrumentation for retreatment of canals filled with different materials. *J Endod*, **2008**; 34:1370-1373.
235. Gao, Y., O.A. Peters, H. Wu, and X. Zhou. An application framework of three-dimensional reconstruction and measurement for endodontic research. *J Endod*, **2009**; 35:269-274.
236. Paque, F., A. Laib, H. Gautschi, and M. Zehnder. Hard-tissue debris accumulation analysis by high-resolution computed tomography scans. *J Endod*, **2009**; 35:1044-1047.
237. Salmon, P.L. and A.Y. Sasov, Application of nano-CT and high-resolution micro-CT to study bone quality and ultrastructure, scaffold biomaterials and vascular networks, in *Advanced Bioimaging Technologies in Assessment of the Quality of*

- Bone and Scaffold Materials: Techniques and Applications. **2007**, Springer: Berlin. 323-331.
238. Tiainen, H., S.P. Lyngstadaas, J.E. Ellingsen, and H.J. Haugen. Ultra-porous titanium oxide scaffold with high compressive strength. *J Mater Sci Mater Med*, **2010**; 21:2783-2792.
239. Sabetrasekh, R., H. Tiainen, S.P. Lyngstadaas, J. Reseland, and H. Haugen. A novel ultra-porous titanium dioxide ceramic with excellent biocompatibility. *J Biomater Appl*, **2011**; 25:559-580.
240. The Physikalisch-Technische Bundesanstalt - Facts about PTB. 2018. [cited; Available from: <https://www.ptb.de/cms/en/about-us-careers/about-us/facts-about-ptb.html>].
241. 3D Systems - IS 3D SYSTEMS SOFTWARE CERTIFIED? 2017. [cited; Available from: <http://support1.geomagic.com/Support/5605/5668/en-US/Article/View/772/Is-3D-Systems-software-certified/0>].
242. Piccinelli, M., A. Veneziani, D.A. Steinman, A. Remuzzi, and L. Antiga. A framework for geometric analysis of vascular structures: application to cerebral aneurysms. *IEEE Trans Med Imaging*, **2009**; 28:1141-1155.
243. Antiga, L., M. Piccinelli, L. Botti, B. Ene-lordache, A. Remuzzi, and D.A. Steinman. An image-based modeling framework for patient-specific computational hemodynamics. *Med Biol Eng Comput*, **2008**; 46:1097-1112.
244. McDonald, C., A Computational Validation of MRI as a Surveillance Tool for Vascular Access in End-Stage Renal Disease, in Physics Department. **2015**, University of St Andrews.
245. Dillard, S.I., J.A. Mousel, L. Shrestha, M.L. Raghavan, and S.C. Vigmostad. From medical images to flow computations without user-generated meshes. *Int J Numer Method Biomed Eng*, **2014**; 30:1057-1083.
246. Klepaczko, A., P. Szczypinski, A. Deistung, J.R. Reichenbach, and A. Materka. Simulation of MR angiography imaging for validation of cerebral arteries segmentation algorithms. *Comput Methods Programs Biomed*, **2016**; 137:293-309.
247. Mirfendereski, M. and O. Peters, Micro-Computed Tomography in Endodontic Research, in *Endodontic Radiology*, B. Basrani, Editor. **2017**, John Wiley & Sons, Inc: New Jersey. 278-284.
248. Ordinola-Zapata, R., C.M. Bramante, M.A. Versiani, B.I. Moldauer, G. Topham, J.L. Gutmann, A. Nunez, M.A. Duarte, and F. Abella. Comparative accuracy of the Clearing Technique, CBCT and Micro-CT methods in studying the mesial root canal configuration of mandibular first molars. *Int Endod J*, **2017**; 50:90-96.
249. Davis, G.R. and F.S. Wong. X-ray microtomography of bones and teeth. *Physiol Meas*, **1996**; 17:121-146.
250. Davis, G.R. and J.C. Elliott. Artefacts in X-ray microtomography of materials. *Mater Sci Tech-Lond*, **2006**; 22:1011-1018.
251. Boas, F.E. and D. Fleischmann. CT artifacts: causes and reduction techniques. *Imag Med*, **2012**; 4:229-240.
252. Barrett, J.F. and N. Keat. Artifacts in CT: recognition and avoidance. *Radiographics*, **2004**; 24:1679-1691.
253. Queiroz, P.M., K. Rovaris, H. Gaeta-Araujo, S. Marzola de Souza Bueno, D.Q. Freitas, F.C. Groppo, and F. Haiter-Neto. Influence of Artifact Reduction Tools in

- Micro-computed Tomography Images for Endodontic Research. *J Endod*, **2017**; 43:2108-2111.
254. Besl, P.J. and N.D. McKay. A method for registration of 3-D shapes. *IEEE T Pattern Anal*, **1992**; 14:239-256.
255. Chen, Y. and G. Medioni. Object Modeling by Registration of Multiple Range Images. 1991 *IEEE International Conference on Robotics and Automation*, Vols 1-3, **1991**; 2724-2729.
256. Nguyen, T., L. Cevidanes, M.A. Cornelis, G. Heymann, L.K. de Paula, and H. De Clerck. Three-dimensional assessment of maxillary changes associated with bone anchored maxillary protraction. *Am J Orthod Dentofacial Orthop*, **2011**; 140:790-798.
257. Boyer, D.M., Y. Lipman, E. St Clair, J. Puente, B.A. Patel, T. Funkhouser, J. Jernvall, and I. Daubechies. Algorithms to automatically quantify the geometric similarity of anatomical surfaces. *Proc Natl Acad Sci U S A*, **2011**; 108:18221-18226.
258. Alqattan, M., J. Djordjevic, A.I. Zhurov, and S. Richmond. Comparison between landmark and surface-based three-dimensional analyses of facial asymmetry in adults. *Eur J Orthod*, **2015**; 37:1-12.
259. Hilaga, M., Y. Shinagawa, T. Kohmura, and T.L. Kunii. Topology Matching for fully automatic similarity estimation of 3D shapes. in *SIGGRAPH 2001 Proceedings of the 28th annual conference on Computer graphics and interactive techniques 2001*. New York, NY, USA.
260. Osada, R., T. Funkhouser, B. Chazelle, and D. Dobkin. Matching 3D models with shape distributions. *International Conference on Shape Modeling and Applications, Proceeding*, **2001**; 154-168.
261. Verhoeven, T., T. Xi, R. Schreurs, S. Berge, and T. Maal. Quantification of facial asymmetry: A comparative study of landmark-based and surface-based registrations. *J Craniomaxillofac Surg*, **2016**; 44:1131-1136.
262. Roumeliotis, G., R. Willing, M. Neuert, R. Ahluwalia, T. Jenkyn, and A. Yazdani. Application of a Novel Semi-Automatic Technique for Determining the Bilateral Symmetry Plane of the Facial Skeleton of Normal Adult Males. *J Craniofac Surg*, **2015**; 26:1997-2001.
263. Markvart, M., L. Bjorndal, T.A. Darvann, P. Larsen, M. Dalstra, and S. Kreiborg. Three-dimensional analysis of the pulp cavity on surface models of molar teeth, using X-ray micro-computed tomography. *Acta Odontol Scand*, **2012**; 70:133-139.
264. Roane, J.B., C.L. Sabala, and M.G. Duncanson, Jr. The "balanced force" concept for instrumentation of curved canals. *J Endod*, **1985**; 11:203-211.
265. Hulsmann, M., O.A. Peters, and P.M.H. Dummer. Mechanical preparation of root canals: shaping goals, techniques and means. *Endod Topics*, **2005**; 10:30-76.
266. Walia, H.M., W.A. Brantley, and H. Gerstein. An initial investigation of the bending and torsional properties of Nitinol root canal files. *J Endod*, **1988**; 14:346-351.
267. Yared, G. Canal preparation using only one Ni-Ti rotary instrument: preliminary observations. *Int Endod J*, **2008**; 41:339-344.
268. Shen, Y., H.M. Zhou, Y.F. Zheng, B. Peng, and M. Haapasalo. Current challenges and concepts of the thermomechanical treatment of nickel-titanium instruments. *J Endod*, **2013**; 39:163-172.

269. Belladonna, F.G., M.S. Carvalho, D.M. Cavalcante, J.T. Fernandes, A.C. de Carvalho Maciel, H.E. Oliveira, R.T. Lopes, E. Silva, and G. De-Deus. Micro-computed Tomography Shaping Ability Assessment of the New Blue Thermal Treated Reciproc Instrument. *J Endod*, **2018**; 44:1146-1150.
270. Burklein, S., K. Hinschitza, T. Dammaschke, and E. Schafer. Shaping ability and cleaning effectiveness of two single-file systems in severely curved root canals of extracted teeth: Reciproc and WaveOne versus Mtwo and ProTaper. *Int Endod J*, **2012**; 45:449-461.
271. De-Deus, G., E.J. Silva, V.T. Vieira, F.G. Belladonna, C.N. Elias, G. Plotino, and N.M. Grande. Blue Thermomechanical Treatment Optimizes Fatigue Resistance and Flexibility of the Reciproc Files. *J Endod*, **2017**; 43:462-466.
272. Keskin, C., U. Inan, M. Demiral, and A. Keles. Cyclic Fatigue Resistance of Reciproc Blue, Reciproc, and WaveOne Gold Reciprocating Instruments. *J Endod*, **2017**; 43:1360-1363.
273. Topcuoglu, H.S. and G. Topcuoglu. Cyclic Fatigue Resistance of Reciproc Blue and Reciproc Files in an S-shaped Canal. *J Endod*, **2017**; 43:1679-1682.
274. de Vasconcelos, R.A., S. Murphy, C.A. Carvalho, R.G. Govindjee, S. Govindjee, and O.A. Peters. Evidence for Reduced Fatigue Resistance of Contemporary Rotary Instruments Exposed to Body Temperature. *J Endod*, **2016**; 42:782-787.
275. Grossman, L.I., *Endodontic practice*. 5th ed. **1960**, Philadelphia: Lea & Febiger. 402.
276. De-Deus, G. New directions in old leakage methods. *Int Endod J*, **2008**; 41:720-721; discussion 721-723.
277. Grossman, L.I. A Study of Temporary Fillings as Hermetic Sealing Agents. *J Dent Res*, **2016**; 18:67-71.
278. Bachicha, W.S., P.M. DiFiore, D.A. Miller, E.P. Lautenschlager, and D.H. Pashley. Microleakage of endodontically treated teeth restored with posts. *J Endod*, **1998**; 24:703-708.
279. Derkson, G.D., D.H. Pashley, and M.E. Derkson. Microleakage measurement of selected restorative materials: a new in vitro method. *J Prosthet Dent*, **1986**; 56:435-440.
280. Barthel, C.R., J. Moshonov, G. Shuping, and D. Orstavik. Bacterial leakage versus dye leakage in obturated root canals. *Int Endod J*, **1999**; 32:370-375.
281. De Bruyne, M.A., R.J. De Bruyne, and R.J. De Moor. Capillary flow porometry to assess the seal provided by root-end filling materials in a standardized and reproducible way. *J Endod*, **2006**; 32:206-209.
282. Torabinejad, M., B. Ung, and J.D. Kettering. In vitro bacterial penetration of coronally unsealed endodontically treated teeth. *J Endod*, **1990**; 16:566-569.
283. Michalesco, P. and P. Boudeville. Calibrated latex microspheres percolation: a possible route to model endodontic bacterial leakage. *J Endod*, **2003**; 29:456-462.
284. Dow, P.R. and J.I. Ingle. Isotope determination of root canal failure. *Oral Surg Oral Med Oral Pathol*, **1955**; 8:1100-1104.
285. Madison, S., K. Swanson, and S.A. Chiles. An evaluation of coronal microleakage in endodontically treated teeth. Part II. Sealer types. *J Endod*, **1987**; 13:109-112.

286. Allison, D.A., C.R. Weber, and R.E. Walton. The influence of the method of canal preparation on the quality of apical and coronal obturation. *J Endod*, **1979**; 5:298-304.
287. Yassen, G.H., J.A. Platt, and A.T. Hara. Bovine teeth as substitute for human teeth in dental research: a review of literature. *J Oral Sci*, **2011**; 53:273-282.
288. Karagenc, B., N. Gencoglu, M. Ersoy, G. Cansever, and G. Kulekci. A comparison of four different microleakage tests for assessment of leakage of root canal fillings. *Oral Surg Oral Med Oral Pathol Oral Radiol Endod*, **2006**; 102:110-113.
289. Eldeniz, A.U. and D. Orstavik. A laboratory assessment of coronal bacterial leakage in root canals filled with new and conventional sealers. *Int Endod J*, **2009**; 42:303-312.
290. Santos, J., L. Tjaderhane, C. Ferraz, A. Zaia, M. Alves, M. De Goes, and M. Carrilho. Long-term sealing ability of resin-based root canal fillings. *Int Endod J*, **2010**; 43:455-460.
291. Pommel, L., B. Jacquot, and J. Camps. Lack of correlation among three methods for evaluation of apical leakage. *J Endod*, **2001**; 27:347-350.
292. Wu, M.K. and P.R. Wesselink. Endodontic leakage studies reconsidered. Part I. Methodology, application and relevance. *Int Endod J*, **1993**; 26:37-43.
293. Goldman, M., S. Simmonds, and R. Rush. The usefulness of dye-penetration studies reexamined. *Oral Surg Oral Med Oral Pathol*, **1989**; 67:327-332.
294. Oliver, C.M. and P.V. Abbott. Correlation between clinical success and apical dye penetration. *Int Endo J*, **2001**; 34:637-644.
295. Susini, G., L. Pommel, I. About, and J. Camps. Lack of correlation between ex vivo apical dye penetration and presence of apical radiolucencies. *Oral Surg Oral Med Oral Pathol Oral Radiol Endod*, **2006**; 102:e19-23.
296. Rechenberg, D.K., T. Thurnheer, and M. Zehnder. Potential systematic error in laboratory experiments on microbial leakage through filled root canals: an experimental study. *Int Endod J*, **2011**; 44:827-835.
297. Lucena, C., J.M. Lopez, C. Abalos, V. Robles, and R. Pulgar. Statistical errors in microleakage studies in operative dentistry. A survey of the literature 2001-2009. *Eur J Oral Sci*, **2011**; 119:504-510.
298. Schuurs, A.H., M.K. Wu, P.R. Wesselink, and H.J. Duivenvoorden. Endodontic leakage studies reconsidered. Part II. Statistical aspects. *Int Endod J*, **1993**; 26:44-52.
299. Fardi, A., K. Kodonas, C. Gogos, and N. Economides. Top-cited articles in endodontic journals. *J Endod*, **2011**; 37:1183-1190.
300. Dummer, P. International Endodontic Journal 50th Anniversary Editorial. *Int Endod J*, **2017**; 50:921-923.
301. Editorial Board of the Journal of, E. Wanted: a base of evidence. *J Endod*, **2007**; 33:1401-1402.
302. Ferracane, J.L. Resin-based composite performance: are there some things we can't predict? *Dent Mater*, **2013**; 29:51-58.
303. AAE. Art and Science of New Materials in Endodontics. 2017. [cited 2018 19.06.2018]; Position Statement]. Available from: <https://www.aae.org/specialty/wp-content/uploads/sites/2/2017/06/newtechnologiesmaterials.pdf>.

304. Ferracane, J.L. Resin composite--state of the art. *Dent Mater*, **2011**; 27:29-38.
305. Khayat, A., S.J. Lee, and M. Torabinejad. Human saliva penetration of coronally unsealed obturated root canals. *J Endod*, **1993**; 19:458-461.
306. Trope, M., E. Chow, and R. Nissan. In vitro endotoxin penetration of coronally unsealed endodontically treated teeth. *Endod Dent Traumatol*, **1995**; 11:90-94.
307. Shipper, G. and M. Trope. In vitro microbial leakage of endodontically treated teeth using new and standard obturation techniques. *J Endod*, **2004**; 30:154-158.
308. Kirkevang, L.L., P. Horsted-Bindslev, D. Orstavik, and A. Wenzel. Frequency and distribution of endodontically treated teeth and apical periodontitis in an urban Danish population. *Int Endod J*, **2001**; 34:198-205.
309. Biggs, S.G., K.I. Knowles, J.L. Ibarrola, and D.H. Pashley. An in vitro assessment of the sealing ability of resilon/epiphany using fluid filtration. *J Endod*, **2006**; 32:759-761.
310. Tunga, U. and E. Bodrumlu. Assessment of the sealing ability of a new root canal obturation material. *J Endod*, **2006**; 32:876-878.
311. Key, J.E., F.G. Rahemtulla, and P.D. Eleazer. Cytotoxicity of a new root canal filling material on human gingival fibroblasts. *J Endod*, **2006**; 32:756-758.
312. Susini, G., I. About, L. Tran-Hung, and J. Camps. Cytotoxicity of Epiphany and Resilon with a root model. *Int Endod J*, **2006**; 39:940-944.
313. Leonardo, M.R., F. Barnett, G.J. Debelian, R.K. de Pontes Lima, and L.A. Bezerra da Silva. Root canal adhesive filling in dogs' teeth with or without coronal restoration: a histopathological evaluation. *J Endod*, **2007**; 33:1299-1303.
314. Duggan, D., R.R. Arnold, F.B. Teixeira, D.J. Caplan, and P. Tawil. Periapical inflammation and bacterial penetration after coronal inoculation of dog roots filled with RealSeal 1 or Thermafil. *J Endod*, **2009**; 35:852-857.
315. Conner, D.A., D.J. Caplan, F.B. Teixeira, and M. Trope. Clinical outcome of teeth treated endodontically with a nonstandardized protocol and root filled with resilon. *J Endod*, **2007**; 33:1290-1292.
316. Cotton, T.P., W.G. Schindler, S.A. Schwartz, W.R. Watson, and K.M. Hargreaves. A retrospective study comparing clinical outcomes after obturation with Resilon/Epiphany or Gutta-Percha/Kerr sealer. *J Endod*, **2008**; 34:789-797.
317. Hiraishi, N., F.T. Sadek, N.M. King, M. Ferrari, D.H. Pashley, and F.R. Tay. Susceptibility of a polycaprolactone-based root canal filling material to degradation using an agar-well diffusion assay. *Am J Dent*, **2008**; 21:119-123.
318. Hiraishi, N., J.Y. Yau, R.J. Loushine, S.R. Armstrong, R.N. Weller, N.M. King, D.H. Pashley, and F.R. Tay. Susceptibility of a polycaprolactone-based root canal-filling material to degradation. III. Turbidimetric evaluation of enzymatic hydrolysis. *J Endod*, **2007**; 33:952-956.
319. Tay, F.R., D.H. Pashley, R.J. Loushine, S. Kuttler, F. Garcia-Godoy, N.M. King, and M. Ferrari. Susceptibility of a polycaprolactone-based root canal filling material to degradation. Evidence of biodegradation from a simulated field test. *Am J Dent*, **2007**; 20:365-369.
320. Tay, F.R., D.H. Pashley, M.C. Williams, R. Raina, R.J. Loushine, R.N. Weller, W.F. Kimbrough, and N.M. King. Susceptibility of a polycaprolactone-based root canal filling material to degradation. I. Alkaline hydrolysis. *J Endod*, **2005**; 31:593-598.

321. Tay, F.R., D.H. Pashley, C.K. Yiu, J.Y. Yau, M. Yiu-fai, R.J. Loushine, R.N. Weller, W.F. Kimbrough, and N.M. King. Susceptibility of a polycaprolactone-based root canal filling material to degradation. II. Gravimetric evaluation of enzymatic hydrolysis. *J Endod*, **2005**; 31:737-741.
322. Tay, F.R., R.J. Loushine, P. Lambrechts, R.N. Weller, and D.H. Pashley. Geometric factors affecting dentin bonding in root canals: a theoretical modeling approach. *J Endod*, **2005**; 31:584-589.
323. Gogos, C., V. Theodorou, N. Economides, P. Beltes, and I. Kolokouris. Shear bond strength of AH-26 and Epiphany to composite resin and Resilon. *J Endod*, **2008**; 34:1385-1387.
324. De-Deus, G., K. Di Giorgi, S. Fidel, R.A. Fidel, and S. Paciornik. Push-out bond strength of Resilon/Epiphany and Resilon/Epiphany self-etch to root dentin. *J Endod*, **2009**; 35:1048-1050.
325. De-Deus, G., F. Namen, and J. Galan, Jr. Reduced long-term sealing ability of adhesive root fillings after water-storage stress. *J Endod*, **2008**; 34:322-325.
326. Baumgartner G, Z.M., Paque F. Enterococcus faecalis type strain leakage through root canals filled with Gutta-Percha/AH plus or Resilon/Epiphany. **2007**.
327. Paque, F. and G. Sirtes. Apical sealing ability of Resilon/Epiphany versus gutta-percha/AH Plus: immediate and 16-months leakage. *Int Endod J*, **2007**; 40:722-729.
328. De Bruyne, M.A. and R.J. De Moor. Long-term sealing ability of Resilon apical root-end fillings. *Int Endod J*, **2009**; 42:884-892.
329. Kadam, P. and S. Bhalerao. Sample size calculation. *Int J Ayurveda Res*, **2010**; 1:55-57.
330. Chan, Y.H. Randomised controlled trials (RCTs)--sample size: the magic number? *Singapore Med J*, **2003**; 44:172-174.
331. Aalen, O.O., *Innføring i statistikk : med medisinske eksempler*. 2. utg. ed. **1998**, Oslo: Gyldendal akademisk.
332. Souza, E. Research that matters: setting guidelines for the use and reporting of statistics. *Int Endod J*, **2014**; 47:115-119.
333. Barker, D.S., C. Schultz, J. Krishnan, and T.C. Hearn. Bilateral symmetry of the human metacarpal: implications for sample size calculations. *Clin Biomech (Bristol, Avon)*, **2005**; 20:846-852.
334. Sumner, D.R., T.M. Turner, and J.O. Galante. Symmetry of the canine femur: implications for experimental sample size requirements. *J Orthop Res*, **1988**; 6:758-765.
335. White, A.A., 3rd, M.M. Panjabi, and R.J. Hardy. Analysis of mechanical symmetry in rabbit long bones. *Acta Orthop Scand*, **1974**; 45:328-336.
336. Orth, P., D. Zurakowski, M. Alini, M. Cucchiaroni, and H. Madry. Reduction of sample size requirements by bilateral versus unilateral research designs in animal models for cartilage tissue engineering. *Tissue Eng Part C Methods*, **2013**; 19:885-891.
337. Hearn, T.C., J.P. Szalai, J.F. Surowiak, and J. Schatzker. Sample size estimates for the use of human bone in the experimental study of cancellous screw extraction mechanics. *J Biomech*, **1996**; 29:569-572.

338. Woodward, H.N., J.R. Horner, and J.O. Farlow. Quantification of intraskeletal histovariability in Alligator mississippiensis and implications for vertebrate osteohistology. *PeerJ*, **2014**; 2:e422.
339. Silveira, S.B., F.R.F. Alves, M.F. Marceliano-Alves, J.C.N. Sousa, V.T.L. Vieira, J.F. Siqueira, Jr., H.P. Lopes, and J.C. Provenzano. Removal of Root Canal Fillings in Curved Canals Using Either Mani GPR or HyFlex NT Followed by Passive Ultrasonic Irrigation. *J Endod*, **2018**; 44:299-303 e291.
340. Lacerda, M., M.F. Marceliano-Alves, A.R. Perez, J.C. Provenzano, M.A.S. Neves, F.R. Pires, L.S. Goncalves, I.N. Rocas, and J.F. Siqueira, Jr. Cleaning and Shaping Oval Canals with 3 Instrumentation Systems: A Correlative Micro-computed Tomographic and Histologic Study. *J Endod*, **2017**; 43:1878-1884.
341. Paque, F. and O.A. Peters. Micro-computed tomography evaluation of the preparation of long oval root canals in mandibular molars with the self-adjusting file. *J Endod*, **2011**; 37:517-521.
342. Guimaraes, L.S., C.C. Gomes, M.F. Marceliano-Alves, R.S. Cunha, J.C. Provenzano, and J.F. Siqueira, Jr. Preparation of Oval-shaped Canals with TRUShape and Reciproc Systems: A Micro-Computed Tomography Study Using Contralateral Premolars. *J Endod*, **2017**; 43:1018-1022.
343. Zuolo, M.L., A.A. Zaia, F.G. Belladonna, E. Silva, E.M. Souza, M.A. Versiani, R.T. Lopes, and G. De-Deus. Micro-CT assessment of the shaping ability of four root canal instrumentation systems in oval-shaped canals. *Int Endod J*, **2018**; 51:564-571.
344. De-Deus, G., J. Marins, E.J. Silva, E. Souza, F.G. Belladonna, C. Reis, A.S. Machado, R.T. Lopes, M.A. Versiani, S. Paciornik, and A.A. Neves. Accumulated hard tissue debris produced during reciprocating and rotary nickel-titanium canal preparation. *J Endod*, **2015**; 41:676-681.
345. De-Deus, G., F.G. Belladonna, E.J. Silva, J.R. Marins, E.M. Souza, R. Perez, R.T. Lopes, M.A. Versiani, S. Paciornik, and A. Neves Ade. Micro-CT Evaluation of Non-instrumented Canal Areas with Different Enlargements Performed by NiTi Systems. *Braz Dent J*, **2015**; 26:624-629.
346. Hildebrand, T. and P. Rueggsegger. Quantification of Bone Microarchitecture with the Structure Model Index. *Comput Methods Biomech Biomed Engin*, **1997**; 1:15-23.
347. Peters, O.A., A. Laib, T.N. Gohring, and F. Barbakow. Changes in root canal geometry after preparation assessed by high-resolution computed tomography. *J Endod*, **2001**; 27:1-6.
348. Salmon, P.L., C. Ohlsson, S.J. Shefelbine, and M. Doube. Structure Model Index Does Not Measure Rods and Plates in Trabecular Bone. *Front Endocrinol (Lausanne)*, **2015**; 6:162.
349. Salmon, P.L., Structure Model Index, G.F. Johnsen, Editor. **2018**.
350. Garn, S.M., A.B. Lewis, and R.S. Kerewsky. The meaning of bilateral asymmetry in the permanent dentition. *Angle Orthod*, **1966**; 36:55-62.
351. Mavroskoufis, F. and G.M. Ritchie. Variation in size and form between left and right maxillary central incisor teeth. *J Prosthet Dent*, **1980**; 43:254-257.
352. Probst, F.A. and A. Mehl. CAD reconstruction using contralateral mirrored anterior teeth: a 3-dimensional metric and visual evaluation. *Int J Prosthodont*, **2008**; 21:521-523.

-
353. Yong, R., S. Ranjitkar, G.C. Townsend, R.N. Smith, A.R. Evans, T.E. Hughes, D. Lekkas, and A.H. Brook. Dental phenomics: advancing genotype to phenotype correlations in craniofacial research. *Australian dental journal*, **2014**; 59 Suppl 1:34-47.
 354. Probst, F.A., Dreidimensionale Untersuchungen zur Morphologie der oberen Frontzähne. **2007**, Dachau: Ludwig-Maximilian University. 136.
 355. Probst, F.A., A.P. Litzemberger, M.J. Richter, and A.C. Mehl. Similarity measure for quality control of dental CAD/CAM-applications. *Comput Biol Med*, **2012**; 42:1086-1090.

APPENDIX I

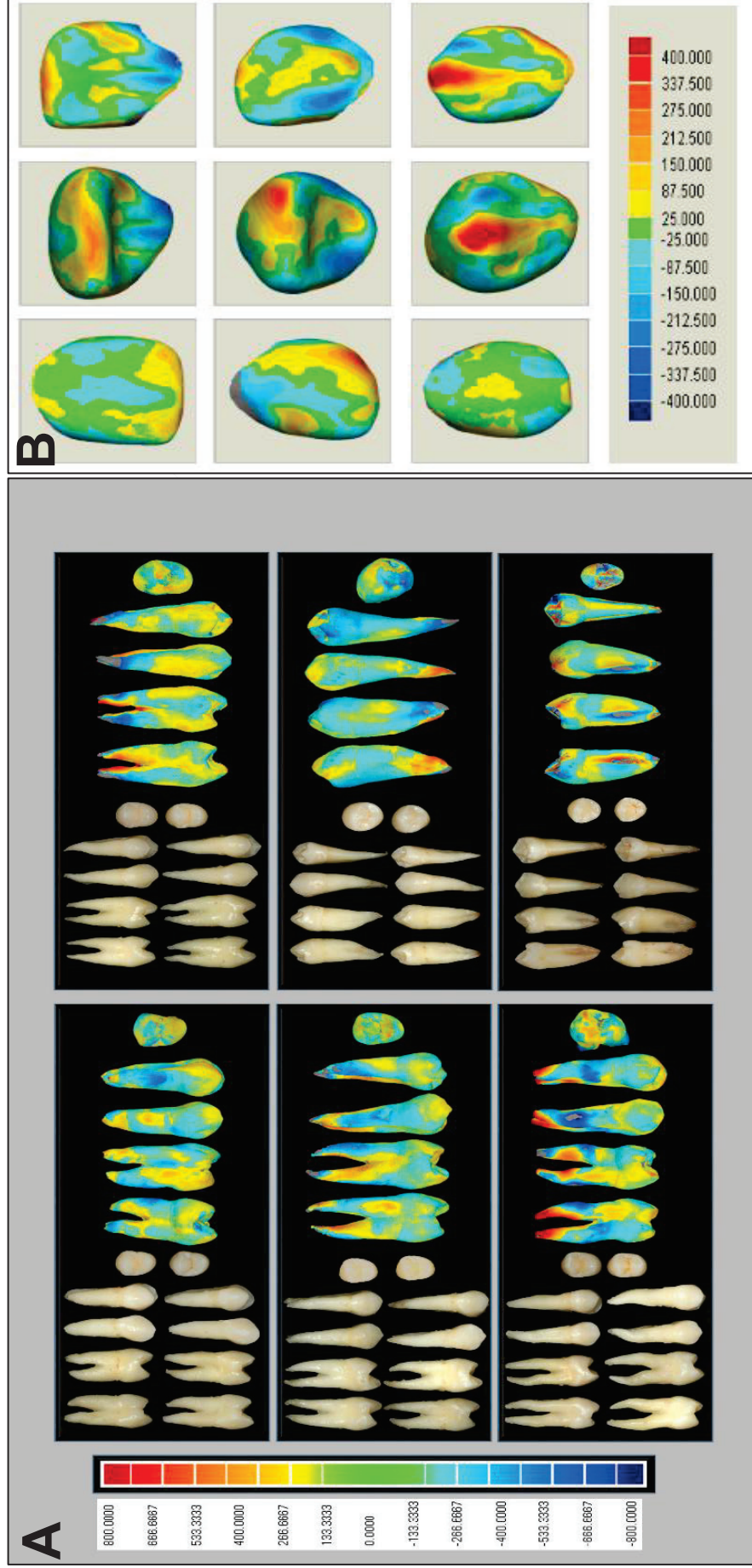


Figure 9. (A) Deviation maps for examples of contralateral premolar tooth pairs showing high degrees of similarity (A). Gray areas represent outliers beyond the maximum and minimum critical values of $\pm 800.00 \mu\text{m}$. (B) Deviation maps for contralateral anterior teeth crowns with maximum and critical values of $\pm 400.00 \mu\text{m}$ [354].

APPENDIX II

Table 2. Comparison of selected parameters in contralateral premolars and simple linear regression values.

Parameter	Contralateral Mean Difference	Standard Deviation	Simple Linear Regression (R)
Volume Total Length Root Canal System	0.831 mm ³	± 0.832	0.9927
Volume Apical Third	0.158 mm ³	± 0.157	0.9519
Average object equivalent circle diameter per slice apical third (AED)	0.645 mm	± 0.390	0.8992
Faciolingual Distance at CEJ	0.323 mm	± 0.562	0.8517
Mesiodistal Distance at CEJ	0.154 mm	± 0.189	0.9467
Faciolingual Distance Halfway	0.273 mm	± 0.301	0.9308
Mesiodistal Distance Halfway	0.0915 mm	± 0.0943	0.9659
Faciolingual Distance 2mm from Apex	0.228 mm	± 0.277	0.9503
Mesiodistal Distance 2mm from Apex	0.189 mm	± 0.175	0.9462

APPENDIX III

Table 3. Paired design sample reduction factors (λ_p), correlation coefficients, and mean sample estimates to detect differences in contralateral pairs

Parameter (unit)	Contralateral	Mean (Standard deviation)	Correlation Coefficient (R)	Mean Difference (Standard deviation)	N_m	N_u	$\lambda_p (N_m/N_u)$	$\lambda_p (1 - R)$																																																																																																																		
Total Volume Root Canal System Pre-instrumentation (mm ³)	1	7.446 (6.896)	0.9927	0.8313 (0.8319)	9	18	0.50	0.0073																																																																																																																		
	2	7.078 (6.080)							Total Volume Root Canal System Post-instrumentation (mm ³)	1	8.575 (7.375)	0.9913	0.9544 (0.7664)	6	12	0.50	0.0087	2	8.237 (6.618)	Volume Apical Third Pre-Instrumentation (mm ³)	1	0.795 (0.608)	0.9519	0.1576 (0.1571)	31	62	0.50	0.0481	2	0.700 (0.499)	Volume Apical Third Post-Instrumentation (mm ³)	1	1.077 (0.655)	0.9358	0.1991 (0.1274)	10	21	0.50	0.0642	2	1.013 (0.626)	Diameter Pre-instrumentation (mm)	1	0.465 (0.168)	0.9927	0.0645 (0.0391)	5	10	0.50	0.0073	2	0.444 (0.153)	Diameter Post-instrumentation (mm)	1	0.552 (0.159)	0.9913	0.0786 (0.0498)	6	12	0.50	0.0087	2	0.542 (0.143)	Root Canal Widths FL CEJ (mm)	1	2.298 (1.057)	0.8517	0.323 (0.562)	48	96	0.50	0.1483	2	1.976 (0.995)	Root Canal Widths MD CEJ (mm)	1	1.106 (0.580)	0.9467	0.154 (0.189)	24	47	0.50	0.0533	2	0.952 (0.523)	Root Canal Widths FL Halfway (mm)	1	2.712 (0.738)	0.9308	0.273 (0.301)	8	35	0.22	0.0692	2	2.985 (0.821)	Root Canal Widths MD Halfway (mm)	1	1.221 (0.357)	0.9659	0.0915 (0.0943)	4	8	0.50	0.0341	2	1.313 (0.325)	Root Canal Widths FL Apical 2 mm (mm)	1	0.791 (0.688)	0.9503	0.228 (0.277)	65	131	0.50	0.0497	2	1.0189 (0.829)	Root Canal Widths MD Apical 2 mm (mm)	1	0.617 (0.425)	0.9462
Total Volume Root Canal System Post-instrumentation (mm ³)	1	8.575 (7.375)	0.9913	0.9544 (0.7664)	6	12	0.50	0.0087																																																																																																																		
	2	8.237 (6.618)							Volume Apical Third Pre-Instrumentation (mm ³)	1	0.795 (0.608)	0.9519	0.1576 (0.1571)	31	62	0.50	0.0481	2	0.700 (0.499)	Volume Apical Third Post-Instrumentation (mm ³)	1	1.077 (0.655)	0.9358	0.1991 (0.1274)	10	21	0.50	0.0642	2	1.013 (0.626)	Diameter Pre-instrumentation (mm)	1	0.465 (0.168)	0.9927	0.0645 (0.0391)	5	10	0.50	0.0073	2	0.444 (0.153)	Diameter Post-instrumentation (mm)	1	0.552 (0.159)	0.9913	0.0786 (0.0498)	6	12	0.50	0.0087	2	0.542 (0.143)	Root Canal Widths FL CEJ (mm)	1	2.298 (1.057)	0.8517	0.323 (0.562)	48	96	0.50	0.1483	2	1.976 (0.995)	Root Canal Widths MD CEJ (mm)	1	1.106 (0.580)	0.9467	0.154 (0.189)	24	47	0.50	0.0533	2	0.952 (0.523)	Root Canal Widths FL Halfway (mm)	1	2.712 (0.738)	0.9308	0.273 (0.301)	8	35	0.22	0.0692	2	2.985 (0.821)	Root Canal Widths MD Halfway (mm)	1	1.221 (0.357)	0.9659	0.0915 (0.0943)	4	8	0.50	0.0341	2	1.313 (0.325)	Root Canal Widths FL Apical 2 mm (mm)	1	0.791 (0.688)	0.9503	0.228 (0.277)	65	131	0.50	0.0497	2	1.0189 (0.829)	Root Canal Widths MD Apical 2 mm (mm)	1	0.617 (0.425)	0.9462	0.189 (0.175)	42	84	0.50	0.0538	2	0.806 (0.511)				
Volume Apical Third Pre-Instrumentation (mm ³)	1	0.795 (0.608)	0.9519	0.1576 (0.1571)	31	62	0.50	0.0481																																																																																																																		
	2	0.700 (0.499)							Volume Apical Third Post-Instrumentation (mm ³)	1	1.077 (0.655)	0.9358	0.1991 (0.1274)	10	21	0.50	0.0642	2	1.013 (0.626)	Diameter Pre-instrumentation (mm)	1	0.465 (0.168)	0.9927	0.0645 (0.0391)	5	10	0.50	0.0073	2	0.444 (0.153)	Diameter Post-instrumentation (mm)	1	0.552 (0.159)	0.9913	0.0786 (0.0498)	6	12	0.50	0.0087	2	0.542 (0.143)	Root Canal Widths FL CEJ (mm)	1	2.298 (1.057)	0.8517	0.323 (0.562)	48	96	0.50	0.1483	2	1.976 (0.995)	Root Canal Widths MD CEJ (mm)	1	1.106 (0.580)	0.9467	0.154 (0.189)	24	47	0.50	0.0533	2	0.952 (0.523)	Root Canal Widths FL Halfway (mm)	1	2.712 (0.738)	0.9308	0.273 (0.301)	8	35	0.22	0.0692	2	2.985 (0.821)	Root Canal Widths MD Halfway (mm)	1	1.221 (0.357)	0.9659	0.0915 (0.0943)	4	8	0.50	0.0341	2	1.313 (0.325)	Root Canal Widths FL Apical 2 mm (mm)	1	0.791 (0.688)	0.9503	0.228 (0.277)	65	131	0.50	0.0497	2	1.0189 (0.829)	Root Canal Widths MD Apical 2 mm (mm)	1	0.617 (0.425)	0.9462	0.189 (0.175)	42	84	0.50	0.0538	2	0.806 (0.511)															
Volume Apical Third Post-Instrumentation (mm ³)	1	1.077 (0.655)	0.9358	0.1991 (0.1274)	10	21	0.50	0.0642																																																																																																																		
	2	1.013 (0.626)							Diameter Pre-instrumentation (mm)	1	0.465 (0.168)	0.9927	0.0645 (0.0391)	5	10	0.50	0.0073	2	0.444 (0.153)	Diameter Post-instrumentation (mm)	1	0.552 (0.159)	0.9913	0.0786 (0.0498)	6	12	0.50	0.0087	2	0.542 (0.143)	Root Canal Widths FL CEJ (mm)	1	2.298 (1.057)	0.8517	0.323 (0.562)	48	96	0.50	0.1483	2	1.976 (0.995)	Root Canal Widths MD CEJ (mm)	1	1.106 (0.580)	0.9467	0.154 (0.189)	24	47	0.50	0.0533	2	0.952 (0.523)	Root Canal Widths FL Halfway (mm)	1	2.712 (0.738)	0.9308	0.273 (0.301)	8	35	0.22	0.0692	2	2.985 (0.821)	Root Canal Widths MD Halfway (mm)	1	1.221 (0.357)	0.9659	0.0915 (0.0943)	4	8	0.50	0.0341	2	1.313 (0.325)	Root Canal Widths FL Apical 2 mm (mm)	1	0.791 (0.688)	0.9503	0.228 (0.277)	65	131	0.50	0.0497	2	1.0189 (0.829)	Root Canal Widths MD Apical 2 mm (mm)	1	0.617 (0.425)	0.9462	0.189 (0.175)	42	84	0.50	0.0538	2	0.806 (0.511)																										
Diameter Pre-instrumentation (mm)	1	0.465 (0.168)	0.9927	0.0645 (0.0391)	5	10	0.50	0.0073																																																																																																																		
	2	0.444 (0.153)							Diameter Post-instrumentation (mm)	1	0.552 (0.159)	0.9913	0.0786 (0.0498)	6	12	0.50	0.0087	2	0.542 (0.143)	Root Canal Widths FL CEJ (mm)	1	2.298 (1.057)	0.8517	0.323 (0.562)	48	96	0.50	0.1483	2	1.976 (0.995)	Root Canal Widths MD CEJ (mm)	1	1.106 (0.580)	0.9467	0.154 (0.189)	24	47	0.50	0.0533	2	0.952 (0.523)	Root Canal Widths FL Halfway (mm)	1	2.712 (0.738)	0.9308	0.273 (0.301)	8	35	0.22	0.0692	2	2.985 (0.821)	Root Canal Widths MD Halfway (mm)	1	1.221 (0.357)	0.9659	0.0915 (0.0943)	4	8	0.50	0.0341	2	1.313 (0.325)	Root Canal Widths FL Apical 2 mm (mm)	1	0.791 (0.688)	0.9503	0.228 (0.277)	65	131	0.50	0.0497	2	1.0189 (0.829)	Root Canal Widths MD Apical 2 mm (mm)	1	0.617 (0.425)	0.9462	0.189 (0.175)	42	84	0.50	0.0538	2	0.806 (0.511)																																					
Diameter Post-instrumentation (mm)	1	0.552 (0.159)	0.9913	0.0786 (0.0498)	6	12	0.50	0.0087																																																																																																																		
	2	0.542 (0.143)							Root Canal Widths FL CEJ (mm)	1	2.298 (1.057)	0.8517	0.323 (0.562)	48	96	0.50	0.1483	2	1.976 (0.995)	Root Canal Widths MD CEJ (mm)	1	1.106 (0.580)	0.9467	0.154 (0.189)	24	47	0.50	0.0533	2	0.952 (0.523)	Root Canal Widths FL Halfway (mm)	1	2.712 (0.738)	0.9308	0.273 (0.301)	8	35	0.22	0.0692	2	2.985 (0.821)	Root Canal Widths MD Halfway (mm)	1	1.221 (0.357)	0.9659	0.0915 (0.0943)	4	8	0.50	0.0341	2	1.313 (0.325)	Root Canal Widths FL Apical 2 mm (mm)	1	0.791 (0.688)	0.9503	0.228 (0.277)	65	131	0.50	0.0497	2	1.0189 (0.829)	Root Canal Widths MD Apical 2 mm (mm)	1	0.617 (0.425)	0.9462	0.189 (0.175)	42	84	0.50	0.0538	2	0.806 (0.511)																																																
Root Canal Widths FL CEJ (mm)	1	2.298 (1.057)	0.8517	0.323 (0.562)	48	96	0.50	0.1483																																																																																																																		
	2	1.976 (0.995)							Root Canal Widths MD CEJ (mm)	1	1.106 (0.580)	0.9467	0.154 (0.189)	24	47	0.50	0.0533	2	0.952 (0.523)	Root Canal Widths FL Halfway (mm)	1	2.712 (0.738)	0.9308	0.273 (0.301)	8	35	0.22	0.0692	2	2.985 (0.821)	Root Canal Widths MD Halfway (mm)	1	1.221 (0.357)	0.9659	0.0915 (0.0943)	4	8	0.50	0.0341	2	1.313 (0.325)	Root Canal Widths FL Apical 2 mm (mm)	1	0.791 (0.688)	0.9503	0.228 (0.277)	65	131	0.50	0.0497	2	1.0189 (0.829)	Root Canal Widths MD Apical 2 mm (mm)	1	0.617 (0.425)	0.9462	0.189 (0.175)	42	84	0.50	0.0538	2	0.806 (0.511)																																																											
Root Canal Widths MD CEJ (mm)	1	1.106 (0.580)	0.9467	0.154 (0.189)	24	47	0.50	0.0533																																																																																																																		
	2	0.952 (0.523)							Root Canal Widths FL Halfway (mm)	1	2.712 (0.738)	0.9308	0.273 (0.301)	8	35	0.22	0.0692	2	2.985 (0.821)	Root Canal Widths MD Halfway (mm)	1	1.221 (0.357)	0.9659	0.0915 (0.0943)	4	8	0.50	0.0341	2	1.313 (0.325)	Root Canal Widths FL Apical 2 mm (mm)	1	0.791 (0.688)	0.9503	0.228 (0.277)	65	131	0.50	0.0497	2	1.0189 (0.829)	Root Canal Widths MD Apical 2 mm (mm)	1	0.617 (0.425)	0.9462	0.189 (0.175)	42	84	0.50	0.0538	2	0.806 (0.511)																																																																						
Root Canal Widths FL Halfway (mm)	1	2.712 (0.738)	0.9308	0.273 (0.301)	8	35	0.22	0.0692																																																																																																																		
	2	2.985 (0.821)							Root Canal Widths MD Halfway (mm)	1	1.221 (0.357)	0.9659	0.0915 (0.0943)	4	8	0.50	0.0341	2	1.313 (0.325)	Root Canal Widths FL Apical 2 mm (mm)	1	0.791 (0.688)	0.9503	0.228 (0.277)	65	131	0.50	0.0497	2	1.0189 (0.829)	Root Canal Widths MD Apical 2 mm (mm)	1	0.617 (0.425)	0.9462	0.189 (0.175)	42	84	0.50	0.0538	2	0.806 (0.511)																																																																																	
Root Canal Widths MD Halfway (mm)	1	1.221 (0.357)	0.9659	0.0915 (0.0943)	4	8	0.50	0.0341																																																																																																																		
	2	1.313 (0.325)							Root Canal Widths FL Apical 2 mm (mm)	1	0.791 (0.688)	0.9503	0.228 (0.277)	65	131	0.50	0.0497	2	1.0189 (0.829)	Root Canal Widths MD Apical 2 mm (mm)	1	0.617 (0.425)	0.9462	0.189 (0.175)	42	84	0.50	0.0538	2	0.806 (0.511)																																																																																												
Root Canal Widths FL Apical 2 mm (mm)	1	0.791 (0.688)	0.9503	0.228 (0.277)	65	131	0.50	0.0497																																																																																																																		
	2	1.0189 (0.829)							Root Canal Widths MD Apical 2 mm (mm)	1	0.617 (0.425)	0.9462	0.189 (0.175)	42	84	0.50	0.0538	2	0.806 (0.511)																																																																																																							
Root Canal Widths MD Apical 2 mm (mm)	1	0.617 (0.425)	0.9462	0.189 (0.175)	42	84	0.50	0.0538																																																																																																																		
	2	0.806 (0.511)																																																																																																																								

APPENDIX IV

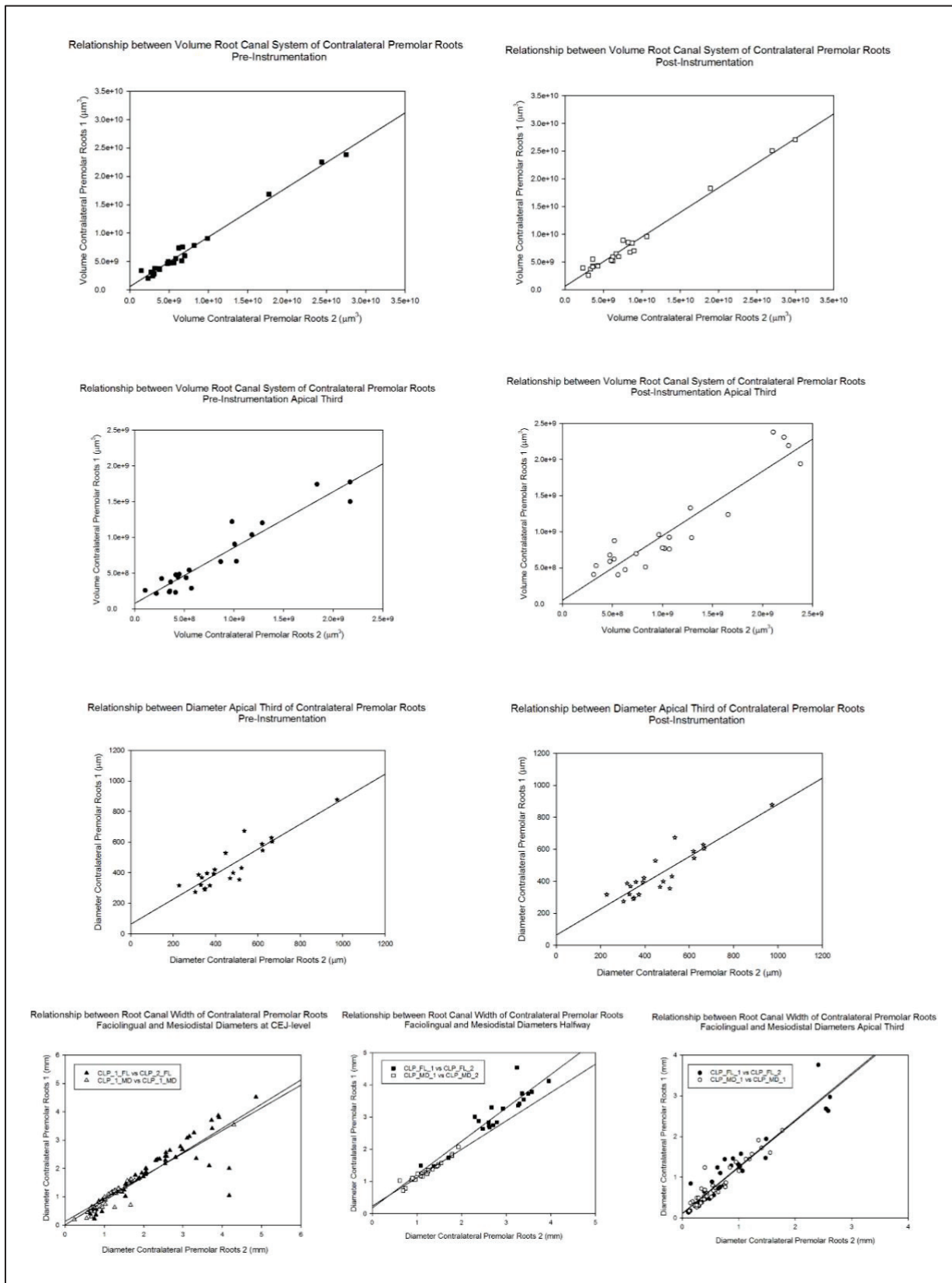


Figure 10. Scatter plots comparing contralateral premolar roots with fitted linear regression lines